Ph.D in Biomedicine and Neurosciences

Ph.D Coordinator: Prof Bucchieri Fabio

Department of Biomedicine, Neuroscience and Advanced Diagnostics

Development of a new anti-cachectic drug based on nano-vesicles

Ph.D Student:
Trovato Eleonora

Academic Tutor:
Prof Di Felice Valentina

Years 2017-2020

List of Contents

List of Figures

List of tables

Abstract

Skeletal muscle is one of the main regulators of protein metabolism and energy production, also involved in important contraction and movement mechanisms. However, alterations of this tissue can cause the onset of certain myopathies such as cachexia, a multifactorial syndrome characterized by a severe loss of muscle mass (with or without loss of fat mass) which is often associated to other chronic illnesses, such as cancer or neurodegenerative diseases (Fearon, 2011).

Currently, there are no specific drugs able to reverse this condition and the few attempts made with the use of appetite stimulants only caused an increase in weight (due to an accumulation of fat), rather than a gain in body mass. However, it has been recently discovered that exercise training may positive affect the state of this disease, primarily improving muscle mass and strength of cachectic patients, but also stimulating specific proteins involved in mitochondrial biogenesis (e.g. PGC1-α) or with cyto-protective effects (e.g. Hsp60). This latter is mainly a mitochondrial molecule involved in several cellular processes, and its levels increase in trained mice, allowing not only a better protein import and folding, but also promoting mitochondrial biogenesis (Barone, 2016). Recently, Hsp60 has also been discovered in the extracellular space, associated with small cellular vesicles (microvesicles or nanovesicles) that cells release during cell-to-cell communication (Caruso Bavisotto, 2017).

Based on these previous data, we first focused on the *in vitro* isolation of micro- nano- vesicles harvested from a murine muscle cell line of C2C12, using different techniques of ultracentrifugation, tangential flow filtration, size exclusion chromatography and commercial kits. The isolation was followed by a morphological and biochemical characterization, in order to better study the characteristics of these potential natural carriers for drug delivery, but also to identify possible pathways by which nanovesicles could inhibit skeletal muscle wasting.

We also investigated possible ways to promote the *in vitro* overexpression of the gene HSPD1 in C2C12 cells, with the final aim to produced vesicles enriched in Hsp60, which may be able to activate PGC-1α isoform 1 in naive C2C12 cells.

1. Introduction

1.1 Muscle Wasting

Skeletal muscle is one of the most extended tissues of the body, implicated in important functions such as movement and contraction (Brown, 2017). Representing around 2/5 of the whole body weight, it also plays a pivotal role in more than 3/4 of the total human metabolism (Westerblad, 2010) (Koistinen, 2002).

Proteins are the main components of this tissue, whose mass is finely regulated by balancing mechanisms of protein synthesis and protein degradation (Thompson, 1998) (Anthony, 2016). However, if alterations in one of these two processes occur, it can lead to the progression of certain myopathies, such as sarcopenia and cachexia (Argilés, 2005) (Bowen, 2015).

Sarcopenia is generally referred to a slow and normal loss of muscle during aging, while cachexia indicates a multifactorial syndrome, characterized by a severe and involuntary loss of muscle mass, with or without loss of fat mass (Fearon, 2011). This latter is a condition that cannot be re-established with the normal nutritional support and may be often associated to several chronic illnesses, such as cancer and neurodegenerative diseases (Yoshida, 2015).

Cachexia has been classified in three main stages: pre-cachexia, cachexia and refractory cachexia (Fearon, 2011). Pre-cachexia is intended when clinical and metabolic signs (anorexia and metabolic alterations, like damages in glucose tolerance) generate a weight loss less than 5%; cachexia develops when there is more than 5% in weight loss, a body max index (BMI) lower than 2%, or in conditions of sarcopenia with more than 2% of weight loss; the last stage, refractory cachexia, develops in presence of an active protein catabolism, with no response to any treatment (e.g. anticancer), causing a life expectation of less than 3 months (Zhou, 2018).

This syndrome is commonly linked with an acute depletion of skeletal muscle mass and a decrease in energy metabolism, triggering a reduction of muscle cells energy capacity (Kyrana, 2012). Multiple molecular proteolytic pathways are involved in the development of cachexia, among which lysosomal (Tardif, 2013), Ca^{2+}-dependent (Costelli, 2001), caspase-dependent (Belizário, 2001) and ubiquitin-proteasome-dependent (Khal, 2005), are the four most representative.

Lysosomal proteolysis is related to the activation of autophagy, a physiological mechanism that cells use for the degradation of cellular compromised organelles, such as mitochondria and peroxisomes (Penna, 2019). It is one of the main processes used from visceral and skeletal muscle tissues, and provokes muscle atrophy through a molecular pathway that involves the tumor necrosis factor-α (TNF-α) and the receptor associated factor (TRAF) 6/Fn14 (Paul, 2010)

(Penna, 2013). Autophagy related 7 protein (Atg7) is also implicated in muscle cell basal autophagy processes, playing a role in the maintenance of an internal cellular homeostasis; however, its depletion may provoke muscle atrophy and consequent decrease of muscle strength (Bowen, 2015) (Masiero, 2009).

In cachexia Ca^{2+}-dependent, specific Ca^{2+}-dependent cysteine proteases (calpains) regulate the proteolytic process (Costelli, 2005). These molecules are strongly dependent on Ca^{2+} levels and stimulate muscle protein degradation when cytosolic Ca^{2+} homeostasis is altered (Wu H. , 2007). Normally present in the cytosolic space in an inactive form, they switch in their active form and move towards the plasma membrane once the intracellular Ca^{2+} concentration increases, cleaving several protein substrates (i.e. cytoskeletal, myofibrillar and membrane proteins) that are subsequently degraded by the activity of proteasome (Huang, 1998).

However, protein degradation may also depend on other protease groups called caspases (Silva, 2015). Similarly to calpains, these molecules are present inside the cell in their inactive form (pro-caspases), but if a cellular traumatic event occurs, they switch in their activated state, forming a molecular complex called apoptosome. Under stress conditions, pro-aptotic signals provoke the mitochondrial release of cytochrome-c in the cytosol of the cell; this latter binds and triggers the activation of the adaptor protein Apaf-1, which in turn stimulates the initiator pro-caspases -9, -3, -6 and -7, promoting the development of the apoptosome complex (Chandra, 2003). Caspase-3, is one of the main molecules acting in muscle degradation, being involved in the cleavage of actomyosin and myofibrillar proteins, thus supplying substrates that are further degraded through the proteasome complex (Du, 2004) (Wang X. , 2010).

This latter is a molecular machinery able to degrade altered proteins that were previously ubiquitinated thanks to the enzymatic activity of ubiquitin-activating enzyme (E1), conjugation enzyme (E2) and ligase enzyme (E3). Ubiquitin is a regulatory protein that covalently binds to damaged proteins, serving as a tag for their degradation. In the ubiquitination process, E1 activates and binds the ubiquitin protein, which is first transferred to E2 enzyme and then to E3 ligase, an important enzyme that regulates the transferring of ubiquin to the target protein. Once ubiquitinated, the damaged protein is then delivered to the proteasome complex for its degradation. Two transcription factors FoxO and NF-kB are mainly involved in this process, both enhancing proteasome activity through the activation of the two muscle-specific E3 ligases MAFbx/atrogin-1 and muscle RING Finger-1 (MuRF1) (Du, 2004). The activation of MuRF-1 (E3-ubiquitin ligase) may be also stress oxidative dependent, causing an increment of the proteasome activity and consequent protein degradation (Li, 2003).

Beyond these four mechanisms, other molecules may also stimulate the development of cachexia. For instance, interleukin-6 (IL-6) and tumor necrosis factor α (TNF-α) cytokines are

among the principal inflammatory molecules associated with cancer muscle wasting (Kayacan, 2006); indeed, it has been shown that the over expression of IL-6 may activate several molecules (e.g. FoxO3, atrogenes, STAT3 and p38) implicated in skeletal muscle atrophy (Puppa, 2014). The role of IL-6 during the initial stages of cachexia is of such importance, since it promotes the activation of lypolisis mechanisms of the white adipose tissue (WAT) with a consequent loss in fat, as well as the parallel white-to-brown trans differentiation of white adipocytes into brown adipocytes during latter stages of cachexia (Han J. , 2018).

TNF-α mainly originate from activated macrophages (as a consequence of invasive stimuli) and it is one of the principal mediators of cancer cachexia (Patel, 2017). Presence of TNF in cachectic subjects provokes a series of dysfunctions, such as the down regulation of muscle actin and myosin (Tracey, 1988), gastrointestinal motility (Tracey, 1986) and suppression of food intake (Dinarello, 1986). In cachectic skeletal muscle it induces the synthesis of IL-1, another kind of pro-inflammatory cytokine, promoting the expression of the uncoupling proteins UCP2 and UCP3, molecules involved in the regulation of mitochondrial energy expenditure and tumor growth (Tijerina, 2004). However, TNF-α role in cachexia seems to be a bit controversial: on one hand, its interaction with specific anti-TNF antibodies seems to inhibit all those lipid metabolic alterations to which the adipose tissue is subjected, but, on the other hand, no correlation has been shown in cachectic patients between the levels of TNF and the gravity of weight loss (Costelli, 1993).

Other molecular factors control protein degradation, such as inflammatory cytokines (Cheung, 2010), angiotensin II (Sanders, 2005), insulin like growth factor-1 (Costelli, 2006) and reactive oxygen species (Ardies, 2002), also impacting the activity of the mitochondrial biogenesis regulator peroxisome proliferator-activated receptor-ɣ coactivator α (PGC-1α) and, consequently, the mitochondrial energy production (Joseph, 2006). Mitochondrion is of such importance in muscle metabolism processes, since it is the most important organelle involved in energy production (Tuena de Gómez-Puyou, 1983), making mitochondria pivotal regulators of muscle loss in wasting diseases (Antunes, 2014).

Mitochondrion is the energy house of each eukaryotic cell. Thanks to an α-proteobacteria endosymbiont that implanted in a host cell, it has its own mtDNA, with a length of ~16.5 kb, containing 37 genes encoding for subunits of the electron transport chain (Ventura-Clapier, 2008). It contributes to most of the total cellular ATP, thus playing an important role in the maintaining of cellular homeostasis (Tuena de Gómez-Puyou, 1983). However, if imbalance in ATP production/consumption occurs, mitochondria may undergo into a series of dangerous disorders, that can be deleterious for the viability of the cell (Spinazzola, 2009).

Mitochondria homeostasis is generally maintained through a regulated mechanism of degradation and biogenesis of new organelles, that replace the ones who were damaged or degraded (Palikaras, 2014). The biogenesis process can be promoted by many factors, such as: cold exposure, caloric restriction, exercise, or oxidative stress; this is a widely complicated process where multiple factors (i.e. nuclear respiratory factors NRF1 and NRF2, peroxisome proliferator receptors-PPARs and estrogen related receptors-ERRs), interact with the peroxisome proliferator-activated receptor-ɣ coactivator α (PGC-1α), the master regulator of mitochondria biogenesis (Wenz, 2009).

PGC-1α belongs to the family of the peroxisome proliferator-activated receptor gamma (PGC) family, a series of transcriptional factors involved in several processes, such as regulation of nuclear receptors PPAR, metabolic and energetic pathways, mitochondrial biogenesis, fatty acid oxidation and angiogenesis (Finck, 2006).

Firstly discovered in brown adipose tissue (BAT), its activity is controlled both at the expression and post-translational levels (Fernandez-Marcos, 2011) (Cantó, 2009). In addition to PGC-1α, other two related co-activators were subsequently discovered: PGC-1β (also known as PERC) and PGC-1–related co-activator (PRC) (Lin, 2002) (Scarpulla, 2002). PGC-1α and PGC-1β are mainly present in tissues with high oxidative activity (i.e. heart, skeletal muscle and BAT), where they control cellular metabolism and mitochondrial activity. In contrast to them, PRC factor is the least studied and there are poor information regarding its biological roles.

Transcribed by different genes, these proteins present similar molecular structures, which reflect their common physiological roles (Lin, 2005). The expression of PGC-1α is controlled by the Pgc-1α gene (PPARGC1A in humans), consisting of an evolutionarily conserved alternative promoter, situated 14 kb upstream of the transcription start site (TSS) (Miura, 2008). The activity of Pgc-1α gene strongly depends on biological conditions of specific tissues, and its expression may generate several mRNAs. In fact, it is composed by many promoter and exon regions that, in association with events of alternative splicing, produce distinct transcripts and protein structures (Martínez-Redondo, 2015) (**Figure 1**).

Transcripts developing from the distal promoter present a new exon-1b sequence (which differs from the classic exon-1a located after the proximal promoter PP) and may be further modified through alternative splicing, thus encoding for two different amino terminal sequences shorter than the proximal exon-1a (16 amino acid long): Pgc-1α-b and Pgc-1α-c, respectively 12 and 3 amino acids long (Chinsomboon, 2009). However, exon-1b sequences may be also present in other two transcripts, Pgc-1α2 and Pgc-1α3, characteristic isoforms of trained skeletal muscle

tissue, which are involved in the expression of the vascular endothelial growth factor (VEGF), for the activation of angiogenesis pathways (Martínez-Redondo, 2016).

PPARGC1A gene also carry two distinct promoters: (LP) and BP. The first one mainly control the expression of a human variant of the liver, while the second one is located 587 kb of distance from exon 1a and is mainly characteristic of the brain tissue (Martínez-Redondo, 2015) (Figure 1). The expression of PGC-1α gene is regulated by different molecular pathways such as Ca^{2+} signalling (Chin, 2004), cyclic AMP and 5′ AMP-activated protein kinase (AMPK) (Irrcher, 2008), that promote the activation and translocation of specific transcription factors to PGC-1α gene regions, for its expression.

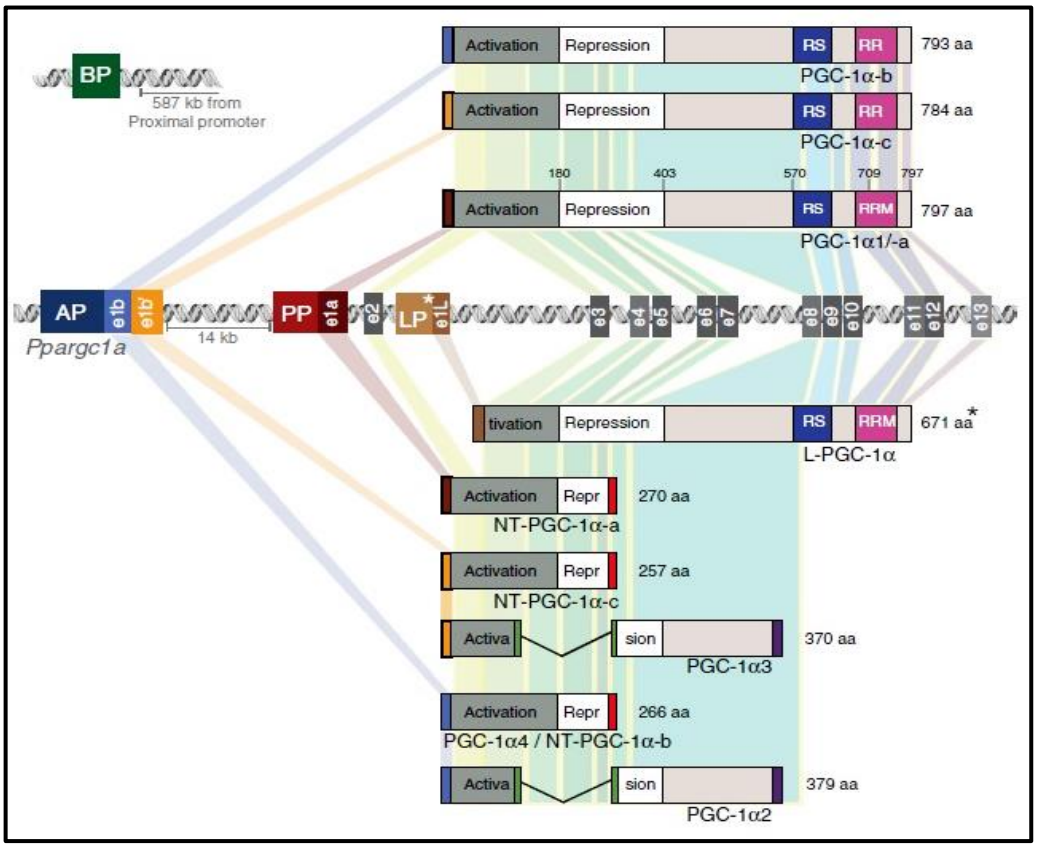

Figure 1 *- PGC-1α isoform structure and transcriptional origin (Martínez-Redondo, 2015).*

However, the expression of this gene may also be suppressed through epigenetic modifications (i.e. DNA methylation) (Bettscheider, 2012), that may alter its activity, causing the development of pathological conditions.

During its activity, PGC-1 interacts with specific transcription factors, enhancing the activation of protein complexes involved in the transcription of nuclear mitochondrial genes. For instance, the binding between the amino-terminal region of PGC-1 with a protein complex constituted by the histone acetyltransferase (HAT), as well as CREB-binding protein/p300 or steroid receptor coactivator-1 (SRC-1), stimulate the activation of chromatin, which modifies its histones, making portions of the genome more accessible to the transcription factors

(Puigserver, 1999) (Wallberg, 2003). Moreover, PGC-1α promotes the activation of nuclear respiratory factor-1 (NRF-1) and -2 (NRF-2), molecules involved in the regulation of the expression of specific mitochondrial transcription factors (i.e. the mitochondrial transcription factor A -TFAM-), important for the expression of nuclear mitochondrial genes (Larsson, 1998) (Gleyzer, 2005).

The activation of PGC-1α is regulated by a considerable number of signaling pathways, and exercise is one of these (Handschin, 2008). During training, contractile activity promotes a consequent increase of intracellular Ca^{2+}, which in turn activates the calcium-dependent phosphatase calcineurin (CaN) and the Ca^{2+}-calmodulin dependent kinase (CaMK), stimulating the expression of PGC-1α and the mitochondria biogenesis (Ventura-Clapier, 2008).

PGC-1α seems to be a positive mediator of some beneficial effects that physical exercise plays in skeletal muscle and its expression is highly concentrated in skeletal muscle fibers (especially in those oxidative), where it promotes mitochondrial respiration and fatty acid oxidation through the conversion of fast glycolytic fibers to slow and oxidative fibers (Zhang L. , 2017). Indeed, it has been demonstrated that both short-term exercise and endurance training may stimulate the expression of PGC-1α in skeletal muscle (Pilegaard, 2003), especially in type IIa fibers after endurance training (Russell A. , 2003). Physical exercise also encourages a reduction of the chromatin methylation of PGC-1α promoter, thus keeping the gene sequence available for its expression (Narkar, 2017). Although the mechanisms underlying the activation of muscle PGC-1α during training activity are still poor understood, it is now known that calcineurin A, CaMK, p38 MAPK and AMPK pathways may be involved in the muscle gene transcription (Egan, 2010) (Schaeffer, 2004).

On the basis of these beneficial effects, exercise could be taken in consideration for all those cachectic conditions that occur during chronic diseases (Eva, 2016). This syndrome is often widely underestimated, since most of the treatments used so far have been ineffective (Tazi, 2010), with disappointing results of most non-pharmacological (e.g. high-calorie diet) and pharmacological strategies (e.g. progesterone therapy based, anabolic steroids, cannabinoids, antidepressants etc). Despite new potential drugs are under investigation (i.e. thalidomide, selective cox-2 inhibitors, ghrelin mimetics, insulin, oxandrolone and olanzapine), they have shown only few auspicious results (Aversa, 2017).

Nowadays, progestogen treatment is the only approved drug in Europa, and constitutes the best available treatment option for cancer-related cachexia. Progestogen is a steroid hormone, which stimulates appetite and weight increase of cachectic patients, through the activity of the neuropeptide Y (Madeddu, 2009). Another novel oral drug named Anamorelin, an analogue of the circulating hormone ghrelin, has demonstrated positive effects in those mechanisms that

influence the development of the syndrome (Currow, 2018). Despite these new evidences, all the currently existing treatments against cachexia appear to be aimed at improving anorectic conditions, thus lacking specificity versus the syndrome.

Therefore, it could be extremely important to identify innovative therapies that can be able to mimic the beneficial effects of exercise in these pathological conditions. Physical activity stimulates muscle strength and function, increasing a fat free mass that positively affect the quality of life. Different cellular responses can be triggered based on the type of training; for instance, non-stressful exercise regulates inflammation processes, through the reduction of cellular response to inflammatory stimuli and pro-inflammatory cytokines (Gould, 2013). On contrary, acute exercise provoke a high expression of cytokines involved in an acute-phase inflammatory response (Ostrowski, 1999), even if levels of classic pro-inflammatory cytokines (TNF-α and IL-1β) seem not to be directly affected, thus suggesting that cytokine cascade induced by physical activity differs from that induced by infections (Gould, 2013).

In a recent study, it has been also shown that endurance training of cachectic mice increased the expression levels of a mitochondrial chaperonine (heat shock protein 60 -Hsp60-) involved in the regulation processes of PGC-1α and mitochondria biogenesis. The study demonstrated a correlation between Hsp60 levels with those of PGC-1α, stressing a potential role of physical activity in the treatment of cachexia syndrome, as well as in the homeostasis of muscle tissue (Barone, 2016).

1.2 Heat Shock Proteins (Hsps)

Heat shock proteins (Hsps) are a family of ubiquitous molecules present in the cells of all organisms (Robert, 2003). Primarily found in the salivary gland of Drosophila, these proteins present a highly conserved genome across species, from Prokaryotes to Eukaryotes (Ritossa, 1962). Originally named, and known, for their expression after exposure to heat stress, this family of proteins can also be activated by a range of other environmental and metabolic stress conditions, such as: ischemia (Nowak, 1990), heavy metal ions (Wagner, 1999), ethanol (Tunici, 1999), nicotine (Hahn, 1991), oxidative stress (Drummond, 1987) and malignant transformation (Vargas-Roig, 1997). Hence, they are of such importance for the cells, as they protect organisms to non-lethal stress, through mechanisms of thermotolerance and cross-tolerance.

Hsps proteins are implicated in many cellular functions, such as protein folding and degradation of damaged-denatured proteins, helping new polypeptides reaching their final functional structure, or re-folding, as well as degrading damaged proteins once exposed to stress events (Wegele, 2004). In addition, they are also implicated to other cellular functions, such as:

regulation of gene expression, cellular differentiation, DNA replication, signal transduction, senescence, programmed cell death and carcinogenesis (Macario, 2005).

Under non-stress conditions, Hsps are less expressed, but if cells alterations occur, levels of specific heat shock transcription factors (HSF) may strongly increase (Pirkkala, 2001). Once activated, these factors (which have a monomer form when inactive) migrate into the nucleus, trimerize into the active form and bind to the promoter site of the Hsps gene, promoting the synthesis of Hsps mRNAs (Sandqvist, 2009) (Whitley, 1999). These proteins play important roles in maintaining cellular homeostasis, controlling apoptotic signaling events (Beere, 2004), antigen processing mechanisms (Li Z. , 2002), but they can also be implicated in the pathology of several diseases (Yujun, 2007).

This class of proteins belong to a multi gene family with a molecular size range from 8 to 150 kDa, and their name generally refers to their molecular weights, classifying them as: low molecular weight Hsp (small Hsps) with a size range of 10-30 kDa, Hsp40, Hsp60 (also called chaperonin), Hsp70, Hsp90, Hsp100 and Hsp110 (also known as chaperons) (Hyunseok, 2016). Depending on their expression patterns, these proteins may be further divided in other two classes: induced and constitutive (heat shock cognate, Hsc) proteins (Somji, 1999). As the name suggests, the first group is generally low expressed in physiologically conditions, but it can widely rise after stress events, while the second group is constitutive expressed within the cell (Garbuz, 2017). Firstly though to be restricted to the only cytoplasm, these proteins are also present in cellular organelles, as well as in the plasma membrane (either in the surface or inside the cellular membranes) and in the extracellular space (Horváth, 2008).

Hsp60 is a mitochondrial protein belonging to the group of chaperonins, multi subunit ATPases molecules involved in the folding of new or damaged proteins (Lund, 2003). This group can be divided in two families: the prokaryotic GroEL-GroES (and their eukaryotic homologs Hsp60-Hsp10) (Haldar, 2015), and the CCT family proteins (chaperonins containing t-complex polypeptide) (Vallin, 2019). In Eukaryotes, the first family works mainly in the mitochondria, while the second one is specific of the cytosol (Garbuz, 2017). In addition to this first classification, chaperonins may be further divided in other two classes: class I (found in prokaryotes and cell organelles) and class II (in Archea and cytosol of eukaryotes), depending respectively on their ability, or not, to interact with other co-chaperonins (Nielsen, 1999).

Unlike from their chaperones counterpart, which interact with protein substrates in a monomeric or dimeric form, functional chaperonins work as oligomeric rings, in which monomeric subunits surround a central cavity where the unfolded protein gets processed (Garbuz, 2017) (Hartl, 1992). For instance, Eukariotic Hsp60 is an ATP dependent oligomer formed by two stacked heptameric rings, each of them composed by the association of 7

monomers and further divided in three domains: apical, intermediate and equatorial; this latter, holds the binding site for ATP molecules, while the intermediate domain serve as a linker for equatorial and apical domains, also promoting all those conformational protein modifications that occur once ATP/ADP and Mg^{2+} are linked to the equatorial subunit (Karlin, 2000). Thanks to this specific conformation, the substrate is literally trapped within the ring and is completely isolated from possible other external interactions. However, as a chaperonin, Hsp60 has to interact with a co-chaperonin to perform its functions (Hsp10) which is arranged to form a sort of cap in the apical and basal areas of the characteristic double ring complex (Vilasi, 2014).

Almost 80-85% of Hsp60 from mammalian cells and tissues resides in the matrix space of mitochondria, while the rest 15-20% of the protein occupies extra-mitochondrial sites, such as the plasma membrane, peroxisomes, the endoplasmic reticulum and the extracellular space (Taldone, 2014) (Campanella, 2012) (Merendino, 2010).

Its synthesis starts from the nuclear gene HSPD1, that is first transcribed into a specific mRNA, which then migrate in the cytosol for its translation. The translated sequence of Hsp60 presents an N-terminal signal sequence of 1-26 amino acids, which is responsible for its translocation inside the mitochondria and its conversion into its mature 58 kDa conformation (Ishida, 2018).

Considering its high mitochondrial distribution, some researchers have speculated a possible correlation between Hsp60 expression and mitochondria biogenesis in muscle cells after training endurance (Barone, 2016) (Frühbeis, 2015), with a release of chaperonine thought via exosomes, since it has been already demonstrated that, under stress conditions, cells are able to secrete high levels of HSPs-bearing EVs (i.e. Hsp-90, Hsp-70, Hsp-60) (Taha, 2019) (Kisho, 2018).

1.3 Extracellular Vesicles: origin and mechanism of biogenesis

Extracellular Vesicles (EVs) are small particles composed of a lipid bi-layer containing multiple molecules derived from the cytosol, and the cellular membrane, of the donor cell (Akers, 2013). First characterized in 1967 in hematopoietic cells (Wolf, 1967), they represent a varied population that differs in cellular origin, size, morphology, antigenic composition and functional properties (**Table 1**).

Originally thought to be exclusively involved in the secretion of transferrin receptors during the maturation of erythrocytes, in the early 1980s, EVs were also found as membranes vesicles released during pre-degenerative processes by dying cells (Coleman, 2001). Recent evidences have demonstrated that the secretion of these vesicles is a well conserved mechanism, common to the majority of the cells (both Prokaryotics or Eukaryotics), and describes vesicles as entities released by living cells, through secretory pathways that occur during physiological and

degenerative processes (Colombo, 2014). Once in the extracellular space, EVs may act as soluble messengers important in cell-to-cell communication among near and distant cells (Colombo, 2014).

Table 1 *-Types of Extracellular Vesicles and most common markers*			
Type	Apoptotic Bodies	Microvesiscles (Ectosomes, Microparticles)	Nano-vesicles (exosomes) (small-medium-large)
Size	> 800 nm	>100 nm-1 μm	30-150 nm
Biogenesis	Apoptosis	outward budding of plasma membrane	Endocytosis
Common Markers	chemokine (C-X3-C motif) ligand 1 CX3CL1; Intercellular adhesion molecule 3 (ICAM-3);	β1 integrins; selectins; CD40; Matrix metalloproteinase (MMP);	Tetraspanins (CD63;CD9; CD81); Hsps (Hsp70; Hsp90); Tumor susceptibility gene 101 (TSG101); Annexin V-VI; Metallopeptidase domain 10 (ADAM10); Alix;
References	(Catchpoole, 1995)	(Surman, 2017)	(Kowal, 2016)

Despite their first classification relied on the basis of their size (e.g. apoptotic bodies 1-5 μm, microparticles from 0.1–1 μm and exosomes, with a diameter of 40–150 nm), their tissue of origin (e.g. prostasomes, oncosomes), their function, or their presence outside the cells, one of their last classification mainly focuses on their mechanism of biogenesis (Kalra, 2016) (**Figure 2**). However, there is still no consensus on specific EV subtypes markers (such as endosome-origin or plasma membrane-derived) that can be used as unique references for their classification into different vesicular sub-groups (i.e. micro- or nano- vesicles); therefore, allocate a vesicle to a particular biogenesis pathway is still very difficult, unless it is captured during its release in live imaging techniques (Choi, 2017). Hence, in order to classify a particular vesicle to a specific subtype, the International Society for studies of Extracellular Vesicles (ISEV) has published the last document about the minimal information for the studies of Extracellular Vesicles (MISEV 2018). They suggested to sort vesicles based on several parameters such as: size [“small EVs” (sEVs) and “medium/large EVs” (m/l- EVs)], density (low, middle, high), biochemical composition (CD63C, CD81C, Annexin A5), description of

their tissue of origin (prostasomes, oncosomes), their function, their presence outside the cells and their biogenesis pathway (Théry, 2018).

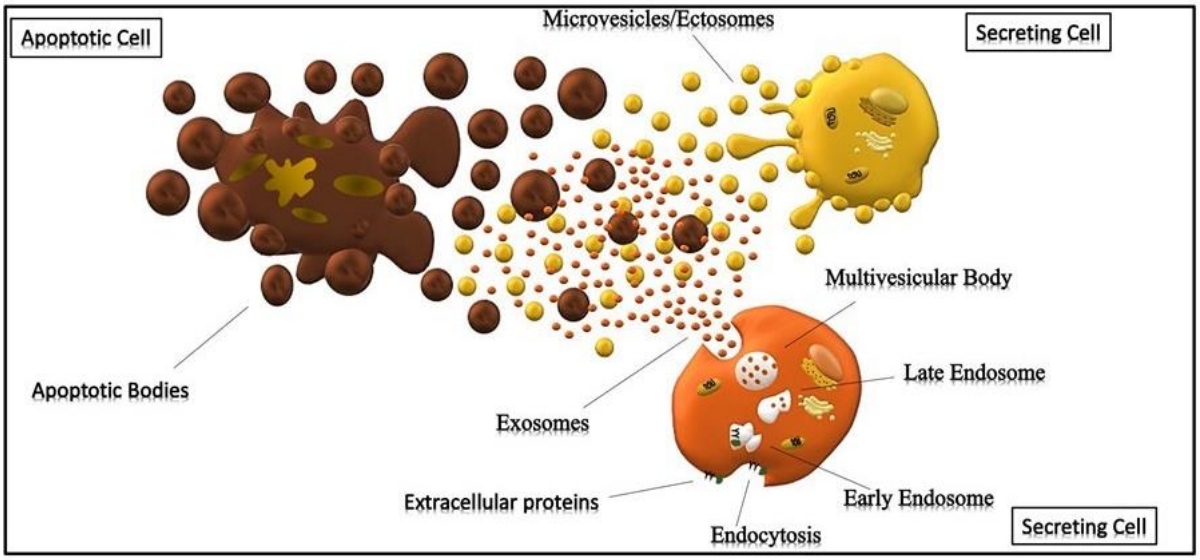

Figure 2 - *Representation of different extracellular vesicles*

The EVs molecular composition is cell-type specific and is represented by several molecules, such nucleic acids (largely constituted by mRNAs and miRNAs), as well as proteins and lipids, all reflecting the similar composition of the cell from which they originate (Gutierrez-Vazquez, 2013). Similarly, their functions are closely related to their cellular origin, being involved in several mechanisms such as immune response, inflammation, etc (Zhang, 2014). In addition, the composition of their molecular cargo may be also influenced by the choice of specific methods of isolation (e.g. ultracentrifugation, SEC, immuno isolation etc.), as well as by the sample from which they are harvested (cell culture medium, bio fluids, or tissues) (Lässer, 2018).

The protein content of exosome is mainly divided in four categories: 1) transmembrane or lipid bound extracellular proteins (tetraspanins like CD9, CD81, CD63), 2) cytosolic proteins normally involved in their biogenesis (RAB proteins, Hsp70, Hsp90), 3) intracellular proteins unique of cellular organelles and often absent in exosomes (calnexin, Golgi and ER proteins) and 4) extracellular proteins, such as acetylcholinesterase (ACHE). Moreover, membrane and cytoskeletal proteins, lysosomal markers enzymes, death receptors (FasL, TRAIL), cytokines, HLA class I and II proteins, and some HSPs can be also part of these vesicles (Choi D. , 2015). On the basis of this classification, when characterizing these particles, at least one protein of each category should be identified (Lotvall, 2014).

EVs lipid composition is the least known, mainly due to the few standardized isolation methods currently used, that have also caused some confusion in the scientific community in the interpretation of results. Moreover, exosomes seem to be more resistant to the use of

detergents than apoptotic bodies and microvesicles, thus complicating the interpretation of analysis (Osteikoetxea, 2015). However, despite these limitations, it is now known that EVs are mainly composed of sphyngolipids, phosphatidyl serine, cholesterol, saturated fatty acids and ceramide (Pfrieger, 2018) (Brouwers, 2013). Moreover, it has been shown that extracellular vesicles of different diameters are made up of different lipids, with exosomes having a higher lipid order than microvesicles or apoptotic bodies (Skotland, 2019).

Among all the few EVs lipidomic studies, exosomes seem to be the most analyzed class. Similarly to other vesicular components, the bilayer of these nano-vesicles is mainly constituted of membrane lipids similar to those of the cell plasma membrane from which they originate (Skotland, 2017). In addition, exosomal membranes may also reflect the asymmetric lipid organization of cell membrane lipids, with sphingolipids and phosphatidylcholines (PC) arranged in the outer leaflet, while the other lipid classes are mostly present in the inner leaflet. Overall, exosomes are rich in cholesteryl-esters (CE), triacylglycerols (TAG) and cardiolipins (Brouwers, 2013). However, these lipids seem also to be respectively present in the core of lipid droplets and in the inner membrane of mitochondria, suggesting that lipid droplets, lipoproteins or mitochondria may co-precipitate with exosomes (Yuana, 2014). Exosomes membranes may also contain cholesterol, sphingomyelins (SM), as well as ether lipids (mainly found as PC and PE), alkenyl-ethers (also called plasmalogens) (Lydic, 2015), glycosphingolipids and phosphatidylserine (PS) with levels 2-3 times more concentrated than in cells (Skotland, 2019). In contrast, phosphatidylethanolamines (PE), phosphatidylcolines and phosphatidylinositols (PI) are respectively present in similar (PE) and low concentrations than in their parent cells.

The biogenesis of extracellular vesicles is a mechanism that differs among various types of vesicles. For instance, secretion of apoptotic bodies (>800 nm) occurs during apoptosis, a process that cells use to discard undesired cells that can alter the physiological homeostasis (Fleisher, 1997). Apoptosis is mainly divided in three steps, which globally describe a process of blebbing and retraction of the cell membrane, with the final formation of membrane protrusions that regulate cell fragmentation and its release in the form of apoptotic bodies vesicles (Tixeira, 2017) (Coleman, 2001). The formation of membrane protrusions is of fundamental importance, since it serves for the detachment of blebs from the plasma membrane and the release of apoptotic vesicles (Atkin-Smith, 2015).

Apoptotic blebbing is monitored by multiple events (hydrostatic pressure, Actin-myosin contraction, microtubules) which promote the translocation of fluids and cell components into these new forming membrane blebs (Mills, 1998). Despite the mechanisms of apoptotic bodies formation are still not well understood, they seem to play an important role in the intercellular communication, since they transport specific biomolecules (such as proteins and microRNAs)

to neighboring cells (Brock, 2019); for instance, apoptotic bodies coming from cancerous processes can deliver altered molecules to other recipient cells, stimulating the proliferation of new cancer cells and the acceleration of metastatic processes (Bergsmedh, 2001).

Microvesicles, also known as shedding vesicles, microparticles, or ectosomes, are particles with a diameter range of 0.1–1 μm, originating from the plasma membrane of the cell through a process of outward budding (Tricarico, 2017). Specifically, the increase of intracellular Ca^{2+}, induced by an external signal, causes changes in the lipid distribution of the bilayer and the concomitant membrane blebbing, also due to the activity alteration of the phospholipid transportation enzymes flippases, translocases and scramblases (Willms, 2018). This increment stimulates the activation of cytosolic proteases (such as calpain and gelsolin), which re-organize the cytoskeleton (through the deconstruction of the actin cytoskeletal protein network) and cause the protrusion of the plasma membrane with consequent detachment of these vesicles (Turturici, 2014) (Cocucci, 2015).

Exosomes are the most studied vesicles, mostly defined by their size and their protein content, despite the fact that in literature the term "exosome" is improperly used to refer to small EVs (Wang, 2017). They are vesicles of 30-150 nm, forming through a well-organized process that starts with the invagination of the plasma membrane of the donor cell and the development of an endocytic pathway (Baietti, 2011).

Cell endocytosis is a molecular mechanism that develops during degradation, recycling, signaling, cytokinesis and migration processes (Besterman, 1983). First described in 1971 (Kerr, 1972), it occurs when plasma membrane introflects towards the center of the cell and forms small vesicles named as "endosomes" (Robinson, 1996). The most described endocytic process is the clathrin-dependent endocytosis (Richard, 2005), however other pathways exist and are classified through their plasma membrane-associated mediators (caveolin, flotillin, etc.) (Rejman, 2005) (Glebov, 2006). Endocytosis is mainly regulated through the ubiquitination mechanism, a three-step process that addresses ubiquitin molecules to target proteins across the activity of ubiquitin -activating, -conjugating and -ligating enzymes (E1,E2 and E3) (Migliano, 2018); nonetheless, endocytosis may be also develops from ubiquitin-independent pathways (Reggiori, 2001).

Endosomal maturation is a deeply regulated process, where proteins and lipids [Rab GTPases and phosphoinositides (PIP) respectively], work in harmony with the Endoplasmic Reticulum (ER) and the trans-Golgi network (TGN), providing enzymes and assisting the exchange of membrane components (Huotari, 2011). Endocytosis starts with the invagination of the plasma membrane and the formation of an endocytic vesicle, that come off the membrane and fuse with previously formed early endosomes (EE), stable structures of the cell that can also form through

the fusion of many endocytic vesicles (Jovic, 2010). At this point, the EE stops absorbing endocytic vesicles and mature into a sorting endosome, composed of two regions: tubular (responsible for the recycling of membrane components) and vacuolar (containing luminal cargo for degradation) (Kurten, 2001) (Pagano, 2004).

Cytoskeleton plays a pivotal role in this maturation process, since through the polymerization of actin it stimulates the movement of both nascent vesicles and early endosome (Oda, 1995); simultaneously, myosin VI guides the transfer of nascent vesicles from the actin-rich areas of the cell to the early endosome (Nielsen E. , 1999). Moreover, microtubules of the cytoskeleton support the interior structure of the endosome, serving as a substrate for the movement of this latter, thanks also to the activity of kinesins and dyneins molecules that enable the exchange of internalized material between compartments (Oda, 1995).

Once endosome matures, it converts into a late endosome (LE), carrying cargo that needs to be destroyed by the lysosomal system (Russell, 2006). The degradation of its vacuolar content starts with the development of intraluminal vesicles (ILVs), that form from the budding of membrane domains in the opposite direction of the tubular region of the early endosomes (EE) (Wenzel, 2018); these latter vesicles (ILVs) acquire late endosome (LE) characteristics and migrates towards the lysosome (in the perinuclear space) for their degradation.

Each step of this maturation is characterized by a distinct luminal pH (6.0–6.5 in EE, 5.0–5.5 in LEs, 4.5 in lysosomes), responsible for the conversion of the late endosome (LE) into a multivesicular body (MVB), as well as for the activation of degrading enzymes (Scott, 2011). The transition of the early endosome (EE) into a late endosome (LE) is also regulated by the interaction between Rabs proteins and Phosphatidylinositol lipids (Wandinger-Ness, 2014) (Fili, 2006).

Rab's proteins belong to a big family of GTPases, which play important roles in membrane organization and mainly serve as platforms for the selection of effector proteins (Stenmark, 2009). Phosphatidylinositols (PIPs) are another group of molecules involved in endosome maturation, from clathrin-coated vesicles (PI(4,5)P2 and PIP4P) to the transition of early-late endosome (EE-LE) (PI(3)P, PI(5)P and PI(3,5)P2) (Hasegawa, 2017) (Antonescu, 2011).

In the early endosome, Rab5 GTPase stimulates the fusion with endocytic and Golgi-derived vesicles (Nagano, 2019). This GTPase has three isoforms in mammalian cells, with Rab5a being the major species involved in the maturation of early endosomes (EE) to late endosomes (LE). During this transition, Rab5 is replaced by Rab7, another GTPase that mediates the fusion between the late endosome (LE) and lysosomes (Rink, 2005). Nonetheless, other Rabs proteins, such as Rab11 (Wilcke, 2000), Rab4 (D'Souza, 2014), and Rab22 (Kauppi, 2002), are also implicated in the recycling pathways of the early endosome.

Rab5 and PI(3)P levels increase at the early development process, dropping in later stages with the concomitant raise of Rab7 and PI(3,5)P2 levels, responsible for the formation of intraluminal vesicles (ILVs) (Rink, 2005). Rab5 inactivation is also accompanied by the reduction of ubiquitinated cargo (sequestered into intraluminal vesicles), the inactivation of Rab4 protein and the acidification of the endosomal pH through the activity of the V-ATPase vacuolar proton pump. In later stages, endosomes interact with the ER and the interaction exponentially expands as the endosome mature, with respectively 50% and 99% of early and late endosomes bound to the ER (Friedman, 2013). This contact between endosome-ER allows several maturation processes (e.g. cholesterol transportation, biogenesis of intraluminal vesicles and the association with the microtubules dynein and kinesin), playing also an important role in the storage of Ca^{2+} levels inside the endosome (provided from the ER storage). Ca^{2+} is an essential ion for the regulation of endosome maturation, since is needed for membrane anchoring and fusion (MacDonald, 2005). Endosome membrane seems also to be generated by lipid droplets that form transient contact sites with endosomes, furnishing membrane components that are used for the maturation of endosome (Liu, 2007). Once Multivesicular bodies (MVBs) are formed, the majority of them undergo lysosome degradation, whereas a few part escapes from this process to be released in the extracellular space as intercellular communicators (exosomes) (Podinovskaia, 2018).

The development of the multivesicular body (MVB) is regulated by the activity of the Endosomal Sorting Complexes Required for Transport (ESCRT) (Bache, 2003). This latter is a molecular machinery composed of a series of 4 protein complexes: ESCRT -0, -I, -II and -III. Working together, they package membrane proteins into ILVs which then convert into multivesicular bodies (MVBs). The first three groups of ESCRT are mainly involved in the binding of ubiquinated proteins on the surface of endosomes (thanks to the presence of specific ubiquitin binding domains), while ESCRT-III interacts primarily with intraluminal vesicles (ILVs) present within the lumen of endosomes. Once the Multivesicular body (MVB) mature, it can follow three fates: fuse with the lysosome causing intraluminal vesicles (ILVs) destruction by lysosomal enzymes (Schuh, 2014), be recycled back from the cell, or can be secreted in the extracellular space as exosomes (Podinovskaia, 2018) (Klumperman, 2014).

Therefore, exosomes are the secretion product of multivesicular bodies (MVBs), which form through an endocytosis of the plasma membrane that introflects into the internal part of the cell and creates an early endosome vesicle (EE), a membrane bounded compartment within the cell (Colombo, 2014). On the basis of the endocytic pathway, the inner budding of the membrane of the early endosome replaces the already existing endosomal luminal space with small intraluminal vesicles (ILVs), forming the multi-vescicular Body (MVB) or late endosome (LE),

filled with proteins, lipids and cytoplasm specifically sorted (Gutierrez-Vazquez, 2013). At this point the multi-vesicular body (MVB) merges with the plasma membrane and release its intraluminar vesicles in the extracellular space as “exosomes” (Hessvik, 2018).

As it happens in endocytic processes, the development of intraluminal vesicles (ILVs) and multivesicular bodies (MVBs) is a mechanism that requires the participation of the Endosomal Sorting Complex Required for Transport (Colombo M. , 2013). Here, ESCRT-0, a heterodimer formed by signal transducing adaptor molecule-STAM and hepatocyte growth factor-regulated tyrosine kinase substrate-HRS molecules, recognizes and sequestrates ubiquitinated trans-membrane proteins into the endosomal membrane and, thanks to the cooperation with phosphatidil inositol-3-phospate (PI(3)P), starts their sorting whitin the multivesicular body (MVB) by recruiting ESCRT-I through the activity of tumor susceptibility gene 101-TSG101 protein (Kojima, 2014). ESCRT-I, instead, is composed of several proteins: vacuolar sorting proteins (VPS), multivesicular body (MVB), ubiquitin associated (UBAP) and the tumor susceptibility gene 101 (TSG101); together with ESCRT-II, it is responsible for the deflection of the membrane of multivesicular bodies, which stretches into buds with specific cargo and forms a sort of vesicle neck; the last complex, ESCRT-III, mainly composed of charged multivesicular body proteins-CHMP, is implicated in the detachment of the formed vesicle and the development of intraluminal vesicles (ILVs). Once formed, ESCRT-III binds Vps4 ATPase for its disassembly (Hanson, 2012).

The development of exosomes is controlled by several components such as syndecans (Baietti, 2011), heparan sulphate (Roucourt, 2015) and syntenin (Friand, 2015). This latter interacts with the auxiliary protein of the ESCRT complex ALIX (also known as PDCD6IP) and assists the invagination of endosomal membranes. ALIX and syntenin are two of the 20 most frequently proteins identified in exosomes, generating a distinctive class of vesicles (flotillin-1-negative) (Baietti, 2011). The presence of all these molecules is very important for the biogenesis of exosomes; for instance, the over expression of syntenin increases the levels of exosomal syndecans, ALIX and other exosomal markers (i.e. CD63 and HSP70), also providing heparan sulphate molecules that are important for many of the signalling events occurring at the cell surfaces during the biogenesis of intraluminal vesicles (ILVs) and exosomes (Fares, 2017). It also collaborates with the small GTPase ADP-Ribosylation Factor 6 (ARF6), located on cell membranes and endosomes, and is involved in various cellular mechanisms (membrane transport, vesicular traffic and membrane remodeling), by controlling the actin cytoskeleton and the metabolism of phosphoinositides (Ghossoub, 2014). ARF6 is extremely important for the development of exosomes, especially at the stage of intraluminal vesicles (ILVs), and its inhactivation causes a considerable decrease in exosomal proteins (Hessvik, 2018).

Various populations of ILVs, with different lipids and cargo, can co-habit and form within MVBs, and can be distinguished based on their size and their mechanism of formation. However, their mechanisms of formation and sorting still remain partially understood, with the complex ESCRT process the best described so far; nonetheless, some other ESCRT-independent pathways have also been identified and might coexist with ESCRT-dependent machinery, thus confirming the presence of different multi-vesicular bodies (MVBs) sub-populations (Babst, 2011).

Despite the mechanism of exosomes secretion is still not well understood, its release might occurs through the remodeling of the cytoskeleton, further controlled by the increase of internal Ca^{2+} and phospholipase D (PLD2) (Laulagnier, 2004). Once in the extracellular space, these vesicles can be either internalized by receiving cells, or they can act as transmembrane signals by binding receptors on the plasma membrane of the cells (Mulcahy, 2014) (Feng, 2010). Indeed, endocytosis is also the mechanism used from EVs during their internalization in receiving cells; however, it has been recently proposed that their uptake could also occur through a mechanism of "passive endocytosis", which appears during the natural recycling of the plasma membrane of the cells and could passively drag exosomes attached to the surface of a cell.

1.4 Methods of isolation and characterization of extracellular vesicles

Currently, characterization of EVs is a combination of several methods that include: microscopy (TEM, SEM, CrioTEM), Western Blot, -omics analysis (proteomic, lipidomic, metabolomic), dynamic light scattering techniques (Nanoparticle Tracking Analysis-NTA and Zetasizer), Tunable Resistive Pulse Sensing (TRPS), as well as immunohistochemical and flow cytometry analysis of specific EVs markers, used to describe their morphology, biochemical composition and receptors localized on their membranes (Momen-Heravi, 2012) (**Table 2**). However, one of the main issue when purifying these particles is that, currently, there is no consensus for a unique standard isolation protocol (Szatanek, 2015).

Ideally, the method used for their isolation should be simple, fast and inexpensive. Overall, three main methodologies are currently used for their isolation: 1) differential centrifugation coupled to ultracentrifugation with, or without, a sucrose gradient/cushion (Iwai, 2016), 2) adsorption to magnetic/non-magnetic micro-beads (Koliha, 2016) and 3) size exclusion chromatography (Nordin, 2015). Each method has its own advantages and disadvantages, and the choice of one rather than another can result in different EV subpopulations with different properties (Davis, 2019). Therefore, at the moment there is no single standardized method for

the isolation of EVs, which could be also able to minimize co-isolating protein aggregates and other membranous particles from a sample of EVs.

Table 2 - *Most common EV isolation and characterization methods*

Isolation	References	Characterization	References
Ultracentrifugation Density gradient	(Théry, 2006) (Zhang Z. , 2014)	Electron Microscopy: TEM; SEM; cryo-EM;	(Escola, 1998) (Sokolova, 2011) (Poliakov, 2009)
Size Exclusion Chromatography (SEC)	(Böing, 2014)	Dinamic Light Scattering (DLS); Nanoparticle Tracking Analysis (NTA); Tunable Resistive Pulse Sensing (TRPS)	(Kesimer, 2015) (Gercel-Taylor, 2012) (Maas, 2014)
Immunological separation: Magnetic beads; ELISA exoTEST	(Pedersen, 2017) (Logozzi, 2009)	Biochemical analysis (Western Blot)	(Théry, 2018)
Polymer-based precipitation	(Brown P. , 2017)	Flow cytometry	(Pospichalova, 2015)
Flow-field fractionation	(Sitar, 2015)	-omics analysis: Proteomic; Lipidomic;	(Schey, 2015) (Haraszti, 2016)
Commercial Kits ExoQuick Total Exosomes Isolation (TEI) Exo-Spin (ExoS)	(Ding, 2018)		
Filtration Stirred Cell Tangential Flow Filtration	(Busatto, 2018)		
PEG based	(Lv, 2018)		

As already mentioned, currently the gold standard method for vesicles preparation is differential centrifugation/ultracentrifugation coupled with sucrose/iodixanol density gradient (Gupta S. , 2018), and EVs obtained from this technology have been classified into: (1) large EVs, pelleted at low speed, (2) medium-sized EVs, pelleted at intermediate speed and (3) small EVs (sEVs), pelleted at high speed. This latter were further divided into four sub-categories:

(1) sEVs rich in tetraspanines CD63, CD9 and CD81 and endosomal markers (better known as exosomes); (2) sEVs without CD63 and CD81, but rich in CD9; (3) sEVs without CD63/CD9/CD81; (4) sEVs rich in extracellular matrix or serum factors. The last two-listed sEV are not associated with exosomes (Kowal, 2016).

In order to compare different isolation methods, several researchers have isolated EVs using 4 of the most common methods (ultracentrifugation, density gradient, exo-kit and total exosome isolation) for the evaluation of yield, size, morphology, protein and RNA content of vesicles (Van Deun, 2014). They demonstrated that density gradient ultracentrifugation gave the purest exosome preparations as respect to the other three techniques which have also co-isolated contaminating factors. Skottvoll et al. evaluated the performance of different isolation methods based on differential ultracentrifugation and a commercial isolation kit (total exosome isolation reagent), demonstrating that the two isolation methods had similar performance with only some differences based on the origin of the cell (Skottvoll, 2019).

In another study, size-exclusion chromatography (SEC) was suggested as capable of eliminating most of the abundant proteins contained in body fluids, also maintaining the vesicular structure and conformation of EVs, thus making this procedure ideal for biomarker discovery, as well as for therapeutic applications (Gamez-Valero, 2016). These data were also confirmed by another research group, which showed that ultrafiltration followed by size exclusion chromatography (UF-SEC) provides well-concentrated EVs for proteomic and functional analysis (Benedikter, 2017). Thanks to its efficient capability to separate EVs from contaminant proteins (especially from large initial volumes), UF-SEC seemed to give a higher yield of pure vesicles if compared to those isolated by simple ultracentrifugation (Nordin, 2015).

Despite the wide range of isolation methods currently available, the scientific community is still arguing about the choice of the best protocol to use, since each of them may be suitable for the analysis of one type of sample, rather than another (Szatanek, 2015). Hence, in absence of a precise standardization, the choice of the isolation method should follow the characteristics of the sample that have to be analyzed.

1.5 Extracellular vesicles in health

Extracellular vesicles are components of cell-to-cell communication, leading physiological and pathological processes in all living organisms, from Prokaryotes to Eukaryotes (Yuana, 2013) (Turturici, 2014) (Soekmadji, 2019) (**Figure 3**).

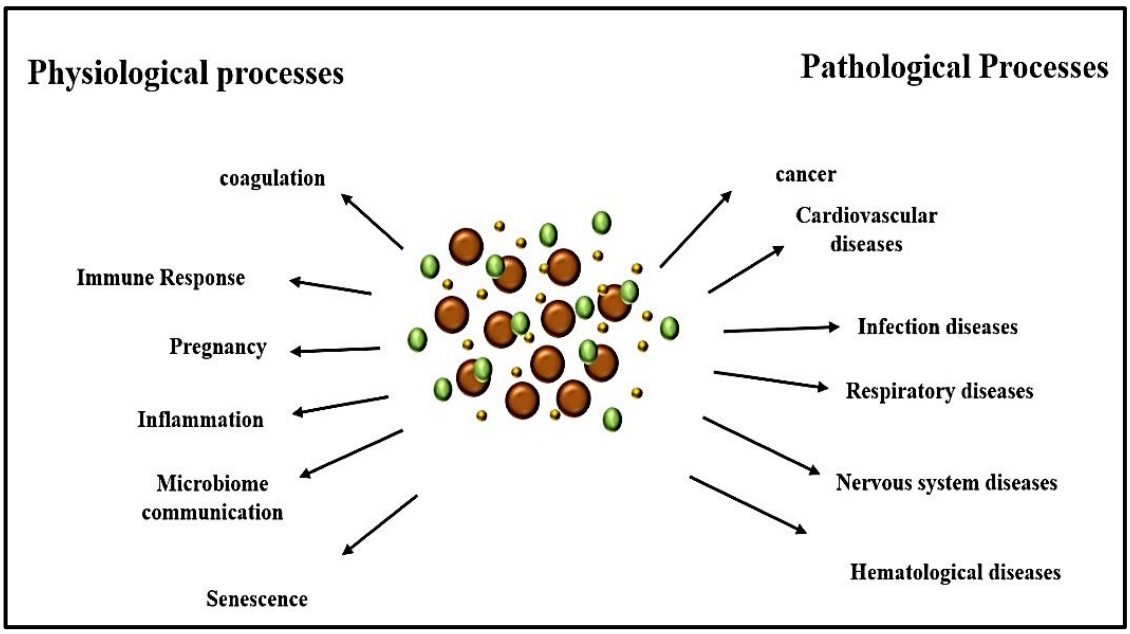

Figure 3 - *Extracellular vesicles in health and diseases*

For instance, Bacteria release small EVs particles from both Gram-negative (known as outer membrane vesicles -OMVs-) and Gram-positive bacteria, during microbiome communication processes (Kulp, 2010) (Lee, 2009). Under physiological conditions, these vesicles are primarily involved in the maintenance of bacterial homeostasis of parent and other bacteria cells (Kang, 2013), transporting nutrients, antimicrobial resistance factors (Lee J. , 2013) and suppressing toxic, or altered, proteins from the cellular environment (Vorkapic, 2016). For instance, commensal Bacteria release a specific type of vesicles implicated in the protection of the host organism against potential inflammatory bowel diseases (Li M. , 2017). Moreover, they can also promote the growth of peculiar species in specific intestinal environments, in order to facilitate bacterial communication. Thanks to these unique features, bacteria EVs could be thought as promising tools for the developments of therapeutic products, such as vaccines (Gnopo, 2017) (Stevenson, 2018).

Similarly to Prokaryotes, Eukaryote EVs also play an important role in several physiological processes such as: coagulation (Berckmans, 2001), pregnancy (Salomon, 2014), metabolism (Tramontano, 2010), immunity (Groot Kormelink, 2018) and apoptosis (Bergsmedh, 2001).

Coagulation is a natural physiological mechanism that occurs during the repair of a wound, in which blood consistency changes from liquid into a sort of gel, thus allowing the closure of the wound and the end of bleeding (process called hemostasis) (Bloom, 1990). Briefly, if a wound occurs, the integral protein membrane tissue factor (TF) rushes to the damaged site and binds with coagulation factors VII and X, promoting the production of thrombine and the conversion of the soluble fibrinogen into the insoluble fibrin, with the formation of a thrombus (Rock,

1997). Coagulation factors need a phospholipid membrane to which they can bind, normally represented by phosphatidyl serine and negative charged phospholipids (Lentz, 2003). Hence, platelet-derived EVs, together with the presence of ion Ca^{2+}, assist the binding of coagulation factors (e.g. tannins complex and the prothrombin complex) through the exhibition of a phospholipid surface, mainly made of phosphatidylserine (Chargaff, 1946) (Tripisciano, 2017) (Müller, 2003).

EVs are also well known in several immunomodulatory processes; indeed, all cells of the immune system are able to collect EVs-signals from non-immune cells (e.g. microbes, tumor cells, etc.), that are then converted and packed into vesicles, allowing the communication among immune system cells (Fernández-Messina, 2015). Therefore, immune cells can, themselves, secrete EVs carrying signals to other cells (Groot Kormelink, 2018) which can participate in various immune regulatory functions (such as immunosuppression and immune activation). For instance, neutrophil-EVs control anti-inflammatory and pro-thrombotic events (Dalli, 2008), while natural killer cells (NK) secrete EVs with specific NK cell markers (FasL and perforin) (Wu, 2019); in addition, monocytes- and macrophages- EVs are implicated in several processes that include antigen presentation, myeloid cell proliferation and differentiation (Garzetti, 2014), while mast cell and dendritic cell derived EVs enhance the proliferation of T- and B- cells, acting also as a reservoir for different immune modulatory proteins involved in antigen presentation (Kim D. , 2018).

In lungs, bronchial epithelial cells-EVs are involved in the regulation of communication among respiratory cells (Kesimer, 2015). Similarly, alveolar macrophage-EVs supervise cellular homeostasis, and the inflammatory signaling, by transferring suppressor cytokines to lung epithelial cells, while epithelial-EVs regulate the innate immunity in the airway, equilibrating lung interactions between epithelial and mesenchymal cells (Schneider, 2017) (Kesimer, 2009).

In stress conditions (e.g. ionizing radiations, osmotic alterations, hypoxia, temperature variations, presence of toxins and infections) (Diaz-Hidalgo, 2016), EVs act as messengers of stress response with close and distant cells (Bewicke-Copley, 2017). Stress events affect not only the amount of secreted EVs, but also their molecular composition, resulting in altered vesicles that can be used as a fount of biomarkers in several diseases (Boukouris, 2015). Indeed, they might act as reservoirs of dangerous molecules (e.g. unfolded proteins, mutated DNA or pathogens), that could modify cell physiology and thus need to be eliminated through normal clearance (Sproviero, 2018) (Cai, 2013). For instance, it seems that the release of endothelial-EVs carrying high levels of caspase-3, an enzyme implicated in programmed death cell, may contribute in the cellular homeostasis, avoiding its aberrant increase inside the cells (Abid Hussein, 2005). In another example, it has been proposed that, when normal activity of the

endoplasmic reticulum fails, due to stress events, cell release stressed EVs that trap damaged/unfolded proteins inside their lumen, in order to preserve the endoplasmic reticulum homeostasis and cell vitality (Diaz-Hidalgo, 2016). Another interpretation of "stressed"-EVs describes these vesicles as sort of alarm bells that warn cells, and the immune system, of possible dangers caused by stressed events (Marcilla, 2014) (Mitsuhashi, 2016). For instance, cells of the immune system may be activated through the interaction with EVs carrying major histocompatibility complex (MHC-complexes), thus taking part to the antigen presentation process to inform cells about stress factors (Kleijmeer, 2001). Moreover, it was also proven that during oxidative stress cells secrete EVs rich in specific RNAs, able to act as messengers in the preservation of receiving cells from oxidative damages (Eldh, 2010).

EVs also regulate the communication among cells of the nervous system. It is now known that neurons secrete EVs able to interact with both neurons and glia cells, and are probably involved in processes of neuronal electrical activity (Frühbeis, 2013). Neuronal communication through EVs is regulated and combined to the neuronal electrical activity and the neurotransmitter signaling, suggesting that brain activity triggers EVs signaling (Borroto-Escuela, 2015). Neural-EVs not only regulate the homeostasis of the central nervous system, helping the plasticity of neural signaling processes, but they also enhance neuronal maintenance and regeneration through the passage of information between the brain and the periphery (Lopez-Verrilli, 2013) (Pegtel, 2014).

Under physiological condition, neuronal-EVs are mainly involved in the regulation of homeostasis and in those mechanisms of plasticity of the nervous system (Chivet, 2012). For instance, oligodendrocytes accumulate high levels of EVs close to the axon, that are then subsequently secreted under the neurotransmitter glutamate signal, this latter released by neurons cells as a consequence of their electrical activity (Frühbeis, 2019) (Frühbeis, 2013). Once in the extracellular space, they are normally internalized by endocytosis from the majority of neuronal cells and absorbed by macropinocytosis in the case of microglial cells (Fitzner, 2011). Oligodendroglial-EVs play important roles in maintaining neuronal homeostasis and regulating neuroprotection during stress conditions (e.g. oxidative stress or nutrient deprivation) (Pegtel, 2014). Similarly, astrocytes secrete different types of EVs, mainly composed of small and large EVs, that seem to be implicated in neuroprotection and in the modulation of inflammatory events of the central nervous system (CNS) (Pascua-Maestro, 2018). Even microglia cells release EVs, which regulate synaptic transmission during excitatory mechanisms, neuro-inflammation processes (Yang Y. , 2018), in the clearance of dangerous or unwanted cellular molecules (Antonucci, 2012), as well as the delivery of endocannabinoids,

molecules responsible for the alteration of the neurotransmission in inhibitory neurons (Lemaire, 2019).

High concentrations of EVs have also been found during senescence pathways. Generally, upon senescence cells undergo a series of modifications that end with their inability to continue proliferative processes, as well as irreversible morphological alterations that convert cells into flat and hypertrophic units (Ohtani, 2013). EVs originating from this type of cells carry different molecules with a modified profile (e.g. genomic DNA fragments), which can take part to many mechanisms like DNA damage activation, tumor progression (in the involved area) and immune cell activation (Xu, 2013).

EVs have also been described in reproductive processes. For instance, EVs isolated from reproductive tracts of both female and man transport messages involved in female reproduction, sperm activity and modulation of female immune response (Almiñana, 2020). Male EVs are implicated in several pathways that include sperm maturation (Nixon, 2019), protection from female immune response, sperm motility and acrosome reaction (Sullivan, 2016). Female EVs are of such importance during reproduction and pregnancy processes, monitoring the maturation of the follicle, as well as in the communication with the embryo (Machtinger, 2016).

Recent studies have demonstrated that, during fertilization, oolemma EVs are directly involved in the interaction between sperm and oolemma (IZUMO1-JUNO), since they carry Juno receptor on their membranes, a molecule responsible for the block of polyspermy. (Bianchi, 2014). In pregnancy, EVs translocate in the uterine tissue for its remodeling, preparing the reproductive tract for the implantation of the embryo (Yang, 2019); their presence persists for the whole period of maternal pregnancy, with higher levels of EVs rich in CD9 and CD63 tetraspanins during early stages of pregnancy, serving as important messengers for the communication between the placenta and the mother (Mellisho, 2017). Among all the placenta derived EVs, those coming from the synctiotrophonblast (STB), the epithelium lining the placenta that provides nutrients circulation between the embryo and the mother, are the most representative (Mincheva-Nilsson, 2014). In normal pregnancy, cells of the synctiotrophonblast secrete extracellular vesicles (called STBEVs) implicated in the down regulation of the innate immune system, also promoting the release of pro-inflammatory cytokines from peripheral blood (Gupta, 2004).

1.6 Extracellular vesicles in diseases

The role of EVs in the development of various pathological conditions has aroused a lot of interest in the recent years, demonstrating their active involvement in several diseases (Ciregia, 2017) (Gao, 2017).

For instance, EVs of Gram-negative and Gram-positive bacteria are involved in many pathophysiological functions, such as bacteria-bacteria (Soler, 2008) and bacteria-host interactions (Bitto, 2017). Bacteria-bacteria interactions are important for antibiotic resistance, bacterial survival and the death of other competitors bacteria (Mashburn-Warren, 2008), while bacteria-host interactions regulate the transmission of virulence factors, as well as processes of bacteria adhesion, invasion and elusion of the host immune system (Bielaszewska, 2017). During bacterial infections, host neutrophil cells produce vesicles able to aggregate around bacteria, causing a reduction in its growth (Timár, 2013). Immune cells can be further activated through the presence of vesicles derived from infected cell, which deliver microbial and viral molecules to antigen presenting cells (Veerman, 2019) (O'Neill, 2008). Moreover, immune-EVs may be implicated in chronic inflammations (such as allergy) and auto-immune diseases (i.e. rheumatoid arthritis), enclosing multiple auto-antigens that can be presented and delivered across EVs, thus causing the beginning of auto immune responses (Wu G. , 2015) (Knijff-Dutmer, 2002).

In pathogenic infection diseases, EVs act as extracellular signals that help the survival of pathogens among inhospitable cellular environments (rendered hostile through the activation of the immune system of the host), through the manipulation of the host responses and the communication with other pathogens (or host cells) during differentiation, transmission, growth and virulence coordination processes (Marcilla, 2014) (Ofir-Birin, 2017) (Rodrigues, 2018). For instance, in cerebral malaria, the presence of Plasmodium falciparum parasite is responsible for an increase of circulating EVs in infected patients, which travel the endothelium of brain infected vessels altering their activity and characteristics (Pierre-Yves, 2014) (Sampaio, 2018).

Enveloped viruses may be considered as another kind of pathogenic EVs, since they are a specific type of nanovesicles, arising from host cells, that use cellular components not only for the duplication of their viral genome, but also for the transport of cellular molecules inside their lumen (Sun, 2006). One example are HIV virions, small vesicles similar to several circulating EVs, which originate from endosomic vesicles (or cholesterol rich domains) of the host membrane through an endocytic pathway, carrying host proteins on their surfaces (Briggs, 2003). They are able to encode proteins present in the plasma membrane of the host cell that allow viruses to co-operate and fuse with the host cell target, infecting this latter with their viral units that will be subsequently released in the extracellular space, eluding the immune system of the host (Vazirabadi, 2003) (Altan-Bonnet, 2016). Of interest, viruses may infect host cells by delivering their genome molecules directly inside extracellular vesicles, without the necessity to use the entire virion (Kouwaki, 2017).

EVs have also been isolated from different fungal species, especially in many human pathogens, where they work as messengers for the communication between both host-fungal and fungal-fungal cells during the modulation of the pathogenesis (Joffe, 2016). These type of vesicles are similar to those of the host cells but, unlike mammalian cells, fungal EVs must cross the cell wall in order to be released in the extracellular space; therefore, some of them may get trapped in this compartment, contributing to the remodeling of the cell wall and serving as surface components (de Toledo, 2019) (Rodrigues M. , 2013).

Mammalian EVs are involved in the regulation of different diseases mechanisms, such as: coagulation, immunity, metabolomic alterations, cancer, etc.

In pathogenic coagulation, EVs vesicles regulate the activation and migration of platelets at a site of the local damage, causing an increase of the levels of different coagulation factors responsible for the formation of plaques that clog the vessels and cause the formation of defective thrombi (Bick, 1992) (Zwicker, 2008). For instance, in cancer-related coagulation processes, circulating tumor EVs are highly concentrated and serve as a reservoir system for the transport of the tissue factor molecule (Thomas, 2009).

Another important role of EVs has been also shown in several metabolic processes (Göran Ronquist, 2019) (Kobayashi, 2018), affecting serum metabolome modifications in different areas of the organism (Royo, 2017). For example, it has been demonstrated that high levels of EVs rich in arginase are involved in the conversion of arginine into ornithine, causing consequent anomalies in processes of vascularization, neuronal toxicity and cancer (Caldwell, 2018). Arginine is an important amino acid, necessary for its conversion into nitric oxide (NO) during normal processes of vasodilation blood vessels. However, if metabolic alterations occurs, circulating EVs cause a reduction of nitric oxide (NO) in favor of an increase of reactive oxygen species within the endothelial cells, thus resulting in endothelial dysfunctions and consequent development of pathological conditions (Bode-Böger, 1998). One of the most representative donors of arginase-EVs are hepatocytes and their levels may strongly increase after liver damage (Royo, 2017) (Eguchi, 2019).

However, these alterations are not limited to the activity of the only liver, but also stem cells, platelets, red blood cells and endothelial cells can release enzymes within EVs that may increase the risk of pathological conditions (e.g. high blood pressure, elevated glucose and triglyceride levels) and dangerous diseases (e.g. type 2 diabetes, dyslipidemia, obesity) (Iraci, 2017) (Lakhter, 2015) (Santamaria-Martos, 2019) (Freeman, 2018).

In the adipose tissue, high levels of EVs may be responsible for different pathological conditions (i.e. insulin resistance and secretion of pro-inflammatory adipokines) and chronic inflammations (Eguchi, 2016). In a diet rich of calories and fats white adipose tissue expand

while oxygen levels decrease, causing a hypoxic environment within the tissue; at the same time, cell macrophages migrate in the tissue secreting pro-inflammatory cytokines and, as a result, adipocytes release compromise EVs that might have effects on other cells and tissues (Maëva, 2017).

Metabolic alterations may also be caused by the activity of the intestinal microbiota. This latter releases outer membrane vesicles (OMVs) that, in normal conditions, maintain gut barrier integrity; however, if alterations in the microbiota occurs, epithelium become more vulnerable and OMVs may migrate from the intestinal barriers to the bloodstream of the host, facilitating the development of inflammatory processes (Jun, 2013) (Ahmadi Badi, 2017).

In pregnancy, circulating EVs can be used as a promising tool for the monitoring of pregnancy disorders caused by placenta dysfunctions such as pre-eclampsia, a severe and dangerous human syndrome that provokes hypertension and proteinuria in the second half of pregnancy, degenerating in maternal mortality. (Han, 2019). Before the development of the syndrome, the placenta undergo a series of modifications, which are also reflected in the number and phenotype of EVs released in maternal circulation (Gill, 2019).

In cancer progression, EVs are implicated in several features of the pathology, especially in the activation of aberrant proliferative and suppressor pathways (Minciacchi, 2015) (Tominaga, 2015). Tumor EVs carry specific molecules that may be taken up by other cells and alter the expression of pro- and anti- proliferation genes (Lunavat, 2015). For instance, they are able to transport specific altered nucleic acids (miRNA and DNA) to recipient cells, provoking morphological changes that may also stimulate the development of new malignant foci (Huber, 2018) (Vagner, 2018).

Tumor micro-environment is a complex dynamic system, made up of several cells (e.g. cancerous cells, fibroblasts, endothelial cells, adipocytes and immune cells) who coexist in the same environment under the regulation of soluble growth factors and other molecules of the extracellular matrix (Hirata, 2017). EVs take part in the modulation of the tumor micro environment, carrying altered molecules that can modify the physiology of the surroundings, increasing tumor growth (Choi, 2014).

Interactions among EVs, cancer cells and the surrounding micro-environment may occurs in several ways: by directly binding the cellular surface of the cell (via the interaction between ligand-membrane receptors), through the release of their luminal content near the target cells, or by simply merging with the plasma membrane of the cells (partially or totally endocytosed) and delivering their cargo within the lumen of the recipient cell (Mulcahy, 2014).

Through these interactions, cancer-EVs may transfer their metastatic phenotype to different cells, influencing their fate. For instance, cancer EVs carry glycolytic enzymes and metabolites

that may provoke a series of endothelial cell alterations, modifying the metabolic activity of cells and enhancing the development of a pro-metastatic micro-environment (Lawson, 2017) (Puhka, 2017). Cancer EVs may also affect the proliferative capacity of donor cells in an autocrine manner, through the interaction with their own plasma membrane (Raimondo, 2015). Cancer-EVs also regulate tumor angiogenesis processes (an essential pathway for tumor growth), controlling the formation of new blood vessels and delivering growth factors and cargo to the cells (Perut, 2019). Tumor micro-environment is highly hypoxic, due to the excessive consumption of glucose by tumor cells (Koukourakis, 2006); under these conditions, levels of alterated EVs increase (as compared to EVs released from normoxic cells) and carry mRNA and microRNA transcripts involved in pro-angiogenesis processess (van der Vos, 2016) (Patton, 2020). Therefore, as a consequence of excessive hypoxia, cancer-EVs stimulate the production of new vessels that will positively affect tumor growth (Ko, 2019). However, tumor angiogenesis may also occur indirectly, through the interaction of EVs with other cells (i.e. fibroblasts), causing the secretion of several pro-angiogenic factors that guide endothelial cells migration and vessels formation (Ko, 2019).

Cancer-EVs are also implicated in the development of cancer-related thrombi (Gheldof, 2017), where they carry coagulant proteins (i.e. tissue factor -TF-) that interact with other clotting factors within the blood and cause the development of a thrombus (Hisada, 2019) (P. Y. Che, 2017).

However, among all these activities, one of the main roles of cancer-EVs occurs during mechanisms of tumor invasion and metastasis (Endzeliņš, 2018). During these processes, cells have to colonize new different cellular sites through a series of events (e.g. disruption of the cellular matrix and interaction with endothelial cells) that end with the passage of cells into the circulation (bloodstream or lymph) and the colonization of a new distinct site (Gkretsi, 2018). The rupture of the extracellular matrix may be also promoted by the activity of metastatic EVs that, thanks to the presence of surface integrins and metalloproteinases, interact with the extracellular matrix and guide the migration of other EVs through this latter (Nawaz, 2018). Metastasization may be also stimulated through the communication between EVs and stromal cells, by the regulation of inflammation processes that increase tumor malignancy and growth (Gener Lahav, 2019). For instance, tumor derived-EVs are able to acquire features similar to those of cancer fibroblasts (the principal cell type within the microenvironment of solid tumors), which can then regulate the activation of these stromal cells for the release of stromal-EVs into the microenvironment, thus contributing in the development of tumor fibroblasts (Vu, 2019). EVs play an important role in the communication between cancer cells and the surrounding stroma, being rich in extracellular matrix components (e.g. heparan sulfate

and proteoglycans) that are essential for the interaction with the extracellular matrix and cells (Cerezo-Magaña, 2019).

Therefore, EVs act as intercellular communicators between tumor cells and distant organs during metastatic colonization; for instance, some kind of metastatic cells preferably colonize precise organs (lung, liver, brain) releasing EVs that, through the blood, migrate to these new sites and prepare them to the metastatic colonization (Valencia, 2014). This is also possible because during tumor growth, the newly formed blood vessels have a weak structural organization, letting cancer cells enter into the circulation for the colonization of distant areas of the body (Nishida, 2006). During these steps, EVs promote cellular proliferation by transferring specific cargoes that may enhance the expression (or mutation) of oncogenes, as well as activate intracellular signaling pathways, or inhibit negative feedback mechanisms (Maacha, 2019) (Ji, 2020).

Metastatization may be also caused by the treatment of tumors with specific chemotherapy drugs that may affect the activity of cancer EVs. For instance, after these treatments, EVs released by cancer cells may deliver resistance proteins and nucleic acids that stimulate the development of a multi-drug resistance phenotype (MDR) in tumor cells (Lopes-Rodrigues, 2017) (Kaye, 1988). According to this hypothesis, it has been shown that cells treated with different type of therapies (e.g. ionizing radiation and chemo-therapeutics), secrete vesicles that may interact with distant cells and provoke stress response or proliferative processes (Kim M. , 2016) (O'Neill C. , 2019). The onset of chemoresistance may be explained by the fact that tumor cells absorb the drug in their cytoplasm and pack it within EVs that are then expelled in the extracellular space (Sousa, 2015). Another reason could be that EVs block cancer toxin drugs through the exposition of specific antigens that are targeted by specific antibodies (Markov, 2019).

Cancer EVs play also an important role during immune evasion, impacting the activity of immune system cells (e.g. NK- and T- cells) and inhibiting their natural functions of killing tumor cells (Ricklefs, 2018) (Abramowicz, 2019). It seems that they regulate the interaction between tumor cells and immune system (Menay, 2017), promoting many pro- and anti-tumoral effects, such as the immunosuppression of dendritic and T-cells, or the decrease of cytotoxicity of NK-cells (Al-Samadi, 2017). Unlike to all these pro-tumor processes, cancer-EVs can also exert anti-tumor effects, acting as antigen vesicles that promote anti-tumor immune responses and activate dendritic, NKs- and macrophages cells (Zhang B. , 2014). For instance, once dendritic cells have absorbed tumor cells and tumor antigens, they release EVs loaded with those antigens that may positively increase immune responses (Zeng, 2018).

Several studies have been performed to modulate cancer EVs secretion *in vivo*, which mainly focused on the activity of small GTPases, molecules involved in the secretion of EVs. For instance, it was demonstrated that the inhibition of RAB27A, or RAB35, reduced the secretion of EVs (especially exosomes) in several tumors (Li W. , 2014) (Yang L. , 2019).

The role of circulating EVs has been also investigated in some cardiovascular diseases. Under physiological conditions endothelial cells, platelets and leukocytes release EVs in the bloody stream (Hutcheson, 2018) (Brahmer, 2019), but their plasma levels increase in subjects with cardiovascular diseases, or with some cardiovascular risk factors, such as: hypertension (Kosanovic, 2019), smoking (Serban, 2016), hypercholesterolemia (Nielsen M. , 2015) and diabetes (Jia, 2016). For instance, it has been shown that circulating levels of leukocyte derived EVs associate with atherosclerotic plaques and can be responsible for some endothelial disorders in patients with coronary diseases (Schiro, 2015). Similarly, plasma levels of platelet EVs seem to intensify in patients with cardiovascular risks, being involved in deleterious effects (e.g. thrombosis) (Bank, 2015). Atherosclerotic EVs accumulate in atherosclerotic lesions expressing specific ligands at their surface (i.e. CD40), which are responsible for plaque progression and thrombi formation (Chistiakov, 2015). Circulating EVs arising from myocardial infarction affect the vascular structure, by altering the release of endothelial nitric oxide (NO) and increasing the expression of tissue factor (TF) and endothelial apoptotic processes (Amabile, 2005) (Boulanger, 2001).

These vesicles can cause both inflammatory and anti-inflammatory effects, stimulating the increase of pro-inflammatory cytokines (e.g. IL-6 and IL-8) from endothelial cells and leukocytes, thus promoting the adhesion of monocytes to the endothelium and its migration through the plaques (Beez, 2019). Endothelial and platelet derived EVs may also encourage endothelial permeability through the delivery of specific apoptotic enzymes within their lumen (i.e. caspase-3), increasing apoptotic processes and enhancing leukocyte adhesion to the endothelial cells (Boulanger, 2017). Similarly, plasma vesicles could also support the adhesion of inflammatory cells to the endothelium, enhancing not only the expression of adhesion molecules (i.e. ICAM-1) and receptors on the surface of monocytes, but also delivering pro-atherogenic chemokines from platelet EVs to the endothelial cells (Boulanger, 2017).

In smooth muscle, EVs may cause arterial micro-calcification (Nik, 2017) and the formation of atherosclerotic plaques (Goettsch, 2016), while cardiomyocytes and other cardiac cells of the heart produce EVs that may be responsible for some hypoxia injuries through the transmission of hypoxic signals to normoxic cardiomyocytes (Yarana, 2018). Cardiomyocytes-EVs can also deliver molecules with glycolytic activity to endothelial cells, exerting

controversial effects that can either stimulate angiogenesis or pro-inflammatory responses in myocardial infaction (Garcia, 2016) (Ribeiro-Rodrigues, 2017).

Another interesting role of pathogenic EVs has been shown on respiratory cells; here, EVs originating during stress events (e.g. cigarette smoke) carry a different cargo that alter cellular homeostasis and may damage lung epithelial and endothelial cells, provoking potential chronic obstructive pulmonary diseases (Benedikter, 2017) (Benedikter, 2019).

EVs may be also implicated in some blood diseases (Tissot J. , 2013). For instance, platelets (Aatonen, 2014), erythrocytes (Nguyen, 2016), leukocytes (Pugholm, 2016), endothelial cells (Cantaluppi, 2015), as well as tissues or organs (i.e. tumor cells), may release altered EVs that can provoke some blood related pathologies (Nomura, 2017).

Platelet-EVs (PEVs), the main type of blood circulating EVs, play several roles in the activation of the immune system through the interaction with leukocytes cells (Weiss, 2018), in atherosclerotic lesions formation (Suades, 2015), in coagulation processes (Suades, 2012) (Zhao, 2016), as well as in inflammation events (Badimon, 2016). Their activity is of such importance and, a reduction of their levels, may be responsible for impaired pro-coagulant and coagulation functions. Beyond platelet-EVs, other circulating blood EVs are involved in pro-coagulant activities, carrying specific molecules on their membranes (e.g. phosphatidylserine and the tissue factor) extremely important during coagulation mechanisms (Del Conde, 2005) (Lentz, 2003). EVs-coagulant function may depends on the presence of these molecules, as microvesicles negative for both of molecules could exert poor pro-coagulant activity, while those expressing one, or both type of molecules are moderate and highly pro-coagulants respectively.

Of interest is the role of EVs in the development of some neurodegenerative diseases (Thompson A. , 2016). All cells of the nervous system are able to release nanovesicles, however its structural complexity makes *in vivo* studies very difficult, with the majority of them coming from the supernatant of cultured cells (Frühbeis, 2013). During inflammation and brain damage events, EVs cross the blood-brain barrier and regulate communication, in both directions, between the central nervous system and the periphery (Dickens, 2017). These type of vesicles carry altered and aggregated proteins (e.g. beta-amyloid or prion proteins) that are associated with some neurodegenerative diseases (Karnati, 2019). For instance, proteins involved in the progression of Alzheimer's disease, such as the normal and oligomeric form of tau protein (Guix, 2018) and the amyloid precursor protein (Laulagnier, 2018), have been found to be transported through EVs. Similarly, in Parkinson’s disease, neuron-EVs carry altered molecules of SOD1 (Silverman, 2016) and alpha-synuclein (Chistiakov, 2017), suggesting their pivotal role in neuronal pathogenic processes.

1.7 Synthetic nanoparticles: current delivery systems

Nanoparticles have been widely proposed in several fields, especially in pharmaceutical and biomedical Industry (Bhatia, 2016). Among all the proposed kind of nanoparticles (e.g. inorganic, polymeric nanoparticles, carbon nanotubes and nanogels), lipid-based nanovesicles (L-NVs) have been the most promising, mainly for their therapeutic and diagnostic potential applications (Elizondo, 2011) (Bulbake, 2017).

They are small bilayered-spherical vesicles, constituted of various lipids of different nature (i.e. fats, waxes, sterols, vitamins, monoglycerides, diglycerides), with hydrophobic or amphipathic properties (Kraft, 2014). Their classification is mainly done on the basis of different parameters, comprising structural characteristics, methods of preparation and lipid composition (Akbarzadeh, 2013) (Dua, 2012). This new kind of colloidal carriers have aroused a lot of interest in the last few years, as they present greater solubility and lifespan in solution, allowing an efficient targeting of organs and tissues through the release of the drug in the specific area (Wu J. , 2018) (Cuenca, 2006).

Their classification is mainly based on morphological and dimensional characteristics and divide them into: small unilamellar vesicles/nanovesicles (SUVs, size < 200 nm and single bilayer) (Hope, 1986), large unilamellar vesicles (LUVs, single bilayered vesicles of 200-1000 nm) (Mimms, 1981), giant unilamellar vesicles (GUVs, single bilayered vesicles >1000 nm) (Bagatolli, 2000), multilamellar vesicles (MLVs, several concentric bilayers) (Lichtenberg, 1984) and multivesicular vesicles (MVVs, several small vesicles entrapped into larger ones) (Kim S. , 1983). Their surface can also be easily functionalized with different ligands, thus providing also multifunctional systems.

Among all kind of nanoparticles, SUVs are the most used in drug delivery system; in fact, thanks to their unique size, they are able to escape from the rapid renal-clearance, facilitating their longer circulation in the body and increasing their possibility to reach the target cells (Blanco, 2015).

Another type of solid lipid nanoparticles are Micro- and Nano- emulsions, thermodynamically stable dispersion of oil and water (Trotta, 1996) (Dipak, 2005). Micro- and Nano- emulsions are significantly different from the conventional emulsions, since they have specific physical properties (transparency, low viscosity, diameter <100–200 nm) and a low energy barrier that allow their spontaneously formation (Mc Clements, 2012).

Micro-emulsions are made from at least three components: a polar phase (usually water), a non-polar phase (usually oil) and a surfactant, with this latter forming an interfacial film that divides the polar and the non-polar domains (Gasco, 2009). Within this film, all reagents form

different microstructures, passing from droplets of oil dispersed in a continuous water phase (O/W-microemulsion), to water droplets dispersed in a continuous oil phase (W/O-microemulsion) (Malik, 2012).

Homogeneous micro-emulsion can be prepared over a wide range of surfactant concentrations of oil-to-water ratios (10–80%), resulting in fluid solution of low viscosity (Solans, 1997). Originally, these nanocarriers were produced with lipid materials such as fatty acids, triglycerides, waxes and oils, with the addition of a surfactant, commonly in combination with a co-surfactant or co-solvent, in order to increase the curvature of the interfacial film on the oil/water interface. These two initial faces (oil and water) are then melted above 40 ºC, since some lipid matrix are solid at body and room temperature and need to be melted (Cavalli, 2007).

The selection of the lipid material to use takes into account some parameters, such as: the lipid structure (it should be similar to the physiological conditions), the state of lipids (solid or liquid), regulatory aspects related to the pharmaceutical Industry and drug properties (the lipid should be able to solubilize the drug into the lipid droplet).

Once synthesized, the new formulation is then followed by steps of purification/separation, mainly based on techniques of Size Exclusion Chromatography, Tangential Flow Filtration and Ultrafiltration, that have been studied and developed for both purification and physic-chemical characterization of the products (Dalwadi, 2007) (Sivamohan, 1999) (Heydenreich, 2003).

In Italy, there are only few Companies expert in this type of nanocarriers, and Nanovector s.r.l. is one of them. It is a small Company, based in Turin, specialized in the research and development of nanostructured lipid systems for drug delivery, in both cosmetic and nutritional field. Nanovector has been operating in the field for over 15 years, taking part at many European projects and developing several families of patents.

Their technology focuses on the formulation of characteristic microemulsions and solid lipid nanoparticles (SLN), which are produced at room temperature, or using their original patented method of warm microemulsions (WμE), which can be furthered functionalized through the incorporation of different kind of drugs. One of their main target focuses on the investigation of new eye drug delivery systems, such as Solin™ product, an eye nanocarrier that can be administrated in form of eye drops and has been efficiently functionalized with different physico-chemical strategies, improving its performance and targeting.

1.8 Latest trends on EVs: tool for delivery system and molecular biomarkers

Interest on EVs is growing very fast over the years. Thanks to their characteristics (specifically their non-immunogenic nature due to their similar composition to the cell from which they

originate) they were recently taken into consideration for their use as drug delivery vehicles (Batrakova, 2015).

Actually, liposomes are the most used drug delivery system, but their biocompatibility and safety are still unknown. Unlike these synthetic systems, natural EVs have long circulating half-life, are biocompatible, stable and have minimal, or no inherent, toxicity issues. Moreover, thanks to their small size, they are able to cross the blood-brain barrier (BBB), thus providing a useful carrier for the delivery of small drugs across this area. Indeed, 98% of drugs potentially effective cannot cross the BBB and their conceptual efficacy shown in labs has not a counterpart in clinical trials (Haney, 2015). In addition, thanks to their capability to carry different molecules (protein and miRNA among others), EVs can also eliminate all those problems related to the instability of drugs based on nucleic acid (Liang, 2018). Of importance, the possibility to isolate them from several biological fluids in non-invasive way, have suggested their use for diagnostic applications, since circulating EVs can be correlated to some specific diseases (Aryani, 2016). Therefore, if compared with their synthetic counterparts, they seem to be a better choice, exceeding those synthetic nanoparticles limitations (Busatto, 2019) and constituting one of the most promising drug delivery systems, especially in the gene therapy of different disorders (e.g. genetic deficiencies or anti tumor progression) (O'Loughlin, 2012). Similarly to natural nano-vesicles, EVs-based semi-synthetic nano-vesicles (NVs) represent another type of vesicle delivery system, that includes all those natural EVs with some modifications for specific purposes.

EVs-based therapies mainly focus on two approaches that differ from the way EVs are used: in their native or modified form. In the first case, EVs are harvested from the sample of interest (e.g. cell type, tissue, or fluid) and directly used for specific analysis (Tian, 2014). In the second case, they undergo specific modifications (e.g. insertion of biological molecules, at the surface of their membrane or inside their lumen), in order to have functional EVs with different capabilities, as respect to their original form (Tian T. , 2018).

The techniques used to package biological molecules into EVs are extremely important and mainly develop through two different ways: one method targets EVs that have already been produced, while the other type targets the cells that secrete these specific EVs (Luan, 2017). In the first case, EVs are normally loaded through a passive incubation with the molecules, or drugs, that have to be associated with EVs (Sun D. , 2010). For instance, some researchers have encapsulated doxorubicin (a drug currently used for breast and solid cancer) into exosomes to increase local dosage of the molecule and reduce its adverse effects on other organs (Gomari, 2018). However, the functionalization of EVs may also require an active intervention, such as electroporation, that temporarily disrupt membrane integrity (Kim M. , 2019).

In the second case, loading of EVs occurs indirectly, through the modification of their parent cells, for instance through the transfection of this latter, thus improving levels of released EVs (Lou, 2015). Once loaded with a specific cargo, EVs are administered to the patient through several methods, including oral and intranasal routes, as well as injection, or under the skin.

Native EVs have been used in many therapeutic approaches, as they are natural reservoirs of biological molecules, important in treating diseases (Batrakova, 2015). For instance, EVs have aroused a lot of interest for the treatment of several chronic and neurodegenerative diseases (Ha, 2016). Indeed, it has been demonstrated that intravenously injected Rabies Virus Glycoprotein (RVG) targeted exosomes delivered GAPDH siRNA specifically in the brain, resulting in a specific gene knockdown (Alvarez-Erviti, 2011). A similar result was also confirmed by others, showing that exogenous siRNA transfected into cells can be packaged by exosomes and delivered into recipient cells to regulate gene silencing, indicating that exosomes can serve as siRNA delivery vesicles in gene therapy for cancer and other diseases (Liu Y. , 2015). In another study, large size plasmid DNA was encapsulated into exosomes and successfully transferred to MSCs (Lin Y. , 2018). Moreover, Khatua group demonstrated that human cytidine deaminase APOBEC3G (A3G), a cellular defense system against human immunodeficiency virus type 1 (HIV-1) and other retroviruses, can be secreted in exosomes, conferring an antiviral phenotype to target cells and limiting replication of the virus in recipient cells (Khatua, 2009).

Thanks to their potential role in drug delivery, EVs have been also taken in consideration sa vaccine technologies. For instance, Bacteria outer membrane vesicles (OMV) could be used as natural vaccines (van der Pol, 2015). However, one of their main limitations is related to their poor productivity and unreliable safety. To overcome these problems, protoplast derived nanovesicles (PDNVs), are arousing a lot of interest as a valid alternative to OMVs (Kim, 2015). They are small nano-vesicles derived from the protoplast (a bacteria cell deprived of its cell wall) of bacteria cells, which are free from all the toxic and dangerous elements present in the cell wall. Thanks to their non-toxic nature, PDNVs may be promising OMVs substitutes, bypassing all the potential harmful effects that OMVs could give (Kim O. , 2017).

Beyond their therapeutic power, EVs can be also used as potent biomarkers in the detection of several pathological conditions (Barile, 2017). For instance, EVs carrying viral components can inform the host organism about the presence of a viral infection, even if the virus has already eluded the immune system response (Rodrigues M. , 2018).

In cancer diagnosis, most current cancer biomarkers are tissue-based and invasive biopsies (Ayala, 1983). However, liquid biopsies may provide a valid alternative to the traditional solid biopsies and, recently, EVs have also arisen attention for their use in this sense (Diaz, 2014)

(Pang, 2020). EVs present in body fluids are non-invasive and easy to access, as respect to solid biopsies. Hence, they could be used to check the progression of the disease, or its response to therapy (Lee C. , 2018). However, there are some limitations in their use, since *in vivo* systems also release EVs from non-cancer related cells. Many kinds of mouse models have been used for the identification of new EVs cancer biomarkers (Moon, 2016) and many research groups have also evaluated EVs from different body fluids [e.g. plasma (Liu W. , 2019), serum (Morio, 2018), urine (Matsuzaki, 2017), cerebral spinal fluid (Akers J. , 2017), saliva (Chiabotto, 2019)] for the same purpose.

Characteristics of EVs that may be taken in consideration as potential cancer biomarkers comprehend their concentration in body fluids and their cargo. As regard cargo, different types of RNAs (mRNA, microRNA, Long non-coding RNA) and DNA molecules have been taken into account, since their levels seem to increase in cancer-EVs (Endzeliņš, 2018) (Vagner, 2018). Indeed, DNA within EVs includes mtDNA and genomic DNA, that can reflect the mutation status of the parental cells (Sansone, 2017). Even proteins have been also proposed as potential EV derived biomarkers, based on their abundance and their role in the progression of the disease (Hurwitz, 2016). Another possibility could be the analysis of EV derived lipids and metabolites, even if only few studies have been currently performed (Puhka, 2017).

Similarly to cancer-EVs, in infarcted patients it could be useful monitoring of endothelial EVs levels, which may be used as tools for the analysis of early biomarkers for the development of cardiovascular diseases (Bei, 2017).

As regard neurodegenerative diseases, it has been shown that dendritic cell derived EVs may act as an immunotherapeutic tool for the modulation of antigen-specific immune responses (Wahlund, 2017), also overcoming those previous drawbacks related to the use of dendritic cells (i.e. delicacy of the cells during freezing procedures) (Babatz, 2003). Therefore, a better characterization of neuronal EVs could be used as a potential tool for the diagnosis of neurological diseases. Neurodegenerative diseases generally do not develop immediately, but slowly evolve after several years, thus affecting levels of potential neurodegenerative proteins on EVs. Hence, neural EVs could be taken into account as a source of biomarkers for these conditions, especially because the diagnosis of neurodegenerative diseases is very difficult in the living patients (Karnati, 2019).

However, one of the main limitations in these studies is strongly linked to the isolation methods used for the investigation of biomarker profiles, since the most common methods currently used result in possible protein contaminants that precipitate with EVs (Cvjetkovic, 2014) (Taylor, 2015). Currently, the most used EVs come from mesenchymal stromal cells, which are able to target different cell types and act in a large spectrum of diseases (Mendt, 2019). For instance,

it has been demonstrated that they may have positive effects in models of stroke (Yang J. , 2017), as well as in traumatic brain injury (Williams, 2019), in glioma (Munoz, 2013) and Alzheimer's diseases (Wang S. , 2018). Despite the way they exert their beneficial effects is not fully understood, it may be that the molecules they carry (e.g. growth factors, cytokines, RNAs) could trigger some disease-modifications.

However, EVs may have controversial effects on health and diseases; for instance, in cancer progression some of them can prevent tumor development (Naseri, 2018) (Rosenberger, 2019), while others provide a communication system between tumor cells and the surrounding tissues (Haga, 2015) (Keklikoglou, 2019). Moreover, one of the principal obstacles for their clinic application is limited to their final yield from donor cells, which is often very poor and strongly related to the protocol of isolation (Van Deun, 2014). Hence, in the last few years, researchers have also started to combine exosomes with synthetic nanoparticles, developing engineered carriers that seem to be more efficient than their natural counterparts. For instance, in order to control and modify the performance of exosomal nanocarriers, some researchers realized hybrid exosomes fusing them with polyethylene glycol (PEG) liposomes (Sato, 2016). They showed that these modifications facilitated cellular uptake of the PEG modified exosomes, reducing also their circulation time in the blood.

To overcome some limitations related to the biology of extracellular vesicles, the bio-nanotechnology sector has also recently focused on the production of fully artificial vesicles (Garcìa-Manrique, 2018). The fabrication of these kinds of particles may occurs in two main ways: top-down and bottom-up approaches (**Figure 4**).

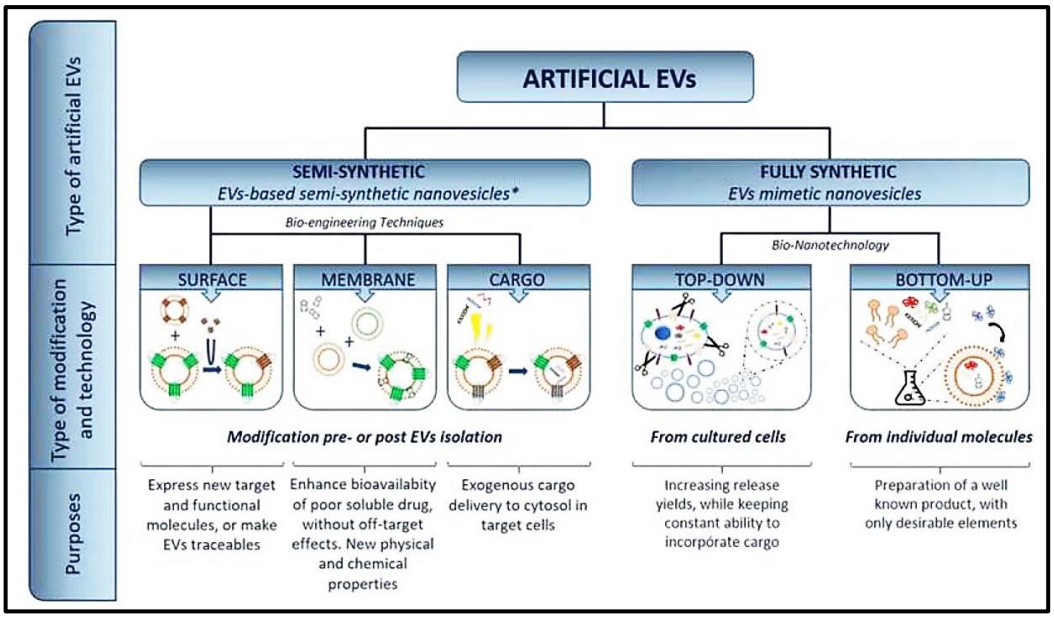

Figure 4 - *Types of artificial EVs*

Top-down methodologies rely on the production of nano-sized materials starting from bigger and complex units (such as cells) which are sequentially broken into smaller parts. In this case, artificial EVs develop from cultured cells, that are gradually fragmented into vesicles of increasingly smaller diameters (Jang, 2013).

Two of the most relevant strategies involve: extrusion over polycarbonate membrane filters (method used to reduce the mean size and homogenize the size distribution of colloidal systems) and microfluidic systems (Senthilkumar, 2018) (Qingfu, 2018). For instance, researchers created exosome-mimetic nano-vesicles by serial extrusions through polycarbonate membranes with pore sizes of 10, 5, and 1 μm, for their utilization in tissue repair and regeneration. These exosome-mimetic nanovesicles (NVs) had a final yield almost 100 times higher than exosomes and promoted cell proliferation and liver regeneration similar to that induced by exosomes (Wu J. , 2018). However, these methods have some drawbacks since, in extrusion methods, cargo sorting lacks selectivity due to the passive encapsulation of the surrounding medium during membrane fragment self-assembly.

By contrast, bottom-up techniques create complex structures starting from molecular components, that are manipulated through the variation of their physical and chemical properties, using similar methods to those of liposomes formulation. The self-assembled synthetic bilayer can be then functionalized with selected proteins to mimic the desired exosomal functions (Garcìa-Manrique, 2018).

Another way to mimic exosomes could be to use plasma membrane phospholipids as starting material for the assembling of the exosomes-like particles. In this case, starting molecules are not artificial, but natural components of the plasma membrane of the cells used. These vesicles, called proteo-liposomes, can be easily functionalized with specific proteins (Pollet, 2018).

2. Aim of the project

This thesis is part of a previous project PRIN 2012, concerning the role of endurance training in mice models Balb/c with neoplastic cachexia. During those experiments, the research group, led by Prof. Di Felice, has discovered natural nanoparticles (exosomes) able to mimic, *in vitro*, the effects of endurance training, consisting in the overexpression of Hsp60 protein and the activation of the mitochondrial biogenesis pathway, to which the PGC-1 co-factor belongs. The purpose of the current project mainly focused on the engineering of a stable transfected C2C12 cell line, overexpressing Hsp60 protein, as well as on the isolation and characterization of extracellular vesicles harvested from cell culture medium of C2C12 murine myoblasts. The project was divided in three phases:

- the first part focused on the engineering of cells (through their transfection with a plasmid containing the gene sequence of Hsp60 protein) capable of producing large quantities of vesicles carrying Hsp60; this latter, as a protein, is not able to easily cross the cell membrane, but can enhance the activation of PGC-1 when it is transported through extracellular vesicles;
- the second part of the project was carried out in Prof. Mülthoff's laboratories, in Germany, where large volumes of cell culture medium were harvested and processed for extracellular vesicle characterization;
- the last part of the project was executed in collaboration with Nanovector srl company, in Turin, where vesicles were further characterized using the same techniques used for the analysis of synthetic lipid nanoparticles.

Understanding the morpho-functional characteristics of these vesicles will allow the design of engineered nanoparticles, able of mimicking the effects of endurance training.

3. Material and Methods

3.1. Cell Culture Methods

3.1.1. Mammalian Cell culture

C2C12 mouse adherent myoblasts (from ATCCH CRL-1772TM) were grown in high glucose Dulbecco Modified Eagle Medium (DMEM) 4.5 g/l glucose supplemented with 10% heat-inactivated Fetal Bovine Serum (FBS), 1000 UI/ml penicillin, 1000 UI/ml streptomycin and 2 mM L-Glutamine at 37 °C, in humidified atmosphere containing 5% CO2.

3.1.2. Plasmid Used

The cloning vector pCMV6-Entry (Cat. PS100001, Origen) is a plasmid composed by several strong promoters (i.e. CMV and T7) that allow the high expression of the target gene.

As illustrated in figure 5, from left to right, the plasmid carry: i) the Kozak sequence, recognized by the pre-initiation complex of translation in eukaryotes; ii) the multiple cloning site (MCS), with several recognition sites for different restriction enzymes, important for the insertion of the target gene; iii) c-tag Myc-DDK, a tag protein added to the target protein using the DYKDDDDK motif of the sequence (where D= aspartic acid, Y= tyrosine and K= lysine); iv) Neo/ Kan, the genes for antibiotic selection of E. Coli bacterial cells and eukaryotic cells respectively; v) SV40 ori, the origin of the replication, important for the synthesis of Kanamycin and Neomycin genes, that confer antibiotic resistance to bacteria and eukaryotic cells that acquired the plasmid (**Figure 5**).

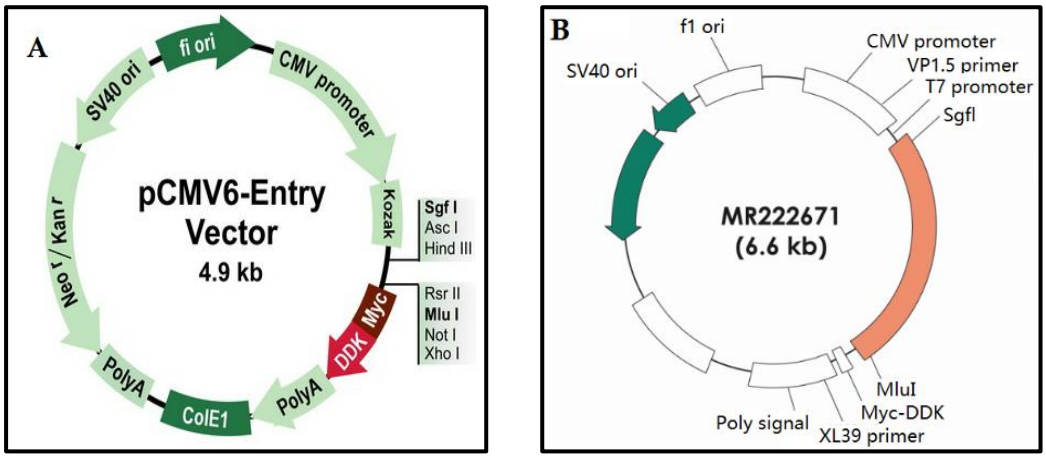

Figure 5 - *(A) Plasmid map of pCMV6-Entry backbone, 4,9 kb; (B) Plasmid map of pCMV6-Entry-HSPD1, 6,6 kb (Cat. MR222671, Origene)*

The gene HSPD1, coding for murine HSP60, is inserted within the site MCS, creating the plasmid pCMV6-Entry-HSPD1. The resulting molecule is a fusion protein between HSP60 and the tag Myc-DDK. HSPD1 used sequence for the synthesis of this new vector, is published on the website of https://www.ncbi.nlm.nih.gov/nuccore/NM_010477, in the database of the National Institute of Heath (NIH).

As regard the other cloning vector pIRES-hrGFP-1a, it is a plasmid composed by: i) a promoter CMV, that allows the expression of the gene of interest; ii) a diastronic cassette, in which MCS is followed by an EMCV-IRES sequence, linked to the hrGFP sequence. EMCV-IRES is the internal ribosomal entry site, derived by the encephalomyocarditis virus, a characteristic nucleotide sequence, able to recruit the ribosomal subunit, thus triggering the translation of the mRNA through a cap-indipendent mechanism; iii) hrGFP sequence, which is merged to the gene target and codes for the recombinant human GFP protein, allowing an easy visualization of the gene of interest after its expression; iv) 3x FLAG, a tag protein added to the target protein, with the same sequence of c-tag-Myc, used in tandem (DYKDHD-G-DYKDHD-I-DYKDDDDK) with a final tag coding for a restriction site for the enterokinase, the enzyme involved in the removing of the tag from the target protein; v) SV40 pA, a DNA sequence able to add a poliA tail to the transcript, avoiding its degradation; vi) pUC ori, the prokaryotic plasmid replication origin; vii) f1 ori, the replication origin of bacteria infected with fagi, important for the synthesis of a single DNA vector; viii) LoxP sequences, derived from the bacteriophage P1 and recognized from Cre recombinase, for the recombination of Cre-Lox; ix) ampicillin, the selection gene of E. Coli cells (**Figure 6**).

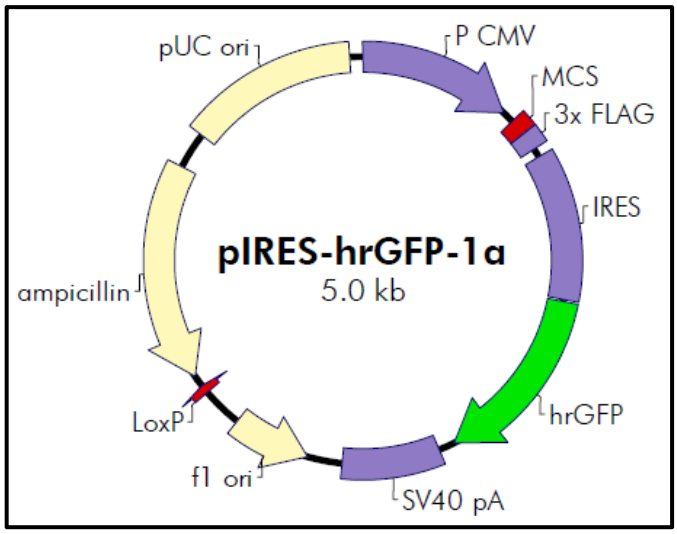

Figure 6 *- Plasmid map of pIRES-hrGFP-1a*

3.1.3. Bacterial transformation

XL10-Gold ultra competent cells (Agilent technologies 200315) are designed for the transformation of DNA molecules with high efficiency.

Briefly, bacterial cells were placed on ice and a cellular aliquot of 100 µl was gently mixed into a pre-chilled tube, with 4 µl of the ß-mercaptoethanol (ß-ME) mix provided with these bacterial batches. Cells were first incubated on ice for 10 minutes and gently swirled every 2 minutes; after, 50 ng of the experimental DNA were added to the bacterial aliquot and incubated for 30 minutes. The mixture was then heat-pulsed at 42 °C, in a water bath, for 30 seconds and passed on ice for other 2 minutes. Subsequently, 0.9 ml of preheated (42 °C) LB-broth were added to the mix and incubated at 37 °C for 1 hour under continuous shaking, at 225-250 rpm.

After the incubation, 150 µL of this transformation mixture was plated on LB agar plates containing the appropriate antibiotic kanamycin (for pCMV6-Entry-HSPD1), or ampicillin (for pcDNA 3.1-mok, pIRES-hrGFP-1a-Hyg and pIRES-hrGFP-1a) and incubated at 37 °C overnight. Once the colonies in the Petri dish have grown, a pure colony was isolated, with the help of a sterile loop, selected and inoculated in a glass flask with 5mL of LB Broth + the specific antibiotic of selection, for 8 hours at 37 °C and 300 rpm continuous shaking.

Then, 150 µL of the starter culture were transferred to a glass flask with 100 mL of LB Broth + antibiotic and incubated for further 14 hours, at 37 °C and under constant shaking at 300 rpm.

3.1.4. Plasmid Extraction

After the incubation, plasmid DNA was extracted from bacterial colonies with the QIAGEN EndoFree Plasmid Maxi Kit (Cat. 12163), following manufacturer's instructions.

This kit provides rapid anion-exchange-based endotoxin-free plasmid DNA purification, thanks to the 2x CsCl gradient centrifugation that drastically reduce the levels of endotoxins. Hence, the purified DNA is highly pure and free from endotoxin, that could significantly reduce transfection efficiencies in endotoxin sensitive cell lines.

The extracted plasmid DNA was washed two times with EtOH 70%, dissolved in 250 µL of TE buffer (provided by QIAGEN kit), read at Nanodrop ND-2000 and used for the transfection of C2C12 cells.

3.1.5. C2C12 transfection via Lipofectamine® 2000

Plasmids were transfected using Lipofectamine® 2000 Reagent according to the manufacturer's instructions, with some modifications.

Briefly, C2C12 cells were plated one day before the transfection in 6-well dishes (5x 10^4 cell/well) in DMEM antibiotic free in order to reach a confluence of 70% the day of the transfection. The second day, 3.5 μg/well plasmid DNA [pCMV6-Entry-HSPD1] for the over expression of Hsp60 (OriGene Technologies Inc., Rockville, MD, USA), and his negative control pcDNA 3.1. plasmid, were diluted in 150 μL of Opti-MEM Medium (without FBS, L-glutamine, penicillin or streptomycin) and incubated for 5 minutes at room temperature (RT).

Similarly, Lipofectamine (in ratio 1:1) was diluted in 150 μL/well of Opti-MEM and incubated for 5 minutes. The mixture was then incubated for 20 minutes and added to growing cells.

After 7-8 h, Opti-MEM medium supplemented with 20% FBS was added to a final volume of 2 mL/well and incubated for 48 hours. Different ratio DNA: Lipofectamine were tried [3.5 μg:mL, 5 μg:mL and 8.75 μg:mL] in order to check which one was the most suitable for a good percentage of transfected cells. After the incubation, transfected cells were selected for 4-5 weeks by using DMEM supplemented with antibiotic G418 in a final concentration range of 4-17 mg/mL. For each well and week, a chamber slide was made, in order to follow the evolution of the transfected cells.

In a different protocol, C2C12 cells were transfected immediately after trypsinization, during the replating (Escobedo, 2003). In this case, the DNA-Lipofectamine complex was added to the cells the same day of the trypsinization, while they were still in suspension.

3.1.6. C2C12 transfection via Electroporation

C2C12 cells were transfected using the Electoroporator Neon Transfection System (Thermo Fisher Scientific, Waltham, Massachusetts, USA) according to the manufacturer's instructions, using the Neon 100 μl Transfection System (Cat. n. MPK10025, Thermo Fisher Scientific, Waltham, Massachusetts, USA).

Briefly, for pCMV6-Entry-HSPD1 transfection, C2C12 cells were plated 1 day before the experiment; on the day of the transfection (70-90% of confluence), they were washed with DPBS without calcium and magnesium, harvested using 10% Trypsin/EDTA (Cat. n. 15400054, Gibco - Thermo Fisher Scientific, Waltham, Massachusetts, USA) and 36 μg of concentrated DNA, 100 μl Buffer R, 1650 pulse voltage, 10 ms pulse width, 2 pulses, were used according to the manufacturer's instructions. After electroporation, cells were plated into 6-well dishes with complete DMEM medium, without antibiotics/anti-mycotics.

Three days after transfection cells were plated into chamber slides for Confocal analysis (5x 10^3 cells/well).

For pIRES-hrGFP-1a-Hyg plasmid transfection, C2C12 cells were plated in a T75 cm^2 flask with fresh medium. On the day of the transfection (70-90% of confluence), cells were harvested

with DPBS without calcium and magnesium and trypsinized with 10% Trypsin/EDTA (Cat. n. 15400054, Gibco - Thermo Fisher Scientific, Waltham, Massachusetts, USA). 5x 10^4 cells/well, 5 µg of pIRES-hrGFP-1a-Hyg and 100 µL of Buffer R were electroporated following different optimization protocols shown in the table below (**Table 3**).

After being electroporated, cells were transferred in 6 well plate and incubated at 37 °C with 2 mL of fresh completed DMEM (Cat. 41966052, Gibco, USA), supplemented with 15 % of FBS (Cat. 16000044, Gilbo) without antibiotic/anti-mycotics. After 48 h, transfected cells were observed and checked under confocal microscopy.

Sample	Well no.	Pulse Voltage	Pulse width	Pulse no.	Sample	Well no.	Pulse Voltage	Pulse width	Pulse no.
1	A1	-----	-----	-----	13	C1	1100	20	2
2	A2	1400	20	1	14	C2	1200	20	2
3	A3	1500	20	1	15	C3	1300	20	2
4	A4	1600	20	1	16	C4	1400	20	2
5	A5	1700	20	1	17	C5	850	30	2
6	A6	1100	30	1	18	C6	950	30	2
7	B1	1200	30	1	19	D1	1050	30	2
8	B2	1300	30	1	20	D2	1150	30	2
9	B3	1400	30	1	21	D3	1300	10	3
10	B4	1000	40	1	22	D4	1400	10	3
11	B5	1100	40	1	23	D5	1500	10	3
12	B6	1200	40	1	24	D6	1600	10	3

Table 3 - *Table representing various combination of parameters for better transfection efficiency*

3.1.7. Total DNA isolation

Due to the impossibility to follow pCMV6-Entry-HSPD1 transfection with a microscope, plasmid DNA was extracted from the transfected cells using Norgen kit for Genomic DNA Isolation (Cat. 24700, 24750) according to the manufacturer's instructions. The DNA was further analyzed by standard PCR and checked by agarose gel electrophoresis (data not shown).

3.1.8. Flow cytometry analysis

Flow cytometry was performed to analyze the percentage of positive GFP cells post pIRES-hrGFP-1a-Hyg plasmid transfection, using a BD FACSVerse ™ (Cat. 651153, BD Biosciences) flow cytometry. Unstained cells, used as negative control, were prepared following manufacturer's instructions of LIVE/DEAD® Viability/Cytotoxicity kit, while fluorescence was detected using FITC filters, at 488 nm.

3.2.Methods of Extracellular vesicles isolation and characterization

3.2.1. Ultracentrifugation

One day before the isolation, C2C12 cells were trypsinized, counted and plated in T175 flasks (1x 10^6 cell/flask) with 20 mL of completed DMEM and incubated at 37 °C in a humidified atmosphere with 5% CO2.

The day after, once they reached a confluence of 70-80%, the complete medium was removed and three washes in DPBS were made to remove any trace of vesicles from FBS. Then, 20 mL/flask of DMEM without FBS were added in each flask and incubated for others 24 h. The next day, the medium was collected and subject to different centrifugations, while cells were trypsinized and counted to be used as cell lysate control for Western Blot analysis.

For EVs isolation, the supernatant was first centrifuged at 300 x g, for 10 minutes at 4 °C, in order to remove the presence of any death cells; then, the supernatant was recovered and further centrifuged at 2,000 x g, 10 minutes at 4 °C, to remove cell debris; the pellet was removed and the supernatant was centrifuged at 15,000 x g, for 45 minutes at 4 °C, to remove microvesicles.

The resulting pellet (EVs larger than 150 nm) was stored at -80 °C for further analysis. At the end of this step, the supernatant was collected and ultracentrifuged for 2 hours, at 110,000 x g at 4 °C, using a micro-ultracentrifuge Sorvall® Discovery M120 with a S55-A rotor. After ultracentrifugation, the supernatant was discarded, while the pellet was washed in DPBS and ultracentrifuged for 2 hours at 110,000 x g at 4 °C, using a S555-A rotor to concentrate the sample. At the end of this step, the supernatant was discarded and the pellet (exosomes, EVs smaller than 150 nm) was resuspended in 30µL of RIPA buffer for protein quantification using BCA protein assay (Ref: 23225, Thermo Scientific), or stored at -80 °C.

3.2.2. Size Exclusion Chromatography (SEC)

Briefly, cell culture medium containing extracellular vesicles was firstly harvested from T175 cm^2 flasks and centrifuged at 300 x g and 2,000 x g, to remove dead cells. The supernatant was then concentrated with 50 mL Stirred Cell Ultrafiltration system (cat. No 5122), mounted with a nitrocellulose filter of 44.5 mm and a nominal molecular weight limit (NMWL) of 100,000 Da (Millipore Cat. No. 14422AM). Up to 10 mL were collected as retentate and further concentrated with a 10 mL stirred Cell Ultrafiltration (cat. No 5121), mounted with an ultracel® regenerated cellulose (RC) disc of 25 mm and a nominal molecular weight limit (NMWL) of 100 kDa (Millipore Corporation, Cat. No. PLHK02510).

A final volume of 2 mL of retentate were harvested and further concentrated with Amicon® Ultra centrifugal Filters (100,000 NMWL of regenerated cellulose), for 15 minutes at 15,000 x g, at 4 °C. The final retentate (500µL) was finally loaded onto a Size Exclusion Chromatography Column (IZON, qEV Original, 70 nm).

Before proceeding with SEC isolation, the column was placed in a holder, left equilibrate at room temperature and then washed with 10-20 mL of 0.2 µm degassed DPBS. Meanwhile, 20 empty plastic vials of 1,5 mL each, were weighed. Once equilibrated the column, with the lower cap still on, excess of DPBS was pipetted out from the top filter and 500 µL of sample were loaded. The lower cap was removed and 20 fractions of 0,5 mL each were collected in 1,5 mL plastic vials.

Each plastic vial, containing the eluate, was weighed and read at the Zetasizer Instrument. Fractions containing vesicles, specifically fraction 7-8-9-10-11, were pooled together and concentrated through Amicon® Ultra centrifugal Filters of 100,000 NMWL regenerated cellulose, for 15 minutes at 15,000 x g, at 4 °C. The final retentate was then used for tunable resistive pulse sensing analysis (where possible) or stored at -20 °C for further analysis.

3.2.3. Tangential Flow Filtration (TFF)

As in SEC, cell culture medium containing extracellular vesicles was initially centrifuged at 300 x g and 2,000 x g, in order to remove dead cells. The supernatant was then concentrated and washed through VIVAFLOW 50 Tangential Flow Filtration system (100,000 Da MWCO); specifically, the retentate was firstly concentrated up to 10 mL, washed 8 times in PBS (to reduce interfering substances present in the medium) and finally recovered in a total volume of 5 mL. This latter, was further concentrated with Amicon® VIVASPIN Ultra centrifugal Filters of 100,000 Da NMWL regenerated cellulose, for 15 minutes at 15,000 x g and 4 °C.

The final concentrate was then used for Zetasizer analysis and tunable resistive pulse sensing (where possible), or stored at -20 °C for further analysis.

3.2.4. Total exosome isolation kit

Total Exosome Isolation (Invitrogen by Life technology; Cat. No 4478359) reagent forces less-soluble components (i.e. exosomes) out of solution, by bounding water molecules and allowing their collection after short and low-speed centrifugation. Here, vesicles were isolated as manufacturer's instructions.

Briefly, cell culture medium (CCM) without serum was harvested from T150 flasks (containing 24 hours starving C2C12 cells) and centrifuged at 2,000 x g, for 30 minutes (in

order to remove cells and debris), at 4 °C. Then, the supernatant was concentrated up to 1mL through VIVASPIN 20 centrifugal concentrator filters (Sartorius, 10,000 MWCO PES, REF_VS2001) at 8,000 x g, for 16 minutes, at 4 °C, and incubated overnight with 0.5 mL of the total exosome isolation reagent, at 4 °C.

The day after, sample was centrifuged at 10,000 x g, 1 hour at 4 °C, after which the supernatant was discarded and the pellet was resuspended with sterile and filtered DPBS or RIPA buffer.

3.2.5. Dinamic Light Scattering (DLS)

Dynamic light scattering determinations of extracellular vesicles was performed with a Zetasizer Nano instrument (Malvern Nano-Zetasizer, λ=532 laser wavelength) and the size data refer to the scattering intensity distribution (z-average). Briefly, extracellular vesicles obtained from different protocols (Ultracentrifugation, SEC and TFF), were resuspended in 0.2 µm filtrate DPBS and 40 µL of undiluted sample-DPBS mix was analyzed at 25 °C, using a precision ultra-micro Quarz Suprasil® cell for low volumes (ZEN2112) for samples isolated with ultracentrifugation, while samples isolated through SEC or TFF were read undiluted in a total volume of ˜300 µL, using a UV-transparent disposable cuvettes (Sarstedt, Germany).

3.2.6. Tunable Resistive Pulse sensing (TRPS)

TRPS is a method used for the characterization of nanoparticles without the use of laser. Here, a voltage is applied across a pore that is filled with an electrolyte solution for the establishment of an ionic current. As particles cross the pore, they briefly increase the electrical resistance, creating a resistive pulse, which is proportional to the particle volume. The rate flow of particles is proportional to the particle concentration, thus obtaining also a particle number estimation. Using this principle, concentration and diameter of extracellular vesicles (EVs) isolated through SEC and TFF were analyzed using Nanopores-NP 200 and 80 nm, at three different pressures: -5,-7 and -10 mbar.

Briefly, samples purified with SEC and TFF were previously concentrated with Amicon® VIVASPIN Ultra centrifugal Filters to a final volume of 20-40 µL, after which they were diluted with 0.22 µm filtered PBS in a final dilution of 1:2 or 1:4 sample-PBS.

Then, a baseline current was established with 75 µL and 40 µL of 0.22 µm filtered PBS, which were respectively loaded in the lower and upper fluid cells. After, the PBS was removed from the upper fluid cell and 40µL of the diluted sample were loaded on it. Two different kinds of nanopores were used: NP-200 (size range 80-400 nm) and NP-80 (size range 40-255 nm).

Sample was read at three different pressures (10, 7 and 5 mbar) and compared to a standard IZON calibrator specific for each nanopore (SKP 200E for NP200 and CPC100 for NP80).

3.3. Microscopy

3.3.1. Immunofluorescence

Immunofluorescence was performed after transfection of C2C12 cells with pCMV6-Entry-HSPD1, in order to evaluate the efficiency post-transfection.

Briefly, transfected cells in chamber slides (5x 10^3/well) were washed twice in DPBS, for 5 minutes and then fixed for 30 minutes in cold Methanol, under ice. After, methanol was removed and cells were washed again in DPBS two times, for 5 minutes, after which they were incubated with Sodium Citrate, 10 minutes at room temperature. After the incubation, fixed cells were washed twice in DPBS, for 5 minutes and blocked with 3% of bovine serum albumin/phosphate buffer saline (BSA/DPBS), for 30 minutes at room temperature. Primary antibodies anti-DDK (OTI4C5) and anti-Hsp60 were added overnight, in a dilution of 1:200 and stored at 4 °C, after which samples were washed twice with DPBS, for 5 minutes, and the secondary antibody has been added for 1 hour, at room temperature.

After the incubation, chamber slide was washed two times with DPBS, for 5 minutes, and 4′,6-diamidino-2-phenylindole (DAPI), diluted 1:1000 in DPBS, was added for 15 minutes. Then, fixed cells were washed again twice in DPBS, for 5 minutes, and assembled with a cover glass for Confocal microscopy visualization.

3.3.2. Transmission Electron Microscopy in 3D Cultures

After 3 days of differentiation in DMEM enriched in 5% Horse serum (HS, Cat. n. 16050130, Gibco - Thermo Fisher Scientific, Waltham, Massachusetts, USA) as previously described (23523921), cells were cultured embedded into collagen I (rat tail, Cat. n. 354236, BD Biosciences, Franklin Lakes, New Jersey, USA) on 24-well plate inserts (200,000 cells/insert; BD Biosciences, BD Biosciences, Franklin lakes, New Jersey, USA).

After 24 hours, inserts were fixed in PFA 4% for 6 hours and washed in Phosphate Buffer Saline (PBS) overnight. After two rapid washes in PBS, inserts were dehydrated in alcohol 30%, 50%, and 70% and embedded into liquid LR-White Medium Grade Resin (Cat. n. 14380, Electron Microscopy Sciences, Hatfield, Pennsylvania, USA) before inclusion into gelatin capsules (Cat. n. 70115, Electron Microscopy Sciences, Hatfield, Pennsylvania, USA). Samples were then cut into 70 nm-thick ultra-thin sections, layered onto Formavar coated gold grids

(FCF100-Au-50,Electron Microscopy Sciences, Hatfield, Pennsylvania, USA) and immunogold labelled.

For staining, grids were rinsed on drops of water for 10 min, incubate in citrate buffer pH 6.0 for 40 minutes and blocked in 3% BSA-c (Cat. n. 900099, Electron Microscopy Sciences, Hatfield, Pennsylvania, USA) in T-PBS for 30 min. Grids were then incubated with the primary antibody (anti-Alix, 1A12, sc-53540, Santa Cruz Biotechnology, Dallas, Texas, USA, diluted 1:10) overnight at 4 °C inside a microplate, washed two times for 5 min in T-PBS, incubated with AuroProbe EM secondary antibody (RPN425, Amersham Biosciences, Little Chalfton, UK, diluted 1:25 in 0.3% BSA-c in T-PBS) for 1 h. The grids, washed twice in T-PBS, were post-fixed with 2% glutaraldehyde in PBS. Washed again were contrasted using conventional techniques. Grid-mounted preparations were stained with uranyl acetate and lead citrate for 5 min, and subsequently observed under the JEM-1220 (Jeol) electron microscope examined at 120 kV.

3.4. Immunoblotting

1 x 10^7 C2C12 cells were homogenized by centrifuging them at 300 x g, 5 minutes at 4 °C; the pellet was resuspended in 1 mL DPBS and centrifuge twice at 300 x g, 5 minutes at 4 °C. Then, 200 µL of lysis buffer RIPA (150 mM NaCl (Roth), 0.5% Sodium Deoxycholate (SigmaAldrich), 1% Triton X-100 (SigmaAldrich), 50 mM Tris, pH 8.0 (Roth), 0.1% SDS (Roth), supplemented with Protease Inhibitor Cocktail (cOmplete ULTRA Tablets, Mini, EDTA-free, EASYpack by Roche) was added to the pellet for 1 hour on ice, by vortexing at the beginning and at the end of the incubation. Then, the homogenates were centrifuged at 20,000 x g for 20 minutes at 4 °C and supernatant fractions were stored at -20 °C, or immediately used.

For Extracellular Vesicles, three ultracentrifugation pellets from three independent experiments were pooled together (˜ 500 mL total of medium), resuspended in a total volume of 80 µL of RIPA buffer and proteins were extracted as mentioned above with cells. Vesicular and cellular proteins were then quantified spectrophotometrically according to Pierce™ BCA protein Assay Kit manufacturer's instructions (Ref: 23225, Thermo Scientific).

Cellular and cellular-vesicle proteins were then denatured in 4X SDS protein Sample Buffer (40% Glicerol, 240 nM Tris/HCl pH 6.8, 8% SDS, 0.04% bromophenol Blue, 5% beta-mercaptoethanol), diluted to a final concentration of 1X, for 5 min at 95 °C and loaded onto a 10% SDS-PAGE gel (30 µg protein/sample).

After Electrophoresis, proteins were blotted onto a nitrocellulose membrane (Nitrocellulose Membrane Filter Paper Sandwich 0.45 µm Pore Size by NOVEX), checked with Red Ponceau, and blocked for 1 hour at room temperature, with 5% Milk in Tris-buffered saline/0.05%

Tween20. The membrane was then cut and incubated overnight at 4 °C, and in gentle shaking, with the antibodies anti-Alix diluted 1:1000 (1A12, sc166028 Santa Cruz), anti-beta-actin diluted 1:5000 (AC-74 SigmaAldrich), anti-Hsp70 diluted 1:1000 (gently provided by Mülthoff's laboratories), anti-Hsp60 diluted 1:1000, and anti-Rab5 diluted 1:1000 (R4654 SigmaAldrich), all diluted in 5% Milk in T-TBS. Polyclonal Rabbit anti-Mouse Immunoglobulins/HRP (Ref: PO260, DAKO) and Polyclonal Swine anti-Rabbit Immunoglobulins/HRP (Ref: PO217, DAKO) diluted 1:2000 in 5% Milk in T-TBS were used as Secondary Antibodies.

The signal was detected by using a Pierce™ ECL Western Blotting Substrate (Ref: 32106 Thermo Scientific) and captured by ChemiDoc, or manually in a dark room.

3.5. Proteomic analysis

Aliquots of 30 µg of Exo and EVs extracts were firstly dialyzed, lyophilized and then purified from PlusOne 2-D Clean-Up Kit (GE Healthcare Life Sciences, Milan, Italy), according to manufacturer's intructions. The obtained pellets were then resuspended in 100 µL of 50 mM ammonium bicarbonate (pH 8.3) and incubated on ice for 15 min. After, 100 µL of 0.2% RapiGest SF (Waters, Milan, Italy) in 50 mM ammonium bicarbonate (pH 8.3) were added and incubated on ice for other 30 min.

Protein concentration was then determined by Qubit Protein Assay kit with the Qubit 1.0 Fluorometer (ThermoFisher Scientific, Milan, Italy) (Higa-Nakamine, 2015). A final concentration of respectively 0.33 and 0.47 µg/µL for Exo and EVs samples was quantified and 0.2 µg of yeast Enolase were added as internal standard to each sample. The reduction was carried out by adding 20.35 µg (Exo sample) and 29.3 µg (EVs sample) of DTT dissolved in the same buffer. The solutions were kept in the dark, for 3 hours, at 25 °C.

Subsequently, alkylation was performed by addition of iodoacetamide, at the same molar ratio over total thiol groups, for 1 hour, in the dark, at 25 °C. Finally, reduced and alkylated proteins were subjected to digestion using modified porcine trypsin (Promega, Milan, Italy), in ammonium bicarbonate (pH 8.3) and at an enzyme-substrate ratio of 1:50 (37 °C overnight) (Saletti, 2018) (Saletti, 2017). The protein digests were dried under vacuum, redissolved in 40 µL 5% FA (final concentration 250 ng/µL).

Mass spectrometry (MS) data were acquired using an Orbitrap Fusion Tribrid (Q-OT-qIT) mass spectrometer (ThermoFisher Scientific, Bremen, Germany) equipped with a ThermoFisher Scientific Dionex UltiMate 3000 RSLCnano system (Sunnyvale, CA). An aliquot of 1 µL of the in-solution digestion was loaded onto an Acclaim ®Nano Trap C18

column (100 μm i.d. × 2 cm, 5 μm particle size, 100Å). After washing the trapping column with solvent A (H_2O + 0.1% FA) for 3 min at a flow rate of 7 μL/min, peptides were eluted from the trapping column onto a PepMap ® RSLC C18 EASY-Spray, 75 μm × 50 cm, 2 μm, 100 Å column and were separated by elution at a flow rate of 0.25 μL/min at 40 °C, with a linear gradient of solvent B (CH_3CN + 0.1% FA) in A, 5% for 3 min, followed by 5% to 20% in 32 min, 20% to 40% in 30 min, 40% to 60% in 20 min and 60% to 98% in 15 min.

The eluted peptides were ionized by a nanospray (Easy-spray ion source, Thermo Scientific) using a spray voltage of 1.7 kV and introduced into the mass spectrometer through a heated ion transfer tube (275 °C). Survey scans of peptide precursors in the m/z range 400–1600 were performed at resolution of 120,000 (@ 200 m/z) with an AGC target for Orbitrap survey of 4.0×10^5 and a maximum injection time of 50 ms.

Tandem MS was performed by isolation at 1.6 Th with the quadrupole, and high-energy collisional dissociation (HCD) was performed in the ion routing multipole (IRM), using a normalized collision energy of 35 and rapid scan MS analysis in the ion trap. Only precursors with charge state 2–4 and an intensity above the threshold of $5 \cdot 10^3$ were sampled for MS2. The dynamic exclusion duration was set to 60 sec with a 10 ppm tolerance around the selected precursor and its isotopes. Monoisotopic precursor selection was turned on. AGC target and maximum injection time (ms) for MS/MS spectra were 10,000 and 100, respectively. The instrument was run in top speed mode with 3 sec cycles, meaning the instrument continuously performed MS2 events until the list of non-excluded precursors diminishes to zero or 3 sec, whichever occurred soonest. MS/MS spectral quality was enhanced enabling the parallelizable time option (i.e., by using all parallelizable time during full scan detection for MS/MS precursor injection and detection). Each sample was injected in triplicate, in order to assess the reproducibility of the MS data. MS calibration was performed using the Pierce ® LTQ Velos ESI Positive Ion Calibration Solution (Thermo Fisher Scientific). MS data acquisition was performed using the Xcalibur v. 3.0.63 software (Thermo Fisher Scientific).

LC–MS/MS data were processed by PEAKS software v. X (Bioinformatics Solutions Inc., Waterloo, ON, Canada). The data were searched against the 17449 "*Mus musculus*" SwissProt database (release February 2019) to whom yeast enolase 1 (P00924) sequence was added. Tryptic peptides with a maximum of three missed cleavage sites were subjected to an in silico search. Cysteine carboxyamidomethylation was set as fixed modification, whereas oxidation of methionine and transformation of N-terminal glutamine and N-terminal glutamic acid residues in the form of pyroglutamic acid were included as variable modifications. The precursor mass tolerance threshold was 10 ppm and the maximum fragment mass error was set to 0.6 Da. Peptide spectral matches (PSM) were validated using Target Decoy PSM Validator node based

on *q*-values at a 1% False Discovery Rate (FDR). Only proteins identified in at least two replicates with a minimum of two peptides matched were considered. Proteins containing the same peptides which could not be differentiated based on MS/MS analysis alone were grouped to satisfy the principles of parsimony. Label-free quantification data were obtained using PEAKS Q software, which detected the reference sample and automatically aligned the sample runs. Enolase tryptic peptides internal standards were employed as normalization factor. Proteins present in distinctly different concentration between the two samples were identified by a statistical analysis tool set with the following filters: protein fold change ≥ 2, protein significance ≥ 20, unique peptides ≥ 2, average area <1·104 and P value < 0.005 The data have been displayed in a volcano plot format for ready visualization.
Raw MS data files, unfiltered protein groups and peptides tables are available at ProteomeXchange (www.proteomexchange.org, accession: 30395289).

3.6. Lipidomic analysis

EVs samples isolated through ultracentrifugation have been further subjected to lipidomic analysis. Briefly, pellet of frozen samples (EVs pelleted at 15,000 x g and EVs pelleted at 110,000 x g) were first recovered in 100 µL of a solution constituted by 70% of an aqueous solvent (A), made of ACN:H2O:Ammonium formate (6:4:1), with 0.1% FA, and 30% of an organic solvent (B), composed by Isopropanolo:ACN (9:1), with 0.1% FA.

Once resuspended in this running solvent, samples were vortexed for 30 sec, transferred in glass reducers of 250 µL each, and further placed in vials for the analysis. Then, 10 µL of sample were injected inside a chromatographic column, Phenomenex Luna C18 3 µm 100 Å 150 x 2.00 mm, using a gradient of an acqueous solvent (A) and an organic solvent (B) (**Table 4**), at a flow speed of 200 µL/min, with a temperature of the sample compartment of 10 °C.

Retention time (min)	%A	%B
0	70	30
5	70	30
45	0	100
50	0	100
55	70	30
70	70	30

Table 4 - *Table representing the gradient of solvents*

Samples were analyzed through the FTMS LTQ Orbitrap mass analyzer, with a mass range m/z of 100-1500. Full scan and dependent scan MS2-MS3 experiments were conducted and positive and negative polarity of samples was examined. Lipid masses were then evaluated through Lipid Maps® software.

3.7. Formulation of synthetic lipid micro-nano emulsions

Two types of synthetic nano-systems have been synthesized, with a diameter of around 400 nm and 100 nm respectively. B-I312-H1 microemulsion (of 300 nm) was prepared from: fatty acid MCT oil, fatty acid lauric acid, monoglyceride Imwitor 312, phospholipid Lipoid S75, detergent TWEEN 20 and water. TPM-A1-T5 microemulsion (of 100 nm) was composed of a mix of phosphatidilcolines, triglycerides, PEG-40 monostearate, Ethanol and short-chain alcohols. In both cases, warm microemulsion method was used for the preparation of nanoparticles, patented by Nanovector s.r.l. (Gasco M. , 1989).

Briefly, all reagents have been weighed and poured in two empty glass vials, one containing the oily phase (with all the lipophilic reagents) and the other one including the water phase (with the hydrophilic surfactants). Then, the two vials have been warmed at 65 °C under magnetic agitation (heating/stirring module, Reacti-Therm™, PIERCE) and, once the oily phase was completely melted, the water phase was added to it, forming the oil in water microemulsion (O/W). Then, the two phases were poured in a large volume of water (dispersing phase) and mixed under mechanical agitation (1800 rpm), allowing the diffusion of the newly formed microemulsion.

The final products were then evaluated for their chemical-physical properties through Dynamic Light Scattering (DLS) and TRPS technologies, using Zetasizer Nano ZS (Malvern Instruments Ltd.) and qNano instruments (from IZON). All DLS measurements have been acquired at 25 °C, with a final dilution of 1:100 in milliQ water, while TRPS evaluation was performed using nanopores NP400 and NP200 respectively, at three different pressures: 5, 7 and 10 mbar.

4. Results

4.1. Transfection of C2C12 cells with pCMV-6-Entry-HSPD1 enhances the expression of Hsp60 and DDK proteins

As already demonstrated in mice models with neoplastic cachexia (Barone, 2016), endurance training seems to stimulate muscle specific expression of Hsp60 chaperonin, which in turn triggers the activation of PGC-1 co-factor, the main regulator of mitochondria biogenesis. To further investigate the role of Hsp60 in mitochondria biogenesis, an *in vitro* model of C2C12 murine myoblast cells was transfected with a plasmid over expressing for Hsp60 protein (pCMV6-Entry-HSPD1). Results shown that, after transfection, these cells were able to release more Hsp60, also associated to a concomitant raise of PGC-1 protein. Since the chaperonine alone was not able to induce PGC-1 protein expression and mitochondria biogenesis, it has been speculated that Hsp60 protein may have acted as a paracrine factor transported within small nano-vesicles, able to activate all those molecules involved in mitochondria biogenesis (Barone, 2016). This latter mechanism is of such importance for muscle cells, since mitochondria are the energetic house of the cell and they are therefore used to provide large energy requirement for all those muscle functions, such as movement of the body.

Based on these preliminary data, we decided to focus on the engineering of a stable transfected cell line, which could be able to mimic those beneficial effects that physical exercise excerted to cells (Barone, 2016).

So, C2C12 cells were transfected by electroporation with the pCMV-6-Entry-HSPD1 plasmid expressing the HSP60 var1 mouse gene, and the corresponding empty negative control plasmid pCMV-6-Entry, previously mentioned in materials and methods section. After 72 h from transfection, cells were plated in chamber slides and immunofluorescence for Hsp60 and DDK-tag proteins was performed. Confocal microscopy analysis of transfected cells confirmed the presence of cells expressing a higher quantity of Hsp60 (green) and Myc-DDK tag (red) in samples transfected with pCMV-6-Entry-HSPD1, with a minor expression in those samples transfected with empty pCMV-6-Entry plasmid. This indicated that tranfection occurred, however we always reached a very low amount of positive tranfected cells that affected transfection efficiency (**Figure 7**).

Due to the low electroporation efficiency, we also tried different methods of transfection, in order to increase the final number of positive transfected cells. Therefore, C2C12 were further seeded in a 6-well plate and transfected through Lipofecatime® 2000, a method based on the use of cationic lipids, which are able to form positive liposome complexes that bind the negative

phosphate groups of DNA molecules, thus facilitating transport and the cellular uptake. Once transfected, C2C12 cells were further selected through the treatment with the antibiotic of selection G-418 geneticin (at a maximum concentration of 17 mg/mL) for 12 days, and constantly monitored under optical microscope. As shown below, among 6, 7 and 12 days of treatment, cells became numerous after each week, developing resistance to the antibiotic used (**Figure 8**).

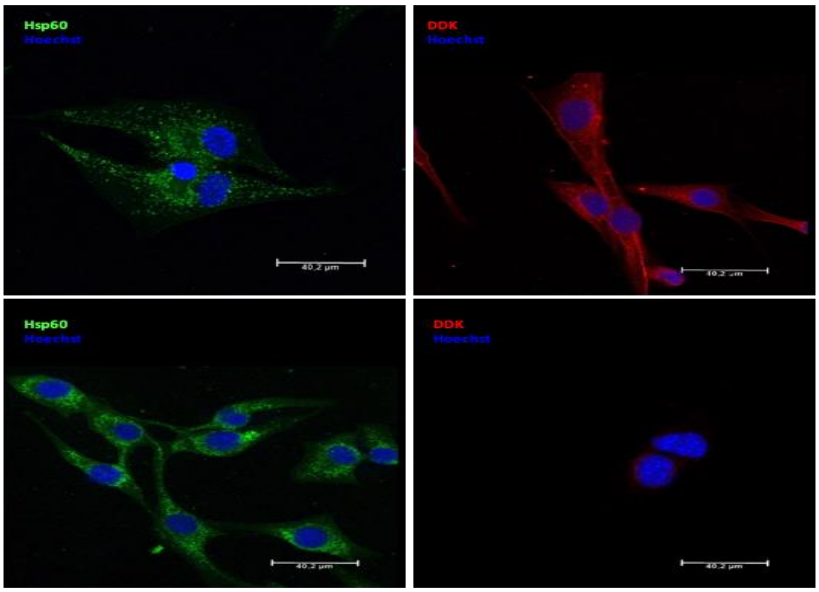

Figure 7 - *Immunofluorescence images of C2C12 myoblasts cell line transfected with pCMV6-Entry-HSPD1 vector (up) and untreated control cells (down). The expression of the tag Myc-DDK demonstrates the presence of the plasmid inside the cell and the expression of the protein, whose sequence has been introduced in the system by the vector.*

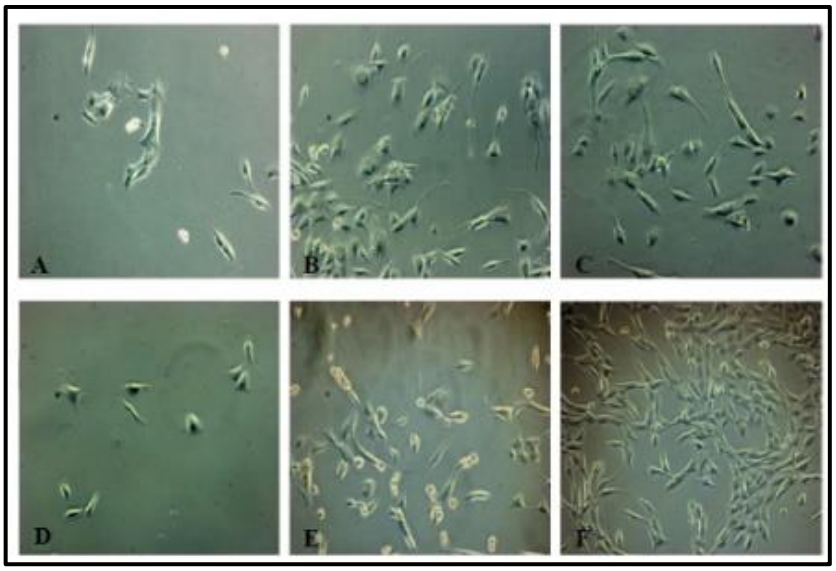

Figure 8 - *Optical microscopy of C2C12 transfected with lipofectamine in presence of 17 mg/mL of G-418 antibiotic. (A, C, E) Cells transfected with the negative control pCMV6-Entry plasmid, after 6, 7 and 12 days, respectively. (B, D, F) Cells transfected with pCMV6-Entry-HSPD1 after 6, 7 and 12 days, respectively.*

4.2. Sensitivity of C2C12 cells to hygromycin B antibiotic and their transfection through the new plasmid pIRES-hrGFP-1a-Hyg

C2C12 cells transfected with the pCMV-6-Entry-HSPD1 plasmid were selected for 4 weeks with the antibiotic of selection G-418 geneticin (gene sequence expressing for the antibiotic was contained within the plasmid), in order to create a stable cell line overexpressing for Hsp60 chaperonin; however, after only few weeks of treatment cells became more abundant and proliferative (**Figure 8**). Therefore, we speculated that cells may have lost the plasmid but not the gene of antibiotic selection, suggesting some kind of resistance to the antibiotic used.

So, due to this potential acquired resistance of transfected C2C12 cells to the G-418 selection antibiotic, we decided to design a new plasmid carrying Hygromycin B, a different kind of antibiotic of selection. However, before proceeding with the transfection of cells, it was first evaluated the sensitivity of C2C12 to this latter antibiotic using different serial dilutions of hygromycin B, up to a final concentration of 500 µg/mL. The Optical microscopy observation of C2C12 after 7 days of treatment revealed that the sensitivity of cells increased proportionally to the increase of hygromicin concentration, improving the number of dead cells in suspension (**Figure 9**).

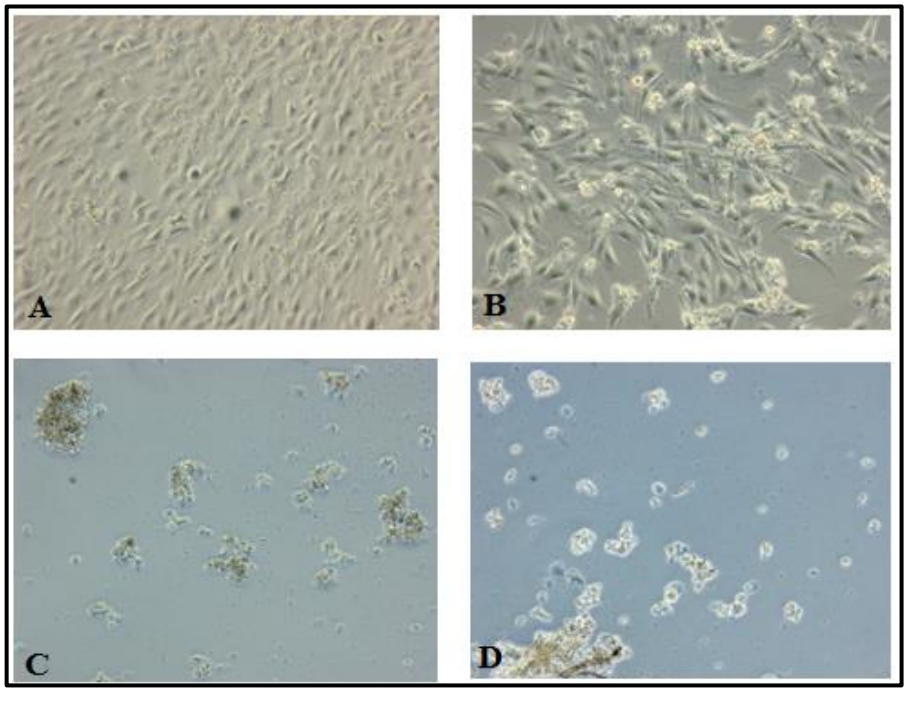

Figure 9 - *Optical microscopy of C2C12 treated with different concentrations of hygromycin B, after 7 days of treatment. (A) Non treated C2C12. (B) C2C12 treated with 0,98 µg/ml of Hygromycin, with cells still alive. (C) Cells aggregates, treated with 250 µg/ml of hygromycin. (D) Dead cells in suspension after 500 µg/ml of hygromycin*

Sensitivity to hygromicyn B was further evaluated through MTT test, at 48 and 72 hours post treatment. As shown in the figure below, the trend curve was similar in both the analyzed situations, with an initial cell viability of around 50 % at a concentration of 7.81 µg/mL of antibiotic, that further decreased as the antibiotic concentration increased (**Figure 10**).

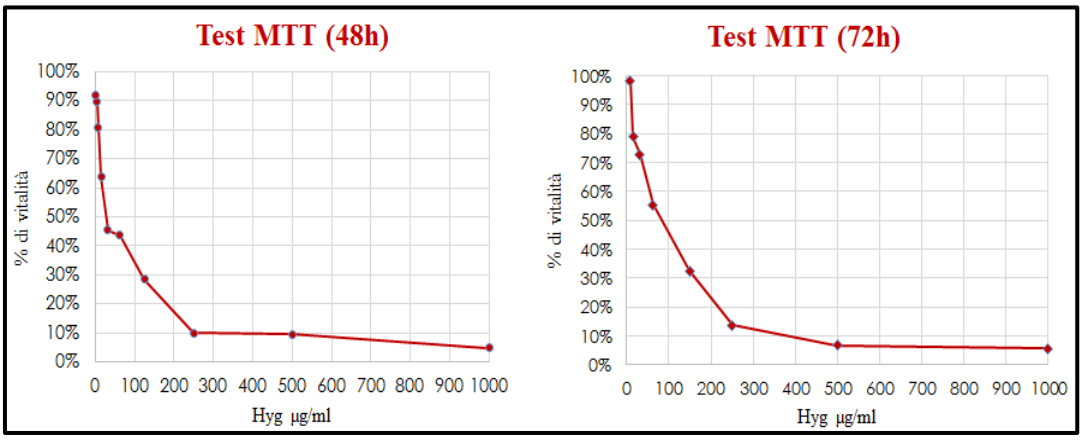

Figure 10 *- MTT test of C2C12 sensitivity to hygromycin B. C2C12 cells were treated with decreasing concentrations of antibiotic, starting from 1 mg/mL to 0,48 µg/mL, after 48h and 72h and MTT test was performed and read under spectrophotometer at an OD570 nm.*

On the basis of these preliminary results, hygromycin B seemed to be more efficient than G-418, hence we decided to change the antibiotic of selection and use HygB for the selection of positive transfected cells.

So, the hygromycin resistance gene was inserted inside the plasmid pIRES-hrGFP-1a (8,1 Kb and devoid of HSPD1 gene) and C2C12 cells were transfected through electroporation, using the system Neon® Transfection System. This latter, is an electroporation device that uses the tip of a special pipet as an electroporation chamber for the transfection of cells. In general, electroporation occurs through the exposure to a short high voltage electrical impulse, which transiently generate pores on the cell membranes, allowing the introduction of the DNA of interest. The efficacy of electroporation depends on three different parameters: voltage, amplitude and pulse number.

To optimize transfection efficiency of C2C12 cells, a pre-set protocol was used in four 6 well plates, in which all the 24 conditions of the electroporation protocol were tested, changing one or two parameters each time. After 48 h, transfected cell were observed under Fluorescent microscope using a FITC filter, since the plasmid DNA carries the hrGFP gene for an easy recognition of transfeted cells. Overall, even if the transfection efficiency was still very low, visible green cells were detected, suggesting that pIRES-hrGFP-1a plasmid was uptaken from cells (**Figure 11**).

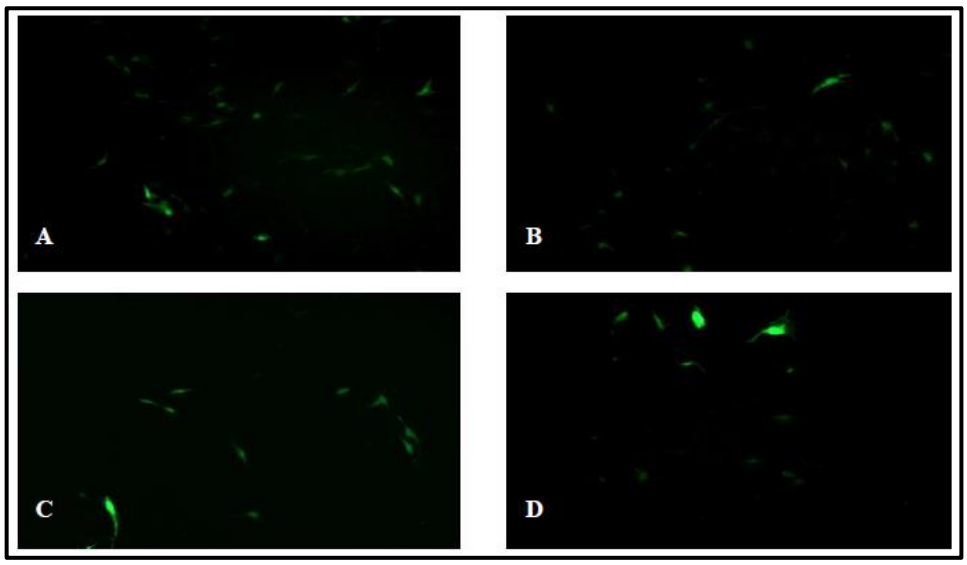

Figure 11 - *Fluorescence images of C2C12 transfected with pIRES-hrGPF-1a-Hyg plasmid. (A-B) C2C12 electroporated following optimization protocols B3 shown in table 1 of material and methods; (C-D) condition A5 and B6 respectively*

After 72 h of electroporation, C2C12 previously subjected to 24 different electroporation protocols (table 1 in material and methods) were also analyzed through flow cytometry, to evaluate the efficiency of transfection. So, from all the 24 conditions used with 5 µg of plasmid pIRES-hrGFP-1a-Hyg and 5x 10^5 cell/well, only conditions C3 (1300 V, 20 °A, 2) and D2 (1150 V, 30 °A, 2) gave efficiency higher than 5 %, with a percentage of 7,22 % and 7,21 %, respectively (**Table 5**).

Condizione	Efficienza	Condizione	Efficienza
A1	0.44 %	C1	0.71 %
A2	0.35 %	C2	2.73 %
A3	1.34 %	C3	7.22 %
A4	2.69 %	C4	0.30 %
A5	3.80 %	C5	0.74 %
A6	1.07 %	C6	1.42 %
B1	2.10 %	D1	2.92 %
B2	3.86 %	D2	7.21 %
B3	3.91 %	D3	0.34 %
B4	0.36 %	D4	3.03 %
B5	2.12 %	D5	4.23 %
B6	4.50 %	D6	0.99 %

Table 5 - *Flow Cytometry of transfected C2C12 with 24 electroporation conditions*

Once defined the best electroporation protocol, 5 x10^5 cells/well and 5 µg of plasmid pIRES-hrGFP-1a-Hyg were further transfected in a 6 well plate, using only conditions C3 and D2. After the electroporation, 500 µL of cell suspension were harvested from each well and seeded

in a chamber slide for Confocal microscopy analysis. As shown below (**Figure 12**), pIRES-hrGFP-1a-Hyg plasmid seemed to be slightly toxic, given the presence of cells under mitotic division (**Figure 12B**); however, the efficiency of transfection was still low and needs some modifications to increase the final yield.

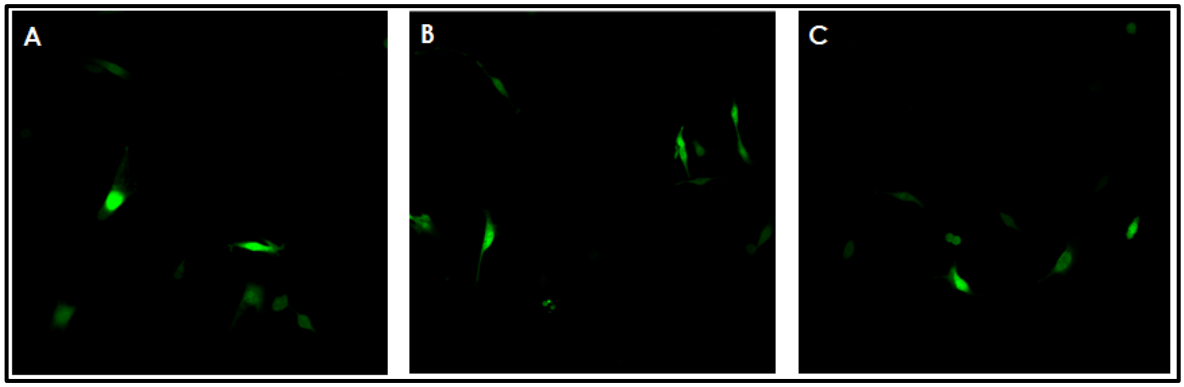

Figure 12 - *Fluorescence images of C2C12 transfected with pIRES-hrGPF-1a-Hyg plasmid. (A-C) C2C12 electroporated using condition D2 from the optimization protocol scheme shown in table 1 of material and methods.*

4.3. C2C12 cells release extracellular vesicles in cell culture medium

Based on previous studies concerning the role of endurance training in mice models with neoplastic cachexia, it has been discovered that physical activity enhances the release of natural nano-particles able to carry the Hsp60 chaperonin, a protein involved in the mitochondrial biogenesis pathway, to which the PGC-1 co-factor belongs. The study has further highlighted a potential active role of Hsp60 only when transported inside EVs, since the protein alone was not able to trigger the activation of PGC-1 co-factor (Barone, 2016). It could be that, thanks to their capability of easily crossing the plasma membrane of the cells, extracellular vesicles may help molecules with low solubility to reach specific targets within the cells.

So, to demonstrate the presence of nano-vesicles in culture medium, C2C12 cells were cultured in T175 cm^2 flasks and kept in starvation for 24 h, after which the supernatant was collected for the isolation of EVs; in parallel, cells were first analyzed for viability through trypan blue assay, and then collected for the production of cell lysate extracts (**Figure 13**). As shown in the figure below, the viability of cells before and after starvation (absence of serum for 24 h) was more than 95%, with only a slight increase of dead cells post-starvation, as compared to those of pre-starvation (**Figure 13**). On the other hand, cell culture medium supernatant was harvested and processed for the isolation of extracellular vesicles using different isolation protocols: ultracentrifugation, size exclusion chromatography, tangential flow filtration and total exosome isolation kit.

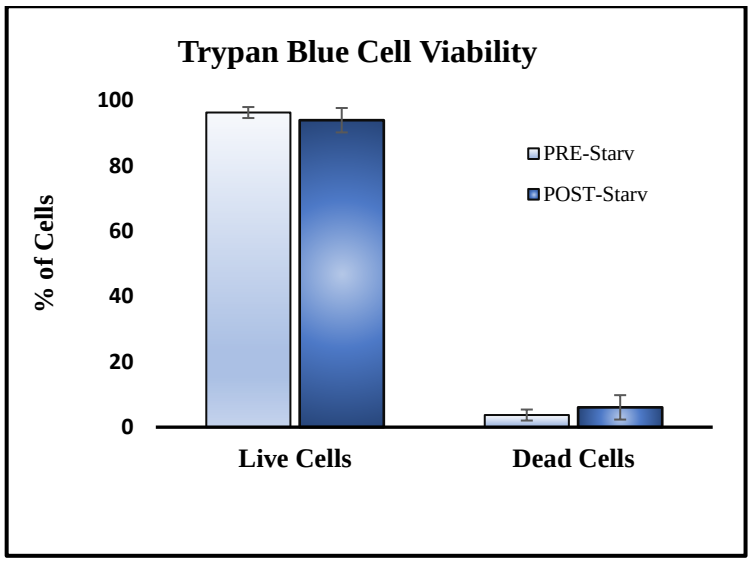

Figure 13 - *Trypan Blue cell viability of C2C12 myoblasts before and after starvation. Black bars: live and dead cells pre-starvation; Gray bars: live and dead cells post-starvation*

As regard ultracentrifugation, vesicles were first isolated through serial centrifugation (300 g for 10 min, 2,000 g for 10 min, 15,000 g for 45 min, and 110,000 g for 2 h, all carried out at 4 °C) and then evaluated with Zetasizer instrument (by Malvern) under dynamic light scattering analysis for size distribution evaluations.

Dynamic light scattering (DLS) is a non-invasive technique that investigates the hydrodynamic size of nanoparticles. This technology relies on particle size measurement, through the estimation of Brownian motion of particles within the sample (this phenomenon occurs when particles suspended in a liquid randomly move due to the collisions with the molecules of the liquid that surrounds the particle). Particles are illuminated with a laser and further analyzed as the intensity fluctuations in the scattered light. Particles speed is then used to determine their size: small particles move quickly and scatter less light, while bigger particles move slowly and scatter much more light than smaller ones. The size distribution generated by the instrument is mainly an intensity distribution, which can be also converted to a volume distribution and a number distribution.

This latter is an important parameter to take in consideration when performing DLS analysis, since it gives an idea of the number of particles, within the sample, with a specific size. For instance, if we consider a sample containing only two sizes of particles (5 nm and 50 nm) with equal numbers of each size particle, the peaks of number distribution, as expected, are of the same size (1:1) as there are equal number of particles. On the other hand, when measuring the intensity distribution, the area of the peak for the 50 nm particles would be 1,000,000 times larger than the peak for the 5 nm (1:1,000,000 ratio), because large particles scatter much more light than small particles (Malvern, 2009).

Two types of EVs were evaluated: those pelleted at 15,000 g and 110,000 g, corresponding to microvesicles and large/small EVs, respectively. On the fractions thus obtained, the Z-Average (d.nm) size distribution by intensity and number of microvesicles was respectively 301,2 nm, while for large/small extracellular vesicles, the Z-Average (d.nm) was of 108,2 nm (**Figure 14-15**).

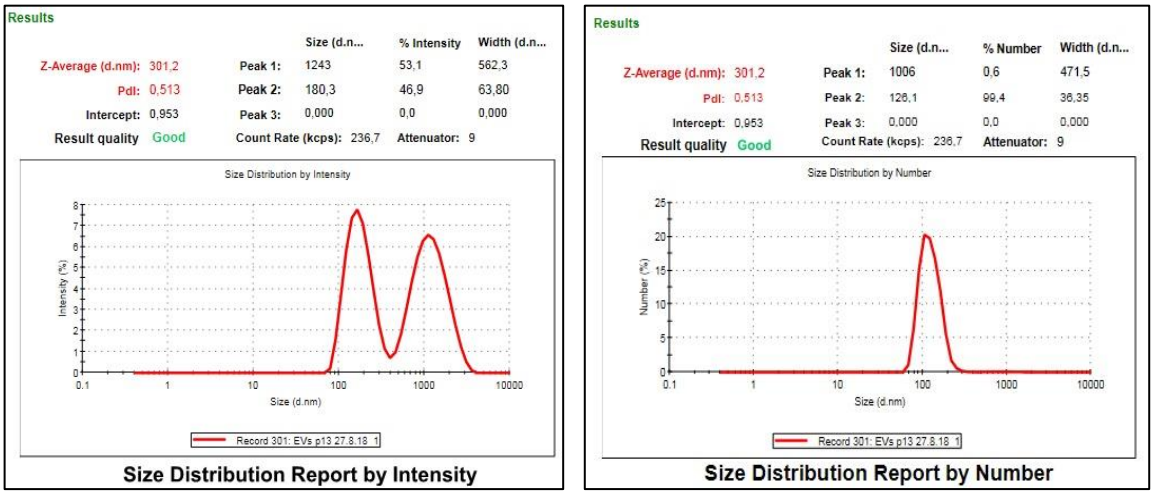

Figure 14 - *Zetasizer images of C2C12 myoblasts derived vesicles isolated with ultracentrifugation protocol at 15,000 g. Left: extracellular vesicles size distribution by intensity, with a main peak at 180,3 nm (95,8 % of the total population), Right: extracellular vesicles size distribution by number, with a main peak at 126,1 nm (99,4 % of the total population)*

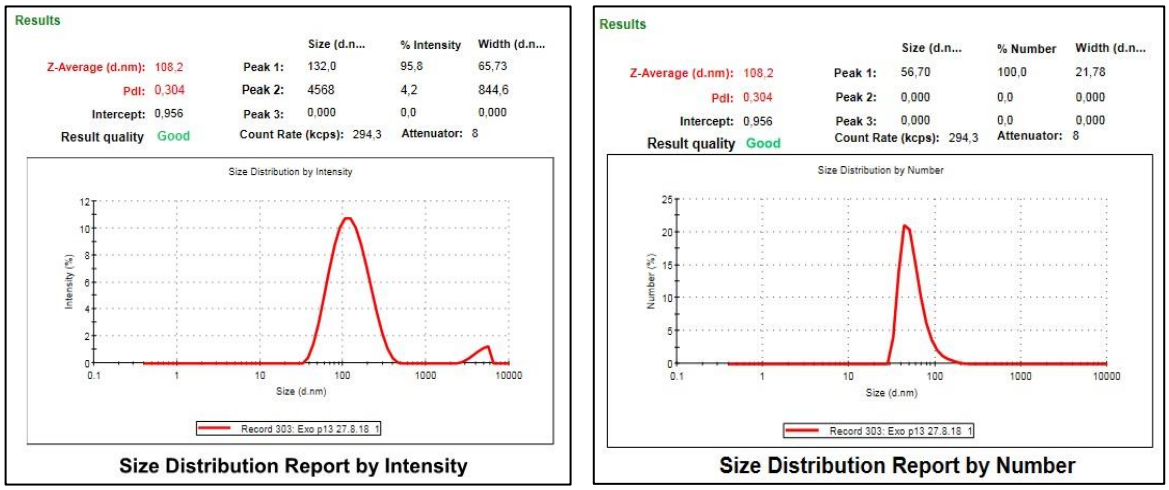

Figure 15 - *Zetasizer images of C2C12 myoblasts derived vesicles isolated with ultracentrifugation protocol at 110,000 g. Left: EVs size distribution by intensity, with a main peak at 132 nm (95,8 % of the total population). Right: EVs size distribution by number, with a main peak at 56,70 nm (100% of the population)*

To further demonstrate the presence of nano-vesicles in the C2C12 culture medium, cells were cultured for 3 days in presence of horse serum, after which they were detached and placed in three-dimensional cultures, in presence of collagen-I (derived from the rat tail) for other 24 h.

This type of procedure is generally used to create a suitable sample for electron microscopy analysis, as well as in order to prevent the dispersion of nano-vesicles in the culture medium (Romancino, 2013).

Electron microscopy images of partially differentiated C2C12 cells, revealed the presence of EVs with a range diameter between 50 to 120-140 nm, situated close to the cell membranes (**Figure 16 A**), as it was also previously demonstrated from Romancino et al. (Romancino, 2013). Moreover, as shown in the figure below (**Figure 16 B-C**), specific antibodies anti-Alix revealed the presence of some nano-vesicles aggregates enriched in Alix protein.

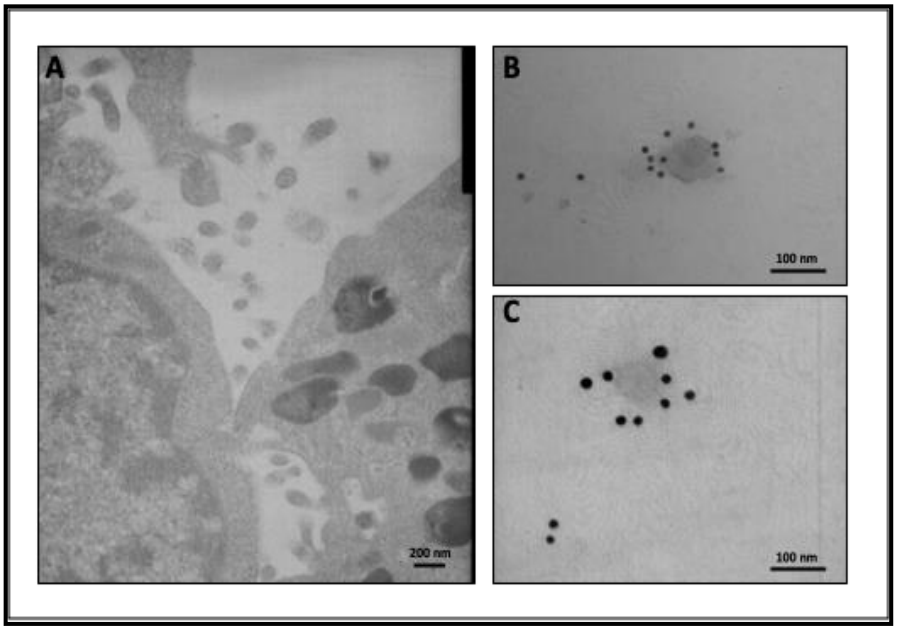

Figure 16 – *C2C12 cells release nano-vesicles. (A) Electron microscopy analysis of 3D cultures of C2C12 cells show the presence of budding intermediates (nascent vesicles) at the plasma membrane or already budded vesicles with an average diameter of 80 nm (see scale bar for reference). (B - C) Transmission electron microscopy shows immunogold labeling of Alix (a known marker of exosomes) in the nanovesicles from 3D cultures of C2C12 myoblasts (10 nm gold particles). The two panels B and C show nano-vesicles released in the collagen gel of the 3D culture (ECM = extra-cellular matrix) (see scale bar for reference)*

Ultracentrifuged samples, from the two fractions 15,000 g and 110,000 g, were further lysed for proteins quantification and used to evaluate the presence of classic EVs protein markers. Western blotting analysis of the EVs obtained from 15,000 g and 110,000 g fractions, as well their whole cell lysate, shown that the 110,000 g fraction contains a significant enrichment of classical exosomes proteins such as Alix, Hsp70 and RAB5, while 15,000 g fraction mainly contains RAB5 and Hsp70, with a less abundance in Alix protein (**Figure 17**). Moreover, total cell lysate (used as a control of the corresponding vesicles) presented smaller quantities of Alix and RAB5 proteins (**Figure 17**).

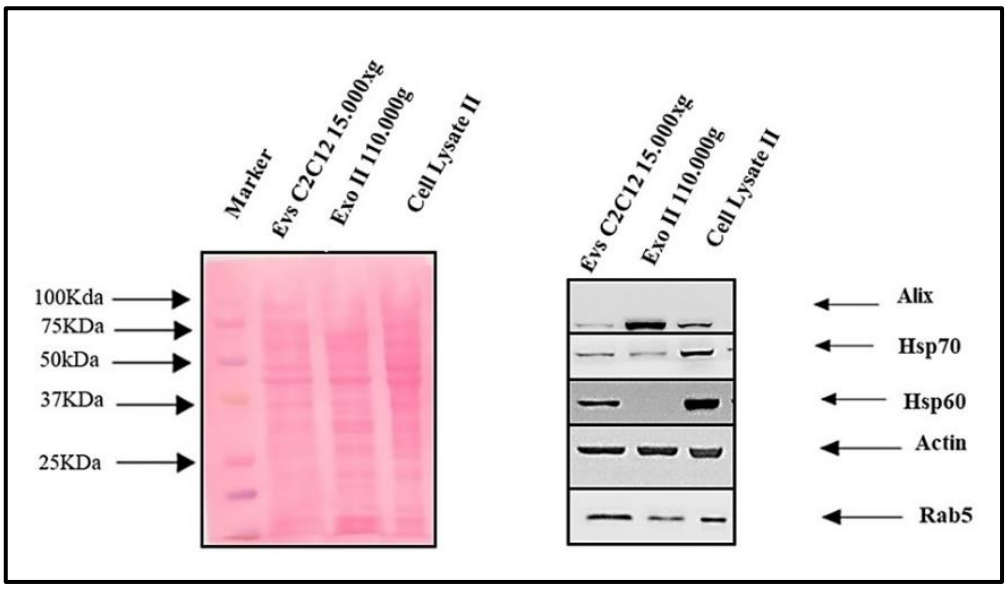

Figure 17 - *Western blot of EVs isolated by ultracentrifugation protocol. Left: red ponceau of microvesicles at 15,000 g, exosomes at 110,000 g and total lysates from C2C12 cells (30 μg of proteins per lane). Right: expression bands of Alix, HSP70, HSP60 and RAB5 proteins. β-Actin was used to verify the correct protein loading*

Despite the presence of some of the most common EVs markers, Hsp60 protein band was detected only in microvesicles and cell lysate protein samples, but not in EVs pelleted at 110,000 g. This may be due to the very low presence of the protein within the entire protein content of EVs pelleted at 110,000 g. Indeed, although western blot for Hsp60 was negative, proteomic results revealed its presence in both samples, 15,000 g and 110,000 g.

For proteomic analysis, EVs isolated from 15,000 g and 110,000 g fractions were further subjected to RP-nUHPLC/nESI-MS/MS analyses and subsequent database search against the *Mus musculus* UniProt database. Respectively, a total of 1531 proteins were identified from samples of EVs isolated at 15.000 g and 1355 in EVs isolated at 110.000 g, including also human ENO1 used as internal standard to quantify relative protein abundance.

A label free based comparative approach was employed to analyse the differential protein content between the two samples. According to the analysis, 389 proteins showed differences greater than 2-fold changes and T-test *P*-value < 0.05 in relative abundances, including 168 up regulated and 227 down regulated proteins in Exo. 560 proteins were identified as common to both samples with differences in relative abundance lower than 2-fold; 405 proteins were exclusively present in Exo and 581 in EVs respectively (**Figure 18**).

Figure 18 shows a volcano plot of the significantly differentially expressed proteins between Evs and Exo samples. Hsp60 (Uniprot Acc. P63038) was identified among the differentially

accumulated protein with higher abundances in EVs isolated at 15.000 g, as respect to EVs isolated at 110.000 g (25-fold change).

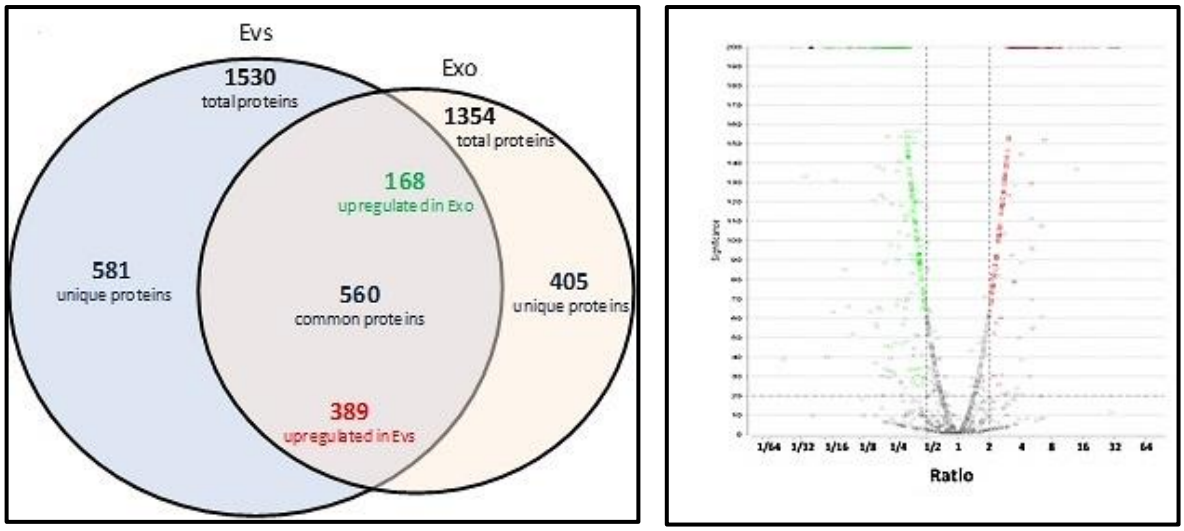

Figure 18 *- Venn diagram and Volcano Plot showing the identified proteins (unique, common and up/down regulated) between EVs and Exo. Left: 560 proteins were identified as common to both samples with differences in relative abundance lower than 2-fold; 405 proteins were exclusively present in EVs pelleted at 15.000 g, while 581 were unique of EVs isolated at 110.000 g. Right: Volcano plot of significantly differentially expressed proteins between Evs and Exo samples. X-axis is the fold change of differentially accumulated proteins represented with the ratio (Evs/Exo), and Y axis is the corresponding significance. Fold change >= 2 and T-test P-value < 0.05 were set as the significant threshold for differential expression. Green color represent down-regulated proteins and red color represent up-regulated proteins (15.000 g EVs/ 110.000 g EVs)*

Proteomic data confirmed the results obtained from western blot analysis concerning the expression of exosomes markers such as Alix, (Uniprot Acc. Q9WU78) identified among the differentially accumulated protein, with lower abundances in microvesicles as respect to exosomes (0.12-fold change).

Hsp70 (Uniprot Acc. P17879 and P16627) and RAB5 (Uniprot Acc. P35278 and Q9CQD1) were identified in both EVs fractions (15,000 g and 110,000 g) without any relative difference in relative abundances. This apparent discrepancy between the western blot analysis may be due by the higher sensibility of the spectrometric analysis. Interesting among the list of top 100 proteins that are often identified in exosomes (derived from exocarta) 44 proteins were also identified in our experiments.

Moreover, the gene interaction network analysis, performed by Fun-Rich (Figure 19) showed that both EVs proteins isolated at 15,000 g and 110,000 g are significantly interconnected with Ubc, Eed, Mib and Foxp3 proteins, while only EVs proteins obtained at 110,000 g, significantly associated with Hdac1. The list of total proteins identified in EVs pelleted ad 15,000 g A) and

EVs pelleted at 110,000 g B) was uploaded and interaction analysis tool was used to obtain the diagrams. Green and Red spheres indicate interacting and selected genes, respectively.

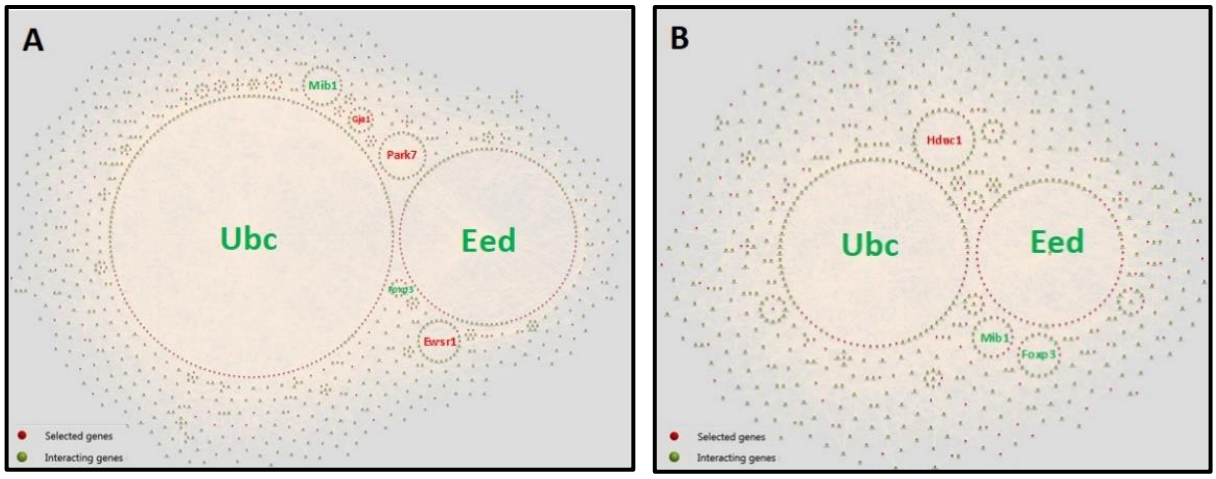

Figure 19 - *Interaction diagrams of EVs pelleted at 15.000 g and 110.000 g identified proteins performed by Fun-Rich*

4.4. Lipid composition of ultracentrifuged EVs

Lipidomic analysis were carried out to investigate the lipid composition of ultracentrifuged EVs fractions obtained at 15,000 g and 110,000 g.

Overall, as shown in the figure below, both microvesicles and small/large EVs are composed by similar categories of lipids, mainly represented by: glycerolipids (GL), sphingolipids (SP), glycerophospholipids (GP), fatty acyls (FA) and sterols (ST). Lipid composition of fractions was slightly different between microvesicles (15,000 g) and small/large EVs (110,000 g), with a decrease in abundance of some glycerolipids (GL) and an increase of sphingolipids (SP), some fatty acyl (FA) and glycerophospholipids (GP) observed in microvesicles as compared to small/large EVs (**Figure 20**). On contrary, small/large EVs seemed to be mainly composed of some triradylglycerols, secosteroids, glycerophosphoserines, glycerophosphoethanolamines and some fatty amides (**figure 20**).

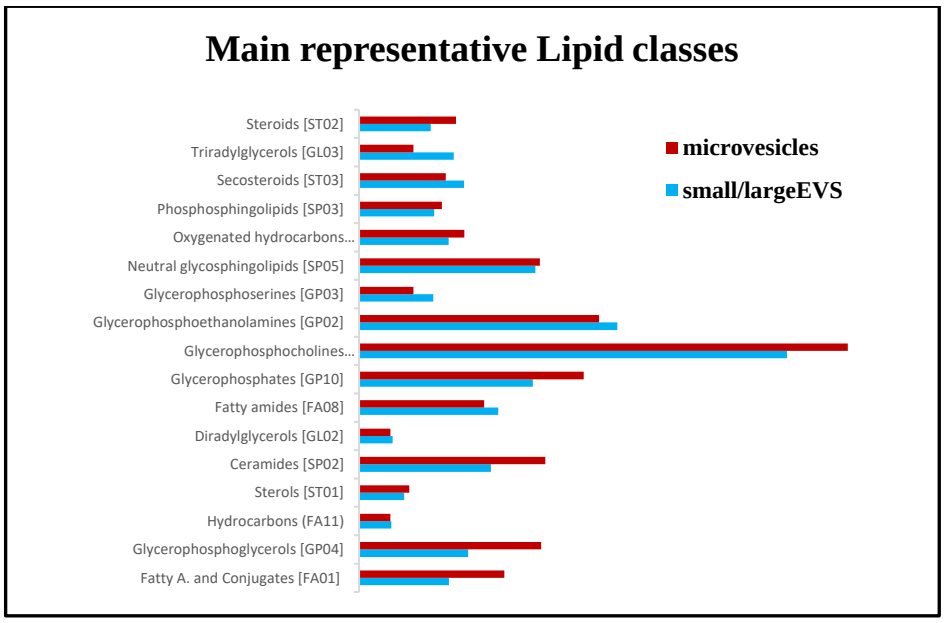

Figure 20 – *Lipidomic analysis of microvesicles pelleted at 15.000 g (red) and small/large EVs pelleted at 110.000 g (light blue)*

4.5. Size exclusion chromatography (SEC) and tangential flow filtration (TFF) as alternative EVs isolation protocols

Currently, standard differential centrifugation/density-gradient ultracentrifugation is the most used protocol for the isolation of extracellular vesicles; however, it may be challenging, since it tends to co-isolate proteins and other contaminant together with vesicles of interest. To overcome this problem, we decided to work on the evaluation of different protocols of isolation (free of any ultracentrifugation step), mainly using techniques based on the separation of particles by different diameters, such as size exclusion chromatography (SEC) and tangential flow filtration (TFF).

Before proceeding with EVs purification, the two techniques were first set through the aid of two different synthetic lipid nano-emulsions of a similar size from that of natural vesicles: 100 nm TPM-A1-T5 formulation for exosomes and 350 nm B-I312-H1 formulation for microparticles. So, the two types of synthetic lipid nanoparticles were first formulated through the technique of warm microemulsion, further purified by using TFF (data not shown) and SEC protocols and finally characterized by the use of DLS and TRPS technologies.

As regard SEC purification, 20 fractions of 500 µL each of TPM-A1-T5 formulation were first collected and subsequently characterized by DLS; size distribution of the most relevant fractions (7, 8, 9 and 10) shown a Z-Average of 127 nm (**Figure 21**).

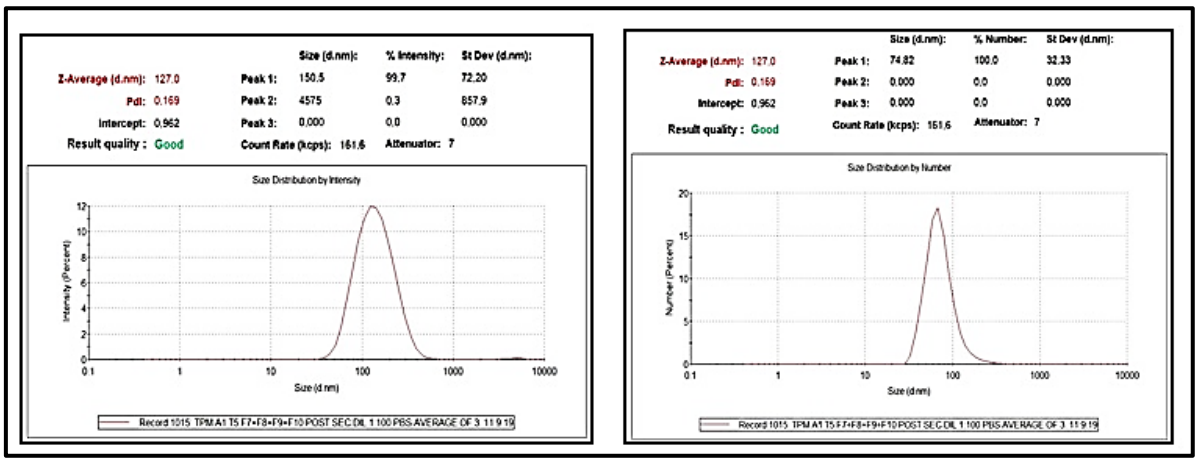

Figure 21 - *Zetasizer size distribution by intensity and by number of synthetic lipid nanoparticles TPM-A1-T5 purified with SEC. Left: size distribution by intensity of TPM-A1-T5 nanoparticles purified with SEC, with a main peak of 150,5 nm (99,7 %). Right: size distribution by number of TPM-A1-T5, with a main peak of 74,82 nm (100 %), respectively. Average of 3.*

To emulate the diameter of microvesicles, B-I312-H1 formulation (of around 300-350 nm) was first prepared, purified through TFF (data not shown) and SEC and finally characterized by DLS and TRPS technologies. DLS analysis of post-SEC fractions 7, 8, 9 and 10 shown a Z-Average (d.nm) of 336,6 nm, with a main peak of 403,8 nm (99, 4 %) and 304,7 nm (82,4 %) for intensity and number distribution respectively (**Figure 22**).

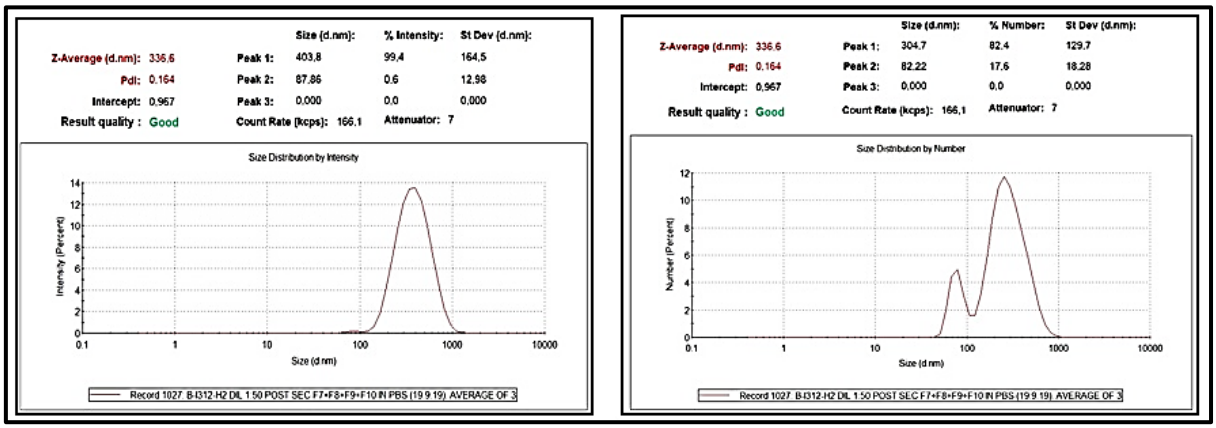

Figure 22 - *Zetasizer size distribution by intensity and by number of synthetic lipid nanoparticles B-I312-H1 purified with SEC. Left: size distribution by intensity of B-I312-H1 fractions (7-10) after SEC purification. Right: size distribution by number of B-I312-H1 fractions (7-10) after SEC purification. Average of 3.*

To better understand the percentage of recovery after SEC purification, we also decided to evaluate, for each SEC fraction of each formulation, the correlation between the size Z-average distribution and the number of particles read as derived count rate (DCR). This latter, is a parameter representative of the scattering intensity measured in the absence of the laser

attenuation filter; it gives a qualitative analysis of the quantity of read particles and is calculated with the formula: *Derived count rate= (Measured Count Rate)/(Attenuation Factor)*.

As shown in the graphs below, the highest percentage of recovery was in fractions 8-10, for both formulations, with a percentage of almost 50 % for TPM-A1-T5 and up to 15 % for B-I312-H1 (**Figure 23**). These data were also in line with qEVoriginal column data sheet, which suggests an elution profile in fraction 7-10 for 500 µL sample loading.

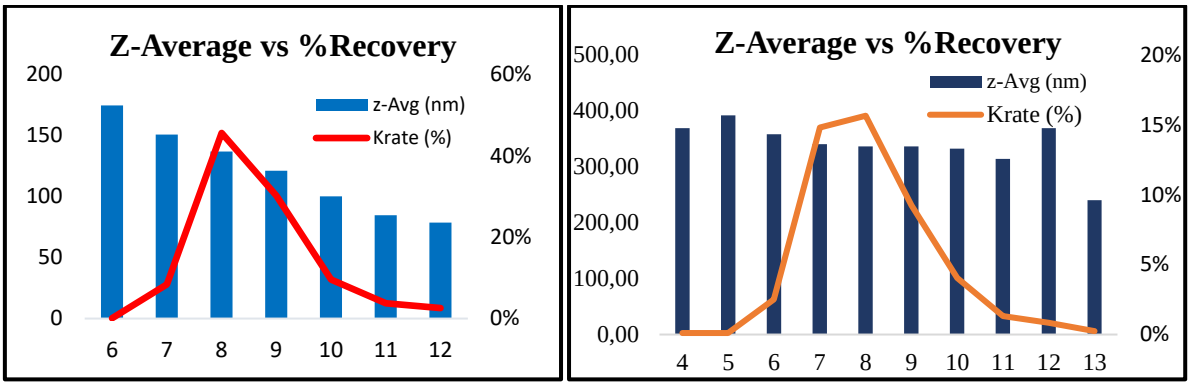

Figure 23 *- Graphic representation of Z-average vs % Recovery of the lipid nanoemulsions TPM-A1-T5 fractions (left) and B-I312-H1 (right) after SEC purification. Correlation between the diameter of particles (Z-Average) in each fraction (blue bars) and the number of particles read at Zetasizer as Derived Count Rate (red and orange lines respectively). Left Y-axis: Z-Average distribution; right Y-axis: percentage of recovery; X-axis: SEC fractions*

To have a comparison with DLS obtained data, synthetic nanoparticles isolated with TFF (data not shown) and SEC protocols, were further evaluated by using tunable resistive pulse sensing technique (TRPS). Unlike DLS, in TRPS system no laser are involved, but a voltage is applied across a pore that is filled with an electrolyte solution for the establishment of an ionic current. As particles cross the pore, they briefly increase the electrical resistance, creating a resistive pulse called blockade event, which is proportional to the particle volume. The rate of flow of particles is proportional to the particle concentration, thus obtaining also a particle number estimation (IZON, 2014). Therefore, larger particles produce a higher resistance and a larger blockade magnitude, while smaller particles generate a lower resistance with a smaller blockade magnitude (**Figure 24**).

TRPS instrument has 5 main components: a fluid cell (where electrodes and sample are located) further divided in upper cell (upper electrode) and lower cell (lower electrode), a nanopore (a polyurethane membrane with a central hole where the sample pass through), a shielding cap (to isolate the electrodes from external interferences), a variable pressure module-VPM (used for concentration measurement, particle mobility and surface charge analysis of the particles) and a base instrument hosting a handle to adjust the nanopore stretch (**Figure 24**).

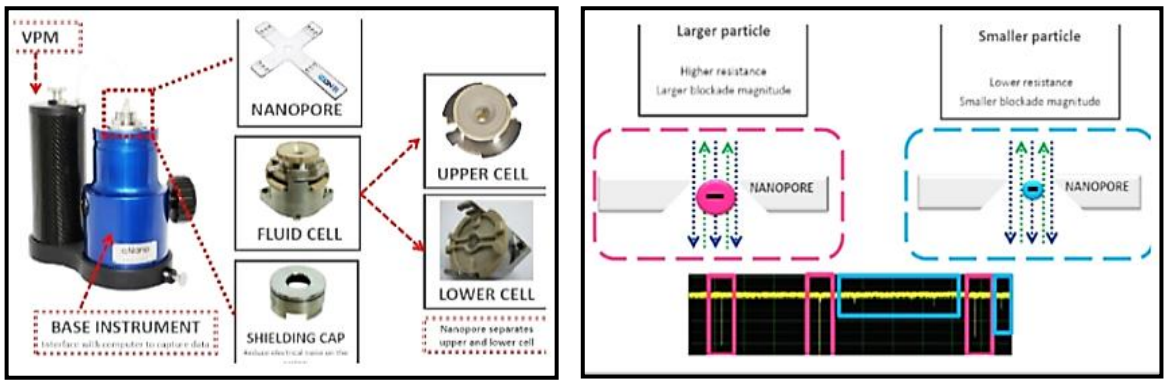

Figure 24 - *qNano instrument. Left: individual components. Right: Generation of blockade event (yellow peaks)*

To use TRPS instrument, a non-conductive nanopore was placed on the 4 arms of the machine and a voltage (dependent on the size of the nanopore) was applied. Then, an electric baseline current was established, filling the two upper and lower fluid cells electrodes with filtered and degassed PBS. For TPM-A1-T5 formulation, a nanopore-NP 200 (with a size range of 85-500 nm) was used, and three different measurements were performed at 4 different pressures: 13, 10, 7 and 5 mbar respectively. Overall, all the measurements conducted shown a similar trend, with an abundance of nanoparticles in the range of 100-150 nm (**Figure 25**). As concern B-I312-H1 formulation, a nanopore-NP 400 (size range of 185-1500 nm) was used, and three different measurements were performed at three different pressures: 10, 7 and 5 mbar respectively. Since in larger nanopores the electrokinetic forces are less than smaller nanopores, we decided to use only three pressure values, rather than the four values used for TPM-A1-T5 formulation (IZON, 2014). Overall, the measurements conducted shown a similar trend, with an enrichment of nanoparticles in the range of 200-350 nm (**Figure 25**).

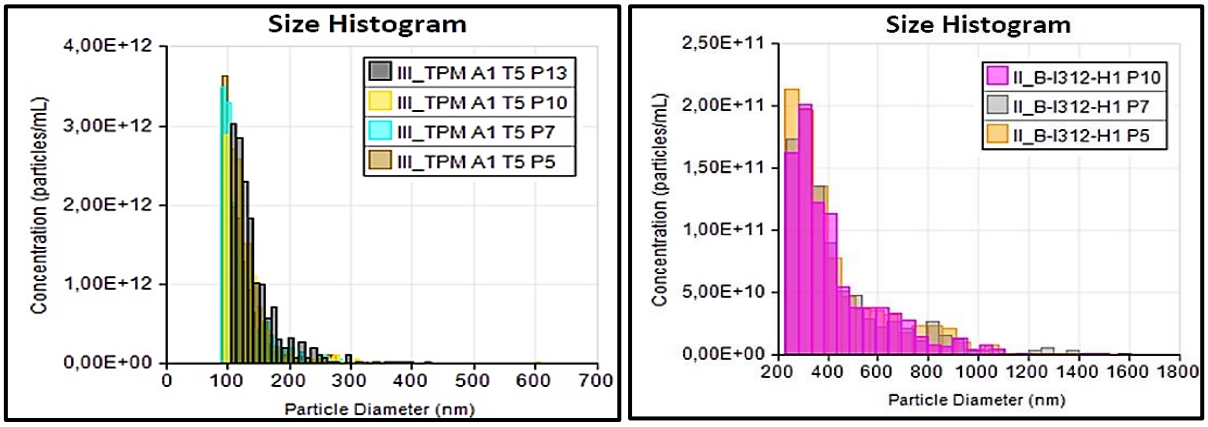

Figure 25 – *Group report histogram of particle diameter vs concentration of TPM-A1-T5 (7, 8 and 9) and B-I312-H1 (7, 8, 9 and 10) formulations fractions post SEC, using nanopores of 200 nm and 400 nm, respectively. Left: size histogram of particle diameter (˜100-300 nm) vs concentration (4,00 E+12) of TPM-A1-T5 fractions. Right: size histogram of particle diameter (˜250-800 nm) vs concentration (2,00 E+11) of B-I312-H2 fractions. Image representative of three measurements at four and three different pressures (13, 10, 7, and 5 mbar), respectively.*

4.6. EVs isolation through size exclusion chromatography (SEC) and tangential flow filtration (TFF)

Once having set TFF and SEC isolation protocols with the aid of synthetic nanoparticles, we further decided to investigate their purification efficiency for the isolation of EVs, evaluating their possible use as alternative technologies to the common ultracentrifugation. This is primarily due by the fact that EVs isolation through differential centrifugation/density-gradient ultracentrifugation may be a challenge, primarily because of the presence of proteins and other contaminant which tend to co-isolate with the vesicles of interest.

For both protocols, C2C12 cell culture medium was first collected from cell flasks and centrifuged by low differential centrifugations to remove dead cells, after which it was processed by TFF and SEC protocols.

As concern SEC, pre-purified cell culture medium was washed, concentrated up to 500 µL and finally loaded to a commercial qEVoriginal column of 70 nm range (provided by IZON Science Ltd.). Then, a total of 20 fractions of 500 µL each were collected and subjected to morpho-dimensional analysis through DLS and TRPS techniques. DLS analysis of isolated fractions demonstrated that most of the recovery was in fractions 7, 8 and 9, with a particle size range of 150-200 nm (**Figure 26**).

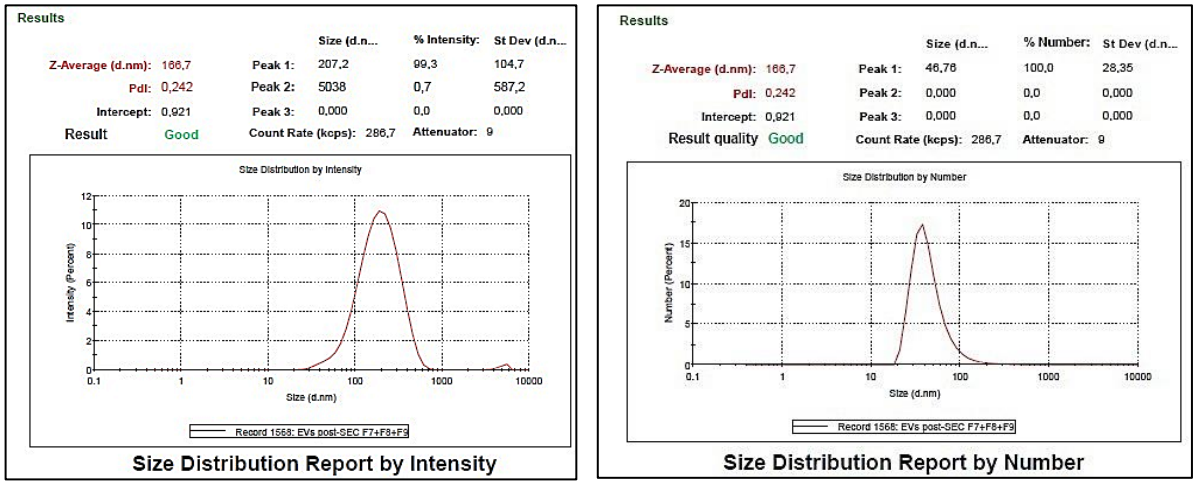

Figure 26 - *Zetasizer images of C2C12 myoblasts derived vesicles, isolated with SEC protocol. Left: EVs size distribution by intensity of fractions 7, 8 and 9 in PBS, with a Z-Average (d.nm) of 166,7 nm and a main peak of 207,2 nm (99,3 %). Right: EVs size distribution by number of fraction 7, 8 and 9 in PBS, with a Z-Average (d.nm) of 166,7 nm and a main peak of 46,76 nm (100 %). Average of three measurements.*

The percentage of recovery for biological nanovesicles, examined by the correlation between the Z-average size distribution and the number of particles read as derived count rate (DCR) in

each SEC fraction, seemed to be in fractions 7, 8 and 9, with just over 20 % of particles recovered (**Figure 27**).

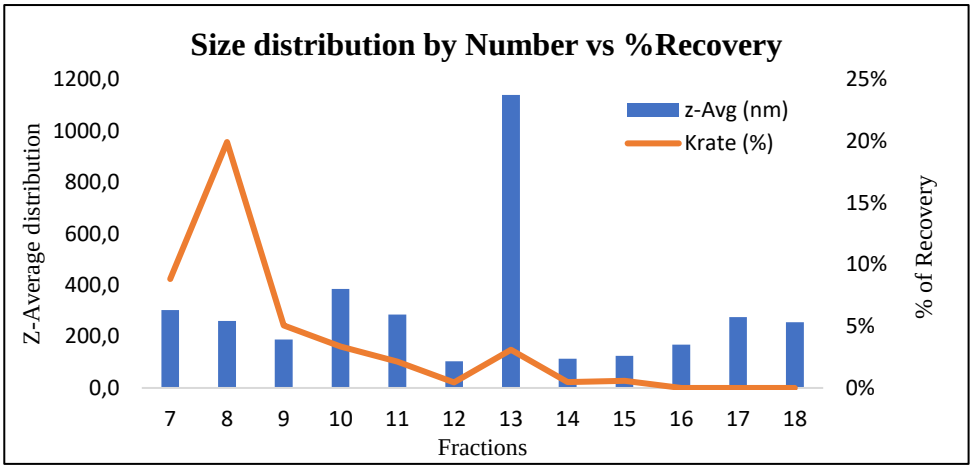

Figure 27 - *Z-Average distribution vs Derived Count Rate (DCR) of SEC Fractions 7-18. Correlation between the Z-Average distribution by size (blue bars) and the number of particles read as Derived Count Rate (orange line), in each fraction.*

These data were also in line with qEVoriginal column data sheet, which suggests that typical elution profile of 500 µL sample should be in fractions 7-10. However, the Z-average distribution was not decreasing by increasing the number of eluted fraction, as one would expect when using SEC technology, probably due by the presence of some aggregates or interfering molecules within the PBS.

Purified SEC fractions were further characterized by tunable resistive pulse sensing (TRPS) technique using qNano instrument (provided by IZON Science Ltd.). However, when performing TRPS analysis, one should keep in mind that the overall size distribution of biological vesicles is widely heterogeneous, with a higher polydispersion index as compared to synthetic nanoparticles; therefore, measuring EVs in biological samples may often result in nanopore clogging, with interruptions of particle rate plot and generation of inaccurate EVs concentration estimations.

For the analysis of EVs fractions (7, 8 and 9) post SEC, a non-conductive nanopore-NP 80 (size range 40-255 nm) was placed on the 4 arms of the machine, stretched at 49,50 mm and a voltage (dependent on the size of the nanopore) was applied. The instrument was first set through the establishment of an electric baseline current (generated by filling the two upper and lower fluid cells electrodes with filtered and degassed PBS), and two different measurements were performed at 84,30 nA, using pressure values of: 10, 7 and 5 mbar, respectively. It was not possible to perform the third measurement, due to the presence of very large particles that they were clogging the nanopore (probably resulting from non-sterile PBS), thus affecting all

the analysis. However, the overall trend of data collected revealed a particle diameter mean and mode of around 160 nm and 110 nm respectively, with an abundance of nanoparticles in the range of 100-150 nm (**Figure 28**).

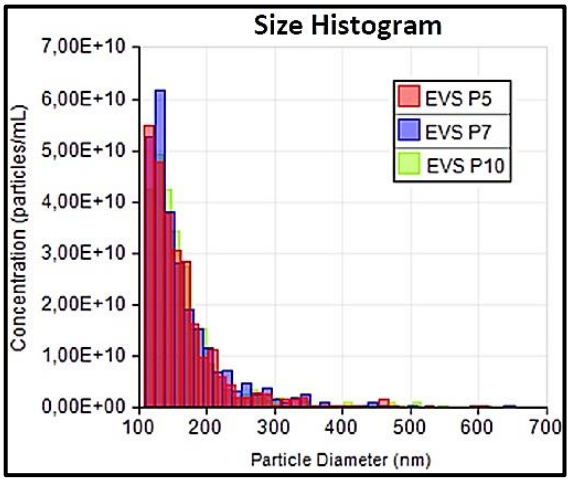

Figure 28 - *Group report histogram of EVs fractions post SEC (7, 8 and 9), using a nanopore-NP 80 at pressures: 5, 7 and 10 mbar. X-axis: particle diameter (nm); Y-axis: particle concentration (particle/mL). Image representative of two measurements.*

Similarly to SEC, biological vesicles were also purified with TFF and further characterized through DLS and TRPS technologies. As shown in the figure below, DLS analysis revealed that most of the recovered particles had a size range between 200-250 nm (**Figure 29**).

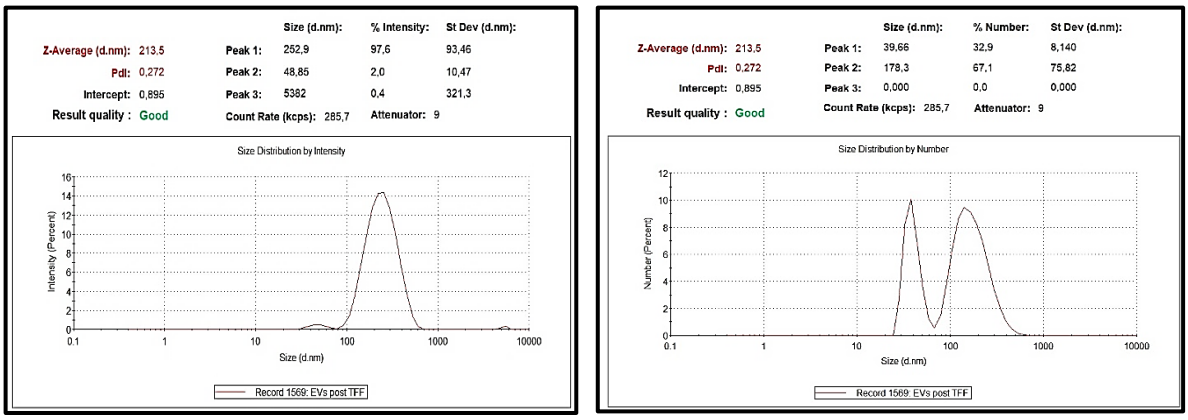

Figure 29 - *Zetasizer images of C2C12 myoblasts derived vesicles, isolated with TFF protocol. Left: EVs size distribution by intensity with a Z-Average (d.nm) of 213,5 nm and a main peak of 252,9 nm (97,6 %). Right: EVs size distribution by number with a Z-Average (d.nm) of 213,5 nm and a main peak of 178,3 nm (67,1 %). Average of three measurements.*

On the basis of DLS results, we decided to use a nanopore-NP 200 (size range 85-500 nm) for TRPS analysis of purified TFF vesicles, which was stretched at 47,26 mm and three different measurements were performed at 69,67 nA, at pressures: 10, 7 and 5 mbar, respectively.

We noticed that, unlike SEC protocol, TFF purified EVs were more spread (**Figure 30**). Overall, all measurements conducted had a similar trend, with an abundance of nanoparticles in the range of 200 nm, and a particle diameter mean and mode of around 250 nm and 190 nm respectively (**Figure 30**). This could be explained by the fact that in TFF we have all population sorted, while when using SEC protocol, particles population is sorted on the basis of its different size.

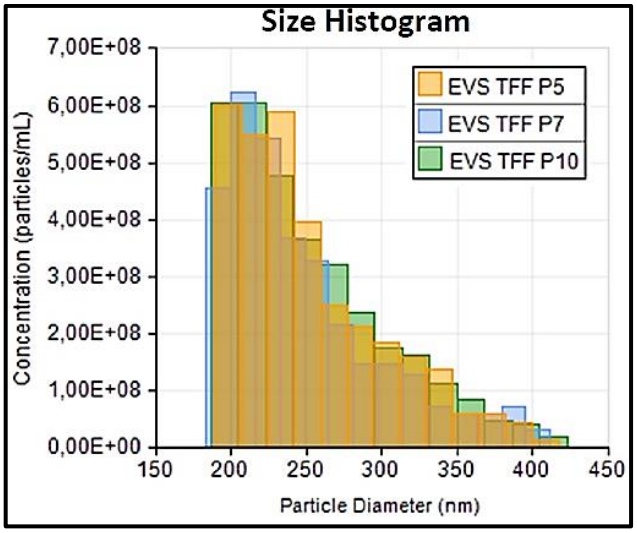

Figure 30 *- Groups report histogram of EVs isolated through TFF. X-axis: particle diameter (nm); Y-axis: particle concentration (particle/mL). Image representative of three measurements.*

5. Discussion

Skeletal muscle tissue plays an important role in human function, being involved in vital processes such as locomotion and respiration. Generally, muscle mass is balanced from a continuous cycle of protein synthesis and protein degradation; however, if this homeostasis is altered, it may lead to the development of specific myopathies, such as sarcopenia and cachexia (Bowen, 2015).

This latter, is a multifactorial syndrome represented by different pathological conditions, such as weight loss, anorexia, loss of muscle mass, systemic inflammation and insulin resistance, which lead to a global functional decline (Fearon, 2011). Despite its gravity, there is still a lack in successful therapeutic interventions, since most of the treatments used so far, resulted not effective, thus provoking its underestimation (Tazi, 2010).

Currently, most used therapeutic approaches are based on pharmacological therapies, mainly focused on the use of appetite stimulants (e.g. megestrol acetate, L-carnitine and melatonin), anti-inflammatory drugs (thalidomide and pentoxyphylline), monoclonal antibodies and ghrelin agonist anamorelin (Von Haehling, 2014). However, most of these drugs demonstrated conflicting results, showing only few auspicious results (**Table 6**).

Drug	Experimental animals	Humans
Progesterone derivatives	++	++
Cannabinoids	++	+
Cyproheptadine	+	+
Corticosteroids	–	–
Ghrelin	++	++
Pentoxifylline	++	?
Thalidomide	+	+
Anti-cytokine antibodies and soluble receptors	+++	–
Anti-inflammatory cytokines	++	?
Anabolic steroids	++	++
β2-adrenergic agonists	+++	?
ω-3-fatty acids	++	++
Prostaglandin inhibitors	++	+
ACE inhibitors	++	?
EPO	?	++
ATP	?	+
Creatine	?	+
Amino acids	++	+
Proteasome inhibitors	?	?

Table 6 – *Efficiency of the different anti-cachexia treatments (Argilés, 2010)*

Despite these limitations, recent literature suggested exercise as a positive modulator of cachexia and other cancer-associated disorders. Indeed, growing evidences proposed chronic exercise as a low-cost and safe defensive tool against systemic inflammations, which positively

modulates muscle metabolism (Lira, 2014). Overall, it promotes the attenuation of some of those signalling pathways related with protein degradation (e.g. FoxO, myostatin and ROS pathways), as well as the activation of specific molecules involved in protein synthesis and mitochondrial biogenesis (i.e. IGF-1 and PGC-1α transcriptor factor) (Belloum, 2017). However, despite its well-documented beneficial effects in the treatment of muscle wasting, only few studies focused on the effect of exercise training in cancer cachexia (Pin, 2015) (Ranjbar, 2019) (Padrão, 2017). For instance, our group of research has recently demonstrated a positive role of endurance training in the treatment of cachectic mice, which stimulated the expression of the mitochondrial chaperonine Hsp60, followed by a further increase of PGC-1α levels (Barone, 2016).

In line with these previous results, the aim of the PhD project focused on the execution of preliminary experiments for the development of a biological drug, based on natural, or engineered, nanovesicles against cachexia. In particular, the group have already isolated biological nanovesicles able to stimulate, in murine myoblast cells, one of the effects induced by endurance training performed by healthy mice. They demonstrated that cell culture medium of C2C12 cells, an immortalized myoblast cell line that simulates the characteristics of muscle cells, transfected with the plasmid pCMV-6-Entry-HSPD1, promote the activation of the mitochondrial biogenesis pathway, to which PGC-1α co-factor belongs (Barone, 2016). Physiactisome, the name of this new drug, aims to be the first direct drug on the treatment of muscle wasting, with the potential to be customizable, since it can be developed directly from muscle stem cells of the patient.

As shown in a recent research, cancer cells are able to release HSP60 protein through lipid raft-exosome pathway; in this alternative secretion mechanism, the chaperonine, previously accumulated in the cytoplasm of the cells, translocates to the periphery of the cells, where it interacts with the lipid rafts of the membrane and localizes on exosome vesicles (Caruso Bavisotto, 2017). Moreover, it was shown that the medium of C2C12 cells transfected with a plasmid overexpressing for Hsp60 protein was able, *in vitro*, to trigger the transcription of PGC-1α and its isoform PGC-1α1, probably thanks to the activity of Hsp60 chaperonine (Barone, 2016). Therefore, on the basis of these evidences, we presumed that the secretion of Hsp60 protein may occur within exocytic vesicles, keeping in mind that Hsp60 protein may be also released in a free active form in the extracellular space.

So, to prove our hypothesis, C2C12 cells were transfected with both pCMV6-Entry-HSPD1 plasmid (expressing for murine HSP60), and its negative control pCMV6-Entry plasmid (empty plasmid). Confocal microscopy analysis confirmed the presence of positive transfected cells, which were positive not only for Myc-DDK tag, (a small oligonucleotide coding for a protein

kinase), present in both plasmids, but also for HSP60 (present only in pCMV6-Entry-HSPD1 plasmid) (Figure 7). However, the antibiotic selection of positive C2C12 transfected clones has not given the desired results, since non- transfected cells acquired antibiotic resistance characteristics, even using high concentration of antibiotic (Figure 8); indeed, cells continued to grow and, more importantly, positive clones lost the plasmid or died, since we couldn't no longer see the expression signal for either HSP60 and Myc-DDK tag (data not shown). So, we speculated that cells tend reject the plasmid, while maintaining the gene for antibiotic resistance, as they continued to grow.

To solve the problem, we decided to design a new plasmid with a different resistance gene, able to facilitate the selection of positive transfected cells, hoping to achieve better results. Among all the possible selection antibiotics, the choice fell on Hygromycin B, an aminoglycoside able of inhibiting protein synthesis of different cells, thus provoking its death in about 48 hours. Once proved the efficacy of free Hygromycin B on C2C12 cells (Figure 9), we further decided to modify and design a new plasmid pIRES-hrGFP-1a-Hyg, (already available at the Human Anatomy laboratories of the Polyclinic of Palermo) in which it was inserted the gene module for hygromycin antibiotic. Unlike the previous plasmid pCMV6-Entry, pIRES-hrGFP-1a-Hyg plasmid was also equipped with green fluorescent human protein (hrGFP), allowing the direct observation of transfected cells under fluorescence microscopy, thus avoiding time-consuming and unreliable methods of fixing cells methods. The hrGFP coding sequence is placed in a distant area from MCS site within pIRES-hrGFP-1a-Hyg plasmid, avoiding the production of a fusion GFP protein, which was instead important in the sequence DDK-tag of pCMV6-Entry plasmid.

The transfection of C2C12 cells with the new plasmid occurred by using an electroporator, an instrument able to generate high voltage electrical impulses, provoking the temporary formation of cell membrane channels (permeabilization), thus allowing the cellular uptake of various molecules which could not spontaneously cross the plasma membrane under physiological conditions. So, C2C12 were first electroporated with the empty control pIRES-hrGFP-1a-Hyg plasmid (with no HSP60 sequence), using different electroporation optimization protocols (Table 3), in order to evaluate the best transfection condition able to give the highest transfection efficiency. Flow cytometry analysis of these transfected cells, revealed that only conditions C3 (1300 V, 2 pulses, 30 °A) and D2 (1150 V, 2 pulses, 30 °A) seem to be the best options for the highest efficiency (**Table 5**). Overall, the new plasmid resulted less toxic as compare to the old one, also confirmed by the confocal microscopy images, in which dividing positive green transfected cells were observed (Figure 12). Despite these preliminary results, in the next experiments it will be necessary to clone Hsp60 gene (HSPD1 sequence) inside the

pIRES-hrGFP-1a-Hyg plasmid, for its insertion within C2C12 cells and the production of high levels of extracellular vesicles bearing Hsp60 protein.

Currently, physiactisome drug is at the preclinical phase, at the level of animal testing phase, and its production is based on the engineering of muscle cells (transfected with a plasmid expressing for Hsp60 protein) able to release high amounts of extracellular vesicles carrying Hsp60. These tiny vesicles may be then used as a delivery system able to bind to the plasma membrane of muscle cells, activating muscle cells repair in all those chronic conditions responsible for muscle atrophy (e.g. cancer, Alzheimer's and heart dysfunction). Physiactisome may be a promising biological drug, able to increase the quality of life of patients, also improving the effectiveness of other therapies. Since the production of this innovative drug is based on biological vesicles, we also focused our attention at some isolation and characterization protocols currently used for the recovery of extracellular vesicles, in order to better study their characteristics to use in the design of engineered nanoparticles, similar to those already discovered.

It was first demonstrated that, even in basal conditions, cultured non transfected C2C12 cells are able to release extracellular vesicles of 50-250 nm in the cell culture medium (**Figure 14-16**), containing some of their most characteristic biomarkers, such as Alix and Rab5 (proteins involved in the biogenesis of EVs), as well as Hsp70, as confirmed by western blotting analysis. These data were also in line with the previous work of Romancino and his collaborators, who have confirmed the presence of Alix protein in C2C12 nanovesicles (Romancino, 2013). Moreover, the work of Guescini and colleagues also demonstrated the presence of extracellular vesicles with an average diameter of 90-99 nm (therefore only exosomes) in the culture medium of C2C12 cells both normal and treated with hydrogen peroxide (Guescini, 2017).

However, despite western blot analysis of ultracentrifuged extracellular vesicles were negative for Hsp60 protein (Figure 17), label free quantitative proteomic data detected its presence, with an abundance 25 folds higher in microvesicles than exosomes (Figure 18). Moreover, proteomic analysis have identified many and common protein profiles between microvesicles and exosomes (**Figure 18**).

Studies of interaction network, revealed a considerable interconnection with the ubiquitin protein (Ubc), for both exosome and the rest of nano-vesicle proteins (**Figure 19**). This molecule is involved in the degradation of altered proteins, through its interaction with the ubiquitin-proteasome system (UPS), one of the major proteolytic machinery systems activated during cachexia (Khal, 2005). In addition, a considerable association was also identified between EVs proteins and two important epigenetic regulators: embryonic ectoderm development (Eed) and histone deacetylase 1 (Hdac1). These genes encode for important

proteins involved in the regulation of chromatin structure, as well as in the control of cell development and differentiation during embryogenesis. For instance, HDAC1 as a component of the histone deacetylase complex, may play an important role in those gene alterations that trigger the development of muscle wasting processes (Tseng, 2015).

Despite the growing interest in the use of EVs as diagnostic and therapeutic tool of pathologies, understanding their physical composition is still a concern, and most of the current researches primarily focused on proteic and nucleic acid characterization of EVs, leaving aside studies on their lipid composition. Indeed, only a few EVs lipidomic studies have been performed so far, also due by the lack of specific standardized isolation methods and the difficulties in the evaluation of pure EVs samples. Moreover, the choice of the lipidomic protocol to use, as well as the competence of the operators using these methods, may affect the interpretation of final data. Nonetheless, despite all these limitations, it is now known that lipid composition of most derived cultured cells EVs is mainly represented by cholesterol, sphingomyelin, glycosphingolipids, and phosphatidylserines (**Table 7**).

Lipids	PC-3 Cells (36)		PC-3 Cells + HG (38)		Oli-neu Cells (30)		HepG2/C3a (39)		B-Lymphocytes (40)		Mast Cells (41)		Dendritic Cells (41)		Reticulocytes (42)		Platelets (45)	Adipocytes (46)
	%	Factor	%	Factor	%[a]	Factor	%[a]	Factor	%	Factor	%[b]	Factor	%[b,c]	Factor	%	Factor	%	%[a]
CHOL	43.5	2.3	59	1.7	43	2.3	43	1.9	42.1	3.0	15	1.0	NR	NR	47	1.03	42.5	43
SM	16.3	2.4	9.1	2.0	8.2	1.5	9.7	10.8	23.0	2.3[d]	12	2.8	20	2.2	8.4[d]	1.31	12.5	12.5
PC	15.3	0.31	10.8	0.33	26.7	0.67	20	0.67	(20.3)[e]	(0.76)[e]	28	0.66	26	0.6	23.5	1.03	15.9	33
PS	11.7	2.1	6.9	1.2	14.9	3.0	15.6	2.4	(20.3)[e]	(0.76)[e]	(16)[e]	(1.2)[e]	(19)[e]	(1.6)[e]	5.9	0.92	10.5	1.1
PE	5.8	0.55	1.1	0.21	10.9	1.0	7.4	1.2	(14.6)[e]	(0.7)[e]	24	1.08	26	1.13	12.7	0.84	3.1	4.0
PE ethers	3.3	1.2	4.7	0.81					(14.6)[e]	(0.7)[e]							3.2	
DAG	1.5	1.5	1.1	0.92														0.8
PC ethers	0.81	0.40	0.7	0.28													1.4	
PG	0.17	0.17	0.1	0.07													NR	
PA	0.16	1.8	0.1	0.33					(20.3)[e]	(0.76)[e]							NR	
PI	0.13	0.13	0.3	0.16	NR		4.1	0.18	(20.3)[e]	(0.76)[e]	(16)[e]	(1.2)[e]	(19)[e]	(1.6)[e]	2.4	1.1	5.2	2.3
Cer	0.32	1.3	0.7	1.2	NR	3.3	0.63	2.0									0.40	0.2
HexCer	0.76	3.8	2.3	2.1		2.0												0.02
LacCer	0.12	3.0[f]	0.7	1.8		NR												

Table 7 - *Lipid composition of exosomes released by individual cell types (Skotland, 2019)*

In line with most of the data presented in the scientific literature, lipidomic analysis of ultracentrifugated EVs (microvesicles and small-EVs) reported the presence of five main lipid categories: glycerophospholipids (GP), glycerolipids (GL), sphingolipids (SP), fatty acyls (FA) and steroids (ST). Nonetheless, there were no substantial differences between the lipid composition of microvesicles and small-EVs, except for some glycerophospholipids, which were more abundant in microvesicles rather than exosomes, as well as glycerolipids, which were more represented in small-EVs fraction rather than in microvesicles (**Figure 20**). Moreover, the online evaluation through XCMS software confirmed that some of the most identified lipids belonged to Phosphatidylcholines (PC), an important component of plasma

membranes, despite the presence of this lipid should be less abundant in EVs than their parent cells (Skotland, 2017). This could be due by the fact that EVs isolation by ultracentrifugation could have also co-isolated some other lipid contaminants, such as lipid droplets or other plasma membrane fragments (Yuana, 2014).

Therefore, the choice of a specific isolation method is an important variable to assess when characterizing these vesicles, since it may influence the efficacy of EVs isolation (Patel G. , 2019). Based on this, we also decided to evaluate other different EVs isolation methods, in order to better understand their biological properties and compare obtained data in terms of EVs purity and quality. So, size exclusion chromatography, tangential flow filtration and Invitrogen total exosome isolation kit (data not shown) methods were also investigated as alternative isolation methods to the classic ultracentrifugation protocol, after having set the protocols with synthetic lipid nanoparticles of similar size to that of EVs, previously formulated by the technique of warm microemulsion (Gasco M. , 1989).

Size Exclusion Chromatography (SEC), is a technology widely used for the separation of heterogeneous samples based on their size, constituting one of the most promising isolation methods in the field of extracellular vesicles (Benedikter, 2017). Indeed, as compared to the classical ultracentrifugation technology, SEC is easy to perform, do not need specific equipments (e.g. ultracentrifuge) and provide a higher quality of isolated EVs, keeping their shape intact, which can instead be damaged by centrifuge force. Nowadays, various group of research have already widely used this technology, demonstrating its ability to obtain sorted purer vesicles subpopulations than ultracentrifugation (Benedikter, 2017) (Mol, 2017). However, one of its main drawbacks is that it dilutes the initial sample, causing its dispersion in several fractions, thus influencing the final yield and subsequent EVs analysis.

On the basis of DLS analysis performed in previous ultracentrifuged samples (**Figure 14-15**), a commercial 10 mL qEVoriginal column of 70 nm range (provided by IZON Science Ltd.) was used for the isolation of pre-centrifuged vesicles. However, this type of columns are only suitable for small sample volumes of about 0.5 ml, hence pre-centrifuged cell culture medium was further concentrated through stirred cell device, using a 100 kDa filter. DLS analysis confirmed that the majority of isolated EVs had a size range between 50 and 300 nm in diameter (**Figure 26-27**). To have an idea of the concentration value of isolated EVs, fractions containing vesicles (F7, F8 and F9) were further analyzed through tunable resistive pulse sensing, an innovative technology able to characterize size, concentration and Z-potential of biological vesicles (**Figure 28**). TRPS technology allows the investigation of small sample size in a short time and without the need to manipulate the sample. The only prerequisite for successful measurement is to maintain the same conditions between calibration and sample particles (i.e.

same sample buffers, instrument settings, nanopore size, voltage and applied pressure) (Maas, 2014). Nonetheless, one of its main limitations is due by the lack of an exact mechanism for the setting of the pressure VPM device, which frequently causes minor differences in applied pressure between samples. Moreover, evaporation of fluid in the VPM may provoke pressure differences if measuring at different time points.

Despite these downsides, C2C12 SEC fractions 7, 8 and 9 were pooled together, concentrated and further analyzed through qNano instrument (provided by IZON Science Ltd.). Overall, the size distribution of EVs was in the range of 100-300 nm (**Figure 28**). However, unlike synthetic nanoparticles (**Figure 21-25**), biological samples were more polydisperse, made by different size of vesicles that had often clogged the nanopore membrane, especially when using smaller nanopores where the electrokinetic forces increased. Moreover, sample contaminants (e.g. sugars, lipids, proteins and other larger debris present in cell culture medium) could have also influenced measurement conditions, affecting the quality of results. Nonetheless, the use of larger nanopores could eliminate the problem, although we noticed that increasing the diameter of the hole in the nanopores may affect the measurement of smaller vesicles, which would pass through it and would be read as background noise. Another possible solution could be filtration of the sample, but the results obtained would not reflect the real concentration value of the sample, since most of the vesicles would remain blocked in the filter, decreasing the final yield (Konoshenko, 2018).

Extracellular vesicles were also purified using tangential flow filtration (TFF), an alternative method of membrane filtration originally used for concentrating and desalting dissolved molecules (Zahka, 1985), but recently adapted in EVs isolation to improve their final yield (Haraszti, 2018). Here, cell culture medium is both concentrated and filtered, in one step, only using a peristaltic system, that can process large volume of medium, thus making the system scalable. Overall, membrane filtration technology can use direct flow filtration (DFF), also known as dead-end filtration, or and Tangential Flow Filtration (TFF). In the first case, the flow of the fluid is perpendicular to the membrane face (Iritani, 1995), while in TFF the feed stream passes parallel to the filter and is recirculated back to the feed reservoir (**Figure 31**).

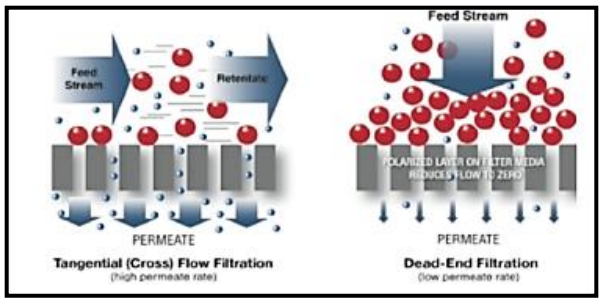

Figure 31 – *Dead end filtration vs tangential flow filtration*

So, similarly to SEC, tangential flow filtration was evaluated as an alternative size-based EV concentration method able of processing scalable volumes of biological fluids. C2C12 pre-centrifuged cell culture medium was purified through VIVAFLOW 50 Tangential Flow Filtration system (100,000 MWCO) and further characterized through DLS ant TRPS analysis. As confirmed in other studies (Busatto, 2018), the size distribution of isolated EVs ranged from 200-250 nm (**Figure 29**), with broader EVs peak diameters, as compared to ultracentrifugation and SEC methods. These data were further confirmed through tunable resistive pulse sensing measurements (**Figure 30**), where it was necessary to use a nanopore with a larger diameter than the nanopore used in SEC isolation. This could be explained by the fact that in TFF technology all EVs population are recovered, unlike SEC and ultracentrifugation, where only specific population are sorted. Therefore, standing to these results, we concluded that TFF technology often requires a second process of purification, often constituted by filtration, size-exclusion chromatography, or a sucrose density gradient, in order to achieve the optimal purity and yield. However, for a complete comparison among all these isolation methods, biochemical analysis focused on the identification of specific EVs biomarkers for the identification of the sub-type of isolated vesicles are needed, and are still under investigation.

6. Conclusions

Given the beneficial effects of physical activity on the general state of cachectic patients, Physiactisome® could represent the first customizable anti-cachectic drug able to act directly on skeletal muscle cells, thus mimicking the effects of exercise. Moreover, it could also improve the lifespan of cancer patients allowing, in parallel, the evaluation of other possible cancer therapies, which are often denied in terminal patients.

We found that *in vitro* transfection of cells was able to reproduce the positive effects of exercise in trained cachectic mice, as suggested by the overexpression of HSP60 protein and the activation of PGC-1α, both regulators of mitochondria biogenesis and muscle homeostasis. However, the efficiency of transfection was always very low, and we still need to design a stable cell line in order to obtain high quantities of product. In addition, since the drug should be based on biological vesicles, further studies are needed to better isolate and characterize these tiny particles. Extracellular vesicles can be isolated through different methods and, the choice of the best method depends on the characteristics of the initial sample. In addition, isolation step is often tricky, especially if the starting cells are under physiological conditions, since they tend to release lower levels of nanovesicles, making their analysis very difficult and linked to the volumes of medium harvested.

7. References

Aatonen, M. (2014). Isolation and characterization of platelet-derived extracellular vesicles. *J Extracell Vesicles.* doi:10.3402/jev.v3.24692

Abid Hussein, M. (2005). Cell-derived microparticles contain caspase 3 in vitro and in vivo. *J Thromb Haemost.*, 3(5):888-96. doi:10.1111/j.1538-7836.2005.01240.x

Abramowicz, A. (2019). Ionizing radiation affects the composition of the proteome of extracellular vesicles released by head-and-neck cancer cells in vitro. *Journal of Radiation Research*, 289–297. doi:10.1093/jrr/rrz001

Ahmadi Badi, S. (2017). Microbiota-Derived Extracellular Vesicles as New Systemic Regulators. *Front Microbiol.*, 8:1610. doi:10.3389/fmicb.2017.01610.

Akbarzadeh, A. (2013). Liposome: classification, preparation, and applications. *Nanoscale Res Lett*, 102. doi:10.1186/1556-276X-8-102

Akers, J. (2013). Biogenesis of extracellular vesicles (EV): exosomes, microvesicles, retrovirus-like vesicles, and apoptotic bodies. *J Neurooncol.*, 1-11. doi: 10.1007/s11060-013-1084-8

Akers, J. (2017). A cerebrospinal fluid microRNA signature as biomarker for glioblastoma. *Oncotarget.*, 8(40):68769-68779. doi:10.18632/oncotarget.18332.

Almiñana, C. (2020). Extracellular vesicles: Multi-signal messengers in the gametes/embryo-oviduct cross-talk. *Theriogenology.*, S0093-691X(20)30090-X. doi:10.1016/j.theriogenology.2020.01.077.

Al-Samadi, A. (2017). Crosstalk between tongue carcinoma cells, extracellular vesicles, and immune cells in in vitro and in vivo models. *Oncotarget.*, 8(36): 60123–60134. doi:10.18632/oncotarget.17768

Altan-Bonnet, N. (2016). Extracellular vesicles are the Trojan horses of viral infection. *Curr Opin Microbiol*, 77-81. doi:10.1016/j.mib.2016.05.004

Alvarez-Erviti, L. (2011). Delivery of siRNA to the mouse brain by systemic injection of targeted exosomes. *Nat. Biotechnol*, 341–345. doi:10.1038/nbt.1807

Amabile, N. (2005). Circulating endothelial microparticles are associated with vascular dysfunction in patients with end-stage renal failure. *J Am Soc Nephrol.*, 16(11):3381-8. doi:10.1681/ASN.2005050535

Anthony, T. (2016). Mechanisms of protein balance in skeletal muscle. *Domest Anim Endocrinol.*, S23-32. doi:10.1016/j.domaniend.2016.02.012.

Antonescu, C. (2011). Phosphatidylinositol-(4,5)-bisphosphate regulates clathrin-coated pit initiation, stabilization, and size. *Mol Biol Cell.*, 22(14): 2588–2600. doi:10.1091/mbc.E11-04-0362

Antonucci, F. (2012). Microvesicles released from microglia stimulate synaptic activity via enhanced sphingolipid metabolism. *EMBO J*, 1231–1240. doi:10.1038/emboj.2011.489

Antunes, D. (2014). Molecular insights into mitochondrial dysfunction in cancer-related muscle wasting. *Biochim Biophys Acta.*, 1841(6):896-905. doi:10.1016/j.bbalip.2014.03.004

Ardies, C. (2002). Exercise, cachexia, and cancer therapy: a molecular rationale. *Nutr Cancer.*, 42(2):143-57. doi:10.1207/S15327914NC422_1

Argilés, J. (2005). Molecular mechanisms involved in muscle wasting in cancer and ageing: cachexia versus sarcopenia. *Int J Biochem Cell Biol*, 37(5):1084-104. doi:10.1016/j.biocel.2004.10.003

Argilés, J. (2010). Optimal management of cancer anorexia-cachexia syndrome. *Cancer Manag Res*, 27-38. doi:10.2147/cmar.s7101

Aryani, A. (2016). Exosomes as a nanodelivery system: a key to the future of neuromedicine? . *Mol. Neurobiol* , 818–834. doi:10.1007/s12035-014-9054-5

Atkin-Smith, G. (2015). A novel mechanism of generating extracellular vesicles during apoptosis via a beads-on-a-string membrane structure. *Nat. Commun.*, 6:7439. doi:10.1038/ncomms8439

Aversa, Z. (2017). Cancer-induced muscle wasting: latest findings in prevention and treatment. *Ther Adv Med Oncol*, 9(5): 369–382. doi:10.1177/1758834017698643

Ayala, A. (1983). Primary bone tumors: percutaneous needle biopsy. Radiologic-pathologic study of 222 biopsies. *Radiology.*, 149(3):675-9. doi:10.1148/radiology.149.3.6580673

Babatz, J. (2003). Large-scale immunomagnetic selection of CD14+ monocytes to generate dendritic cells for cancer immunotherapy: a phase I study. *J Hematother Stem Cell Res.*, 12(5):515-23. doi:10.1089/152581603322448222

Babst, M. (2011). MVB Vesicle Formation: ESCRT-Dependent, ESCRT-Independent and Everything in Between. *Curr Opin Cell Biol*, 452–457. doi:10.1016/j.ceb.2011.04.008

Bache, K. (2003). Hrs regulates multivesicular body formation via ESCRT recruitment to endosomes. *J Cell Biol.*, 162(3): 435–442. doi:10.1083/jcb.200302131

Badimon, L. (2016). Role of Platelet-Derived Microvesicles As Crosstalk Mediators in Atherothrombosis and Future Pharmacology Targets: A Link between Inflammation, Atherosclerosis, and Thrombosis. *Front Pharmacol.*, 7: 293. doi:10.3389/fphar.2016.00293

Bagatolli, L. (2000). Giant phospholipid vesicles: comparison among the whole lipid sample characteristics using different preparation methods: A two photon fluorescence microscopy study. *Chemistry and Physics of Lipids*. doi:10.1016/S0009-3084(00)00118-3

Baietti, M. (2011). Syndecan–syntenin–ALIX regulates the biogenesis. *Nature Cell Biology*, 677-85. doi:10.1038/ncb2502

Bank, I. (2015). The diagnostic and prognostic potential of plasma extracellular vesicles for cardiovascular disease. *Expert Rev Mol Diagn.*, 15(12):1577-88. doi:10.1586/14737159.2015.1109450

Barile, L. (2017). Exosomes: Therapy delivery tools and biomarkers of diseases. *Pharmacol Ther*, 63-78. doi:10.1016/j.pharmthera.2017.02.020.

Barone, R. (2016). Skeletal muscle Heat shock protein 60 increases after endurance training and induces peroxisome proliferator-activated receptor gamma coactivator 1 α1 expression. *Sci Rep*, 6:19781. doi:10.1038/srep19781

Batrakova, E. (2015). Using exosomes, naturally-equipped nanocarriers, for drug delivery. *J Control Release*, 396-40. doi:10.1016/j.jconrel.2015.07.030

Beere, H. (2004). "The stress of dying": the role of heat shock proteins in the regulation of apoptosis. *J Cell Sci*, 2641-51. doi:10.1242/jcs.01284

Beez, C. (2019). Cardiac Extracellular Vesicles (EVs) Released in the Presence or Absence of Inflammatory Cues Support Angiogenesis in Different Manners. *Int J Mol Sci.*, 20(24): 6363. doi:10.3390/ijms20246363

Bei, Y. (2017). Extracellular Vesicles in Cardiovascular Theranostics. *Theranostics.*, 7(17): 4168–4182. doi:10.7150/thno.21274

Belizário, J. (2001). Cleavage of caspases-1, -3, -6, -8 and -9 substrates by proteases in skeletal muscles from mice undergoing cancer cachexia. *Br J Cancer*, 1135–1140. doi:10.1054/bjoc.2001.1700

Belloum, Y. (2017). Cancer-induced cardiac cachexia: Pathogenesis and impact of physical activity (Review). *Oncol Rep*, 2543-2552. doi:10.3892/or.2017.5542

Benedikter, B. (2017). Cigarette smoke extract induced exosome release is mediated by depletion of exofacial thiols and can be inhibited by thiol-antioxidants. *Free Radic Biol Med*, 334-344. doi:10.1016/j.freeradbiomed.2017.03.026

Benedikter, B. (2017). Ultrafiltration combined with size exclusion chromatography efficiently isolates extracellular vesicles from cell culture media for compositional and functional studies. *Sci. Rep*, 7:15297. doi:10.1038/s41598-017-15717-7

Benedikter, B. (2019). Proteomic analysis reveals procoagulant properties of cigarette smoke-induced extracellular vesicles. *J Extracell Vesicles*, 1585163. doi:10.1080/20013078.2019.1585163

Berckmans, R. (2001). Cell-derived microparticles circulate in healthy humans and support low grade thrombin generation. *Thromb Haemost.*, 85(4):639-46.

Bergsmedh, A. (2001). Horizontal transfer of oncogenes by uptake of apoptotic bodies. *Proc Natl Acad Sci U S A.*, 98(11):6407-11. doi:10.1073/pnas.101129998

Besterman, J. (1983). Endocytosis: a review of mechanisms and plasma membrane dynamics. *Biochem J.*, 210(1):1-13. doi:10.1042/bj2100001

Bettscheider, M. (2012). Optimized analysis of DNA methylation and gene expression from small, anatomically-defined areas of the brain. *J Vis Exp*, (65):e3938. doi:10.3791/3938

Bewicke-Copley, F. (2017). Extracellular vesicles released following heat stress induce bystander effect in unstressed populations. *J Extracell Vesicles.*, 6(1):1340746. doi:10.1080/20013078.2017.1340746

Bhatia, S. (2016). Nanoparticles Types, Classification, Characterization, Fabrication Methods and Drug Delivery Applications. *Natural Polymer Drug Delivery Systems*. doi:10.1007/978-3-319-41129-3_2

Bianchi, E. (2014). Izumo meets Juno: preventing polyspermy in fertilization. *Cell Cycle.*, 13(13):2019-20. doi:10.4161/cc.29461.

Bianchi, E. (2014). Juno is the egg Izumo receptor and is essential for mammalian fertilization. *Nature.*, 508(7497):483-7. doi:10.1038/nature13203.

Bick, R. (1992). Coagulation abnormalities in malignancy: a review. *Semin Thromb Hemost.*, 18(4):353-72. doi:10.1055/s-2007-1002575.

Bielaszewska, M. (2017). Host cell interactions of outer membrane vesicle-associated virulence factors of enterohemorrhagic Escherichia coli O157: Intracellular delivery, trafficking and mechanisms of cell injury. *PLoS Pathog.*, 13(2):e1006159. doi:10.1371/journal.ppat.1006159.

Bitto, N. (2017). Bacterial membrane vesicles transport their DNA cargo into host cells. *Sci Rep.*, 7(1):7072. doi:10.1038/s41598-017-07288-4.

Blanco, E. (2015). Principles of nanoparticle design for overcoming biological barriers to drug delivery. *Nat Biotechnol*. doi:10.1038/nbt.3330

Bloom, A. (1990). Physiology of blood coagulation. *Haemostasis.*, 1:14-29. doi:10.1159/000216159

Bode-Böger, S. (1998). L-arginine-induced vasodilation in healthy humans: pharmacokinetic-pharmacodynamic relationship. *Br J Clin Pharmacol.*, 46(5):489-97. doi:10.1046/j.1365-2125.1998.00803.x

Böing, A. (2014). Single-step isolation of extracellular vesicles by size-exclusion chromatography. *J Extracell Vesicles*. doi:10.3402/jev.v3.23430

Borroto-Escuela, D. (2015). The role of transmitter diffusion and flow versus extracellular vesicles in volume transmission in the brain neural-glial networks. *Philos Trans R Soc Lond B Biol Sci.*, 20140183. doi:10.1098/rstb.2014.0183

Boukouris, S. (2015). Exosomes in bodily fluids are a highly stable resource of disease biomarkers. *Proteomics Clin Appl.*, 9(3-4):358-67. doi:10.1002/prca.201400114.

Boulanger, C. (2001). Circulating microparticles from patients with myocardial infarction cause endothelial dysfunction. *Circulation.*, 104(22):2649-52. doi:10.1161/hc4701.100516

Boulanger, C. (2017). Extracellular vesicles in coronary artery disease. *Nat Rev Cardiol.*, 14(5):259-272. doi:10.1038/nrcardio.2017.7

Bowen, T. (2015). Skeletal muscle wasting in cachexia and sarcopenia: Molecular pathophysiology and impact of exercise training. *journal of Cachexia, Sarcopenia and Muscle*, 197-207. doi:10.1002/jcsm.12043

Brahmer, A. (2019). Platelets, endothelial cells and leukocytes contribute to the exercise-triggered release of extracellular vesicles into the circulation. *J Extracell Vesicles.*, 8(1):1615820. doi:10.1080/20013078.2019.1615820

Briggs, J. (2003). Structural organization of authentic, mature HIV-1 virions and cores. *EMBO J*, 1707–1715. doi:10.1093/emboj/cdg143

Brock, C. (2019). Stem cell proliferation is induced by apoptotic bodies from dying cells during epithelial tissue maintenance. *Nat Commun.*, 1044. doi:10.1038/s41467-019-09010-6

Brouwers, J. (2013). Distinct lipid compositions of two types of human prostasomes. *Proteomics*, 1660-6. doi:10.1002/pmic.201200348

Brown, P. (2017). Polymer-Based Purification of Extracellular Vesicles. *Methods Mol Biol*, 91-103. doi:10.1007/978-1-4939-7253-1_8

Brown, S. (2017). Basics of Skeletal Muscle Function and Normal Physiology. *Cardioskeletal Myopathies in Children and Young Adults*, 21-38. doi:org/10.1016/B978-0-12-800040-3.00002-9

Bulbake, U. (2017). Liposomal Formulations in Clinical Use: An Updated Review. *Pharmaceutics*, E12. doi:10.3390/pharmaceutics9020012

Busatto, S. (2018). Tangential Flow Filtration for Highly Efficient Concentration of Extracellular Vesicles from Large Volumes of Fluid. *Cells*, E273. doi:10.3390/cells7120273

Busatto, S. (2019). Organotropic drug delivery: Synthetic nanoparticles and extracellular vesicles. *Biomed Microdevices*, 46. doi:10.1007/s10544-019-0396-7

Cai, J. (2013). Extracellular vesicle-mediated transfer of donor genomic DNA to recipient cells is a novel mechanism for genetic influence between cells. *J Mol Cell Biol.*, 5(4):227-38. doi:10.1093/jmcb/mjt011.

Caldwell, R. (2018). Arginase: A Multifaceted Enzyme Important in Health and Disease. *Physiol Rev.*, 98(2):641-665. doi:10.1152/physrev.00037.2016.

Campanella, C. (2012). The Odyssey of Hsp60 from Tumor Cells to Other Destinations Includes Plasma Membrane-Associated Stages and Golgi and Exosomal Protein-Trafficking Modalities. *PLoS ONE*. doi:10.1371/journal.pone.0042008

Cantaluppi, V. (2015). Endothelial progenitor cell-derived extracellular vesicles protect from complement-mediated mesangial injury in experimental anti-Thy1.1 glomerulonephritis. *Nephrol Dial Transplant.*, 30(3):410-22. doi:10.1093/ndt/gfu364

Cantó, C. (2009). PGC-1alpha, SIRT1 and AMPK, an energy sensing network that controls energy expenditure. *Current Opinion in Lipidology*, 98-105. doi:10.1097/MOL.0b013e328328d0a4

Caruso Bavisotto, C. (2017). Exosomal HSP60: a potentially useful biomarker for diagnosis, assessing prognosis, and monitoring response to treatment. *Expert Rev Mol Diagn*, 815-822. doi:10.1080/14737159.2017.1356230

Catchpoole, D. R. (1995). Formation of apoptotic bodies is associated with internucleosomal DNA fragmentation during drug-induced apoptosis. *Exp. Cell Res.*, 216 169–177. doi:10.1006/excr.1995.1021

Cavalli, R. (2007). THE EFFECT OF ALCOHOLS WITH DIFFERENT STRUCTURES ON THE FORMATION OF WARM O/W MICROEMULSIONS. *Journal of Dispersion Science and Technology*, 717-734. doi:10.1080/01932699608943535

Cerezo-Magaña, M. (2019). The pleiotropic role of proteoglycans in extracellular vesicle mediated communication in the tumor microenvironment. *Semin Cancer Biol.*, S1044-579X(19)30162-2. doi:10.1016/j.semcancer.2019.07.001.

Chandra, D. (2003). Mitochondrially localized active caspase-9 and caspase-3 result mostly from translocation from the cytosol and partly from caspase-mediated activation in the organelle. Lack of evidence for Apaf-1-mediated procaspase-9 activation in the mitochondria. *J Biol Chem*, 278(19):17408-20. doi:10.1074/jbc.M300750200

Chargaff, E. (1946). The biological significance of the thromboplastic protein of blood. *J Biol Chem.*, 166(1):189-97.

Cheung, W. (2010). Inflammation and cachexia in chronic kidney disease. *Pediatr Nephrol*, 711–724. doi:10.1007/s00467-009-1427-z

Chiabotto, G. (2019). Salivary Extracellular Vesicle-Associated exRNA as Cancer Biomarker. *Cancers (Basel)*, 11(7): 891. doi:10.3390/cancers11070891

Chin, E. (2004). The role of calcium and calcium/calmodulin-dependent kinases in skeletal muscle plasticity and mitochondrial biogenesis. *Proc Nutr Soc*, 63(2):279-86. doi:10.1079/PNS2004335

Chinsomboon, J. (2009). The transcriptional coactivator PGC-1alpha mediates exercise-induced angiogenesis in skeletal muscle. *Proc Natl Acad Sci U S A*, 106(50):21401-6. doi:10.1073/pnas.0909131106

Chistiakov, D. (2015). Extracellular vesicles and atherosclerotic disease. *Cell. Mol.*, 2697–2708. doi:10.1007/s00018-015-1906-2

Chistiakov, D. (2017). α-Synuclein-carrying extracellular vesicles in Parkinson's disease: deadly transmitters. *Acta Neurol Belg*, 43–51. doi:10.1007/s13760-016-0679-1

Chivet, M. (2012). Emerging Role of Neuronal Exosomes in the Central Nervous System. *Front Physiol*, 3: 145. doi:10.3389/fphys.2012.00145

Choi. (2017). Structural Analysis of Exosomes Using Different Types. *Apllied Microscopy*, 171-175. doi:10.9729/AM.2017.47.3.171

Choi, D. (2014). Extracellular vesicles shed from gefitinib-resistant nonsmall cell lung cancer regulate the tumor microenvironment. *Proteomics*, 14(16):1845-56. doi:10.1002/pmic.201400008.

Choi, D. (2015). Isolation of extracellular vesicles for proteomic profiling. *Methods Mol Biol*, 167-77. doi:10.1007/978-1-4939-2550-6_14

Ciregia, F. (2017). Extracellular Vesicles in Brain Tumors and Neurodegenerative Diseases. *Front Mol Neurosci.*, 10:276. doi:10.3389/fnmol.2017.00276.

Cocucci, E. (2015). Ectosomes and exosomes: shedding the confusion between extracellular vesicles. *Trends Cell Biol.*, 25 364–372. doi:10.1016/j.tcb.2015.01.004

Coleman, M. (2001). Membrane blebbing during apoptosis results from caspase-mediated activation of ROCK I. *Nat. Cell Biol.*, 3 339–345. doi:10.1038/35070009

Colombo, M. (2013). Analysis of ESCRT functions in exosome biogenesis, composition and secretion highlights the heterogeneity of extracellular vesicles. *J Cell Sci*, 5553-65. doi:10.1242/jcs.128868

Colombo, M. (2014). Biogenesis, secretion, and intercellular interactions of exosomes and other extracellular vesicles. *Annu Rev Cell Dev Biol.*, 255-89. doi:10.1146/annurev-cellbio-101512-122326

Costelli, P. (1993). Tumor Necrosis Factor-a Mediates Changes in Tissue Protein Turnover. *J Clin Invest*, 92(6):2783–2789. doi:10.1172/JCI116897

Costelli, P. (2001). Activation of Ca2+-dependent proteolysis in skeletal muscle and heart in cancer cachexia. *Br J Cancer*, 84(7): 946–950. doi:10.1054/bjoc.2001.1696

Costelli, P. (2005). Ca(2+)-dependent proteolysis in muscle wasting. *Int J Biochem Cell Biol.*, 37(10):2134-46. doi:10.1016/j.biocel.2005.03.010

Costelli, P. (2006). IGF-1 is downregulated in experimental cancer cachexia. *Am J Physiol Regul Integr Comp Physiol*, 291(3):R674-83. doi:10.1152/ajpregu.00104.2006

Cuenca, A. (2006). Emerging implications of nanotechnology on cancer diagnostics and therapeutics. *Cancer*, 459-66. doi:10.1002/cncr.22035

Currow, D. (2018). Efficacy of Anamorelin, a Novel Non-Peptide Ghrelin Analogue, in Patients with Advanced Non-Small Cell Lung Cancer (NSCLC) and Cachexia—Review and Expert Opinion. *Int J Mol Sci*, 19(11): 3471. doi:10.3390/ijms19113471

Cvjetkovic, A. (2014). The influence of rotor type and centrifugation time on the yield and purity of extracellular vesicles. *J Extracell Vesicles.* doi:10.3402/jev.v3.23111

D'Souza, R. (2014). Rab4 Orchestrates a Small GTPase Cascade for Recruitment of Adaptor Proteins to Early Endosomes. *Curr Biol.*, 24(11):1187-98. doi:10.1016/j.cub.2014.04.003.

Dalli, J. (2008). Annexin 1 mediates the rapid anti-inflammatory effects of neutrophil-derived microparticles. *Blood*, 2512-2519. doi:10.1182/blood-2008-02-140533

Dalwadi, G. (2007). Purification of PEGylated Nanoparticles Using Tangential Flow Filtration (TFF). *Drug Development and Industrial Pharmacy*, 1030-9. doi:10.1080/03639040601180143

Davis, C. (2019). The importance of extracellular vesicle purification for downstream analysis: A comparison of differential centrifugation and size exclusion chromatography for helminth pathogens. *PLoS Negl Trop Dis*, e0007191. doi:10.1371/journal.pntd.0007191

de Toledo, M. (2019). Extracellular Vesicles in Fungi: Composition and Functions. *Curr Top Microbiol Immunol*, 45-59. doi:10.1007/82_2018_141

Del Conde, I. (2005). Tissue-factor-bearing microvesicles arise from lipid rafts and fuse with activated platelets to initiate coagulation. *Blood.*, 106(5):1604-11. doi:10.1182/blood-2004-03-1095

Diaz, L. (2014). Liquid Biopsies: Genotyping Circulating Tumor DNA. *J Clin Oncol.*, 32(6): 579–586. doi:10.1200/JCO.2012.45.2011

Diaz-Hidalgo, L. (2016). Transglutaminase type 2-dependent selective recruitment of proteins into exosomes under stressful cellular conditions. *Biochim Biophys Acta.*, 1863(8):2084-92. doi:10.1016/j.bbamcr.2016.05.005

Dickens, A. (2017). Astrocyte-shed extracellular vesicles regulate the peripheral leukocyte response to inflammatory brain lesions. *Sci Signal*, eaai7696. doi:10.1126/scisignal.aai7696

Dinarello, C. (1986). Tumor necrosis factor (cachectin) is an endogenous pyrogen and induces production of interleukin 1. *J Exp Med*, 163(6): 1433–1450. doi:10.1084/jem.163.6.1433

Ding, M. (2018). Comparison of commercial exosome isolation kits for circulating exosomal microRNA profiling. *Anal Bioanal Chem*, 3805-3814. doi:10.1007/s00216-018-1052-4

Dipak, K. (2005). Engineering of Nanoemulsions for Drug Delivery. *Current Drug Delivery*. doi:10.2174/156720105774370267

Drummond, I. (1987). The role of oxidative stress in the induction of Drosophila heat-shock proteins. *Exp Cell Res*, 439-49. doi:10.1016/0014-4827(87)90284-9

Du, J. (2004). Activation of caspase-3 is an initial step triggering accelerated muscle proteolysis in catabolic conditions. *J Clin Invest*, 113(1): 115–123. doi:10.1172/JCI200418330

Dua, J. (2012). LIPOSOME: METHODS OF PREPARATION AND APPLICATIONS. *International Journal of Pharmaceutical Studies and Research*, 14-20.

Egan, B. (2010). Exercise intensity-dependent regulation of peroxisome proliferator-activated receptor coactivator-1 mRNA abundance is associated with differential activation of upstream signalling kinases in human skeletal muscle. *J Physiol*, 588(Pt 10):1779-90. doi:10.1113/jphysiol.2010.188011

Eguchi, A. (2016). Circulating adipocyte-derived extracellular vesicles are novel markers of metabolic stress. *J Mol Med.*, 1241–1253. doi:10.1007/s00109-016-1446-8.

Eguchi, A. (2019). Circulating Extracellular Vesicles and Their miR "Barcode" Differentiate Alcohol Drinkers With Liver Injury and Those Without Liver Injury in Severe Trauma Patients. *Front Med (Lausanne).*, 6:30. doi:10.3389/fmed.2019.00030

Eldh, M. (2010). Exosomes communicate protective messages during oxidative stress; possible role of exosomal shuttle RNA. *PLoS One.*, 5(12):e15353. doi:10.1371/journal.pone.0015353.

Elizondo, E. (2011). Liposomes and other vesicular systems: structural characteristics, methods of preparation, and use in nanomedicine. *Prog Mol Biol Transl Sci*, 1-52. doi:10.1016/B978-0-12-416020-0.00001-2

Endzeliņš, E. (2017). Detection of circulating miRNAs: comparative analysis of extracellular vesicle-incorporated miRNAs and cell-free miRNAs in whole plasma of prostate cancer patients. *BMC Cancer.*, 17(1):730. doi: 10.1186/s12885-017-3737-z

Endzeliņš, E. (2018). Extracellular Vesicles Derived from Hypoxic Colorectal Cancer Cells Confer Metastatic Phenotype to Non-metastatic Cancer Cells. *Anticancer Res.*, 38(9):5139-5147. doi:10.21873/anticanres.12836.

Escobedo, J. (2003). Improved transfection technique for adherent cells using a commercial lipid reagent. *Biotechniques*, 936-8. doi:10.2144/03355bm06

Escola, J. (1998). Selective enrichment of tetraspan proteins on the internal vesicles of multivesicular endosomes and on exosomes secreted by human B-lymphocytes. *J Biol Chem*, 20121-7. doi:10.1074/jbc.273.32.20121

Eva, P. (2016). Aerobic Exercise and Pharmacological Treatments Counteract Cachexia by Modulating Autophagy in Colon Cancer. *Scientific Reports*, 6:26991. doi:10.1038/srep26991

Fares, J. (2017). Syntenin: Key player in cancer exosome biogenesis and uptake? *Cell Adh Migr*, 124–126. doi:10.1080/19336918.2016.1225632

Fearon, K. (2011). Definition and classification of cancer cachexia: an international consensus. *Lancet Oncol*, 489-95. doi:10.1016/S1470-2045(10)70218-7

Feng, D. (2010). Cellular internalization of exosomes occurs through phagocytosis. *Traffic*, 675–687. doi:10.1111/j.1600-0854.2010.01041.x

Fernandez-Marcos, P. (2011). Regulation of PGC-1α, a nodal regulator of mitochondrial biogenesis. *Am J Clin Nutr*, 93(4): 884S–890S. doi:10.3945/ajcn.110.001917

Fernández-Messina, L. (2015). Immunomodulatory role of microRNAs transferred by extracellular vesicles. *Biol Cell.*, 107(3):61-77. doi:10.1111/boc.201400081

Fili, N. (2006). Compartmental signal modulation: Endosomal phosphatidylinositol 3-phosphate controls endosome morphology and selective cargo sorting. *Proc Natl Acad Sci U S A.*, 103(42): 15473–15478. doi:10.1073/pnas.0607040103

Finck, B. (2006). PGC-1 coactivators: inducible regulators of energy metabolism in health and disease. *J Clin Invest*, 116(3): 615–622. doi:10.1172/JCI27794

Fitzner, D. (2011). Selective transfer of exosomes from oligodendrocytes to microglia by macropinocytosis. *J Cell Sci*, 447-58. doi:10.1242/jcs.074088

Fleisher, T. (1997). Apoptosis. *Ann Allergy Asthma Immunol.*, 245-250. doi:10.1016/S1081-1206(10)63176-6

Freeman, D. (2018). Altered Extracellular Vesicle Concentration, Cargo, and Function in Diabetes. *Diabetes.*, 67(11):2377-2388. doi:10.2337/db17-1308.

Friand, V. (2015). Syntenin and syndecan in the biogenesis of exosomes. *Biol Cell*, 331-41. doi:10.1111/boc.201500010. Epub 2015 Jun 30

Friedman, J. (2013). Endoplasmic reticulum–endosome contact increases as endosomes traffic and mature. *Mol Biol Cell.*, 24(7): 1030–1040. doi:10.1091/mbc.E12-10-0733.

Frühbeis, C. (2013). Extracellular vesicles as mediators of neuron-glia communication. *Front Cell Neurosci*, 7: 182. doi:10.3389/fncel.2013.00182

Frühbeis, C. (2013). Neurotransmitter-Triggered Transfer of Exosomes Mediates Oligodendrocyte–Neuron Communication. *PLoS Biol*, e1001604. doi:10.1371/journal.pbio.1001604

Frühbeis, C. (2015). Physical exercise induces rapid release of small extracellular vesicles into the circulation. *J Extracell Vesicles*, 4:28239. doi:10.3402/jev.v4.28239

Frühbeis, C. (2019). Oligodendrocyte-derived exosomes promote axonal transport and axonal long-term maintenance. *bioRxiv*. doi:10.1101/2019.12.20.884171

Gamez-Valero, A. (2016). Size-exclusion chromatography-based isolation minimally alters extracellular vesicles' characteristics compared to precipitating agents. *Sci. Rep*, 6:33641. doi:10.1038/srep33641

Gao, X. (2017). Extracellular Vesicles from Adipose Tissue-A Potential Role in Obesity and Type 2 Diabetes? *Front Endocrinol (Lausanne).*, 8:202. doi:10.3389/fendo.2017.00202

Garbuz, D. (2017). The evolution of heat shock genes and expression patterns of heat shock proteins in the species from temperature contrasting habitats. *Genetika*, 12-30. doi:10.1134/S1022795417010069

Garcia, N. (2016). Cardiomyocyte exosomes regulate glycolytic flux in endothelium by direct transfer of GLUT transporters and glycolytic enzymes. *Cardiovasc Res.*, 109(3):397-408. doi:10.1093/cvr/cvv260.

Garcìa-Manrique, P. (2018). Fully Artificial Exosomes: Towards New Theranostic Biomaterials. *Trends Biotechnol*, 10-14. doi:10.1016/j.tibtech.2017.10.005

Garcìa-Manrique, P. (2018). Therapeutic biomaterials based on extracellular vesicles: classification of bioengineering and mimetic preparation routes. *J Extracell Vesicles*, 1422676. doi:10.1080/20013078.2017.1422676

Garzetti, L. (2014). Activated macrophages release microvesicles containing polarized M1 or M2 mRNAs. *J Leukoc Biol.*, 95(5):817-825. doi:10.1189/jlb.0913485

Gasco, M. (1989). Microemulsions as topical delivery vehicles: ocular administration of timolol. *J Pharm Biomed Anal*, 433-9. doi:10.1016/0731-7085(89)80030-5

Gasco, M. (2009). Chapter 10 - Solid lipid nanoparticles and microemulsions for drug delivery The CNS. *Prog Brain Res.*, 181-92. doi:10.1016/S0079-6123(08)80010-6

Gener Lahav, T. (2019). Melanoma-derived extracellular vesicles instigate proinflammatory signaling in the metastatic microenvironment. *Int J Cancer.*, 145(9):2521-2534. doi:10.1002/ijc.32521.

Gercel-Taylor, C. (2012). Nanoparticle analysis of circulating cell-derived vesicles in ovarian cancer patients. *Anal Biochem*, 44-53. doi:10.1016/j.ab.2012.06.004

Gheldof, D. (2017). Procoagulant activity of extracellular vesicles as a potential biomarker for risk of thrombosis and DIC in patients with acute leukaemia. *J Thromb Thrombolysis*, 224–232. doi:10.1007/s11239-016-1471-z

Ghossoub, R. (2014). Syntenin-ALIX exosome biogenesis and budding into multivesicular bodies are controlled by ARF6 and PLD2. *Nat Commun*, 3477. doi:10.1038/ncomms4477

Gill, M. (2019). Placental Syncytiotrophoblast-Derived Extracellular Vesicles Carry Active NEP (Neprilysin) and Are Increased in Preeclampsia. *Hypertension.*, 73(5):1112-1119. doi:10.1161/HYPERTENSIONAHA.119.12707.

Gkretsi, V. (2018). Cell Adhesion and Matrix Stiffness: Coordinating Cancer Cell Invasion and Metastasis. *Front Oncol.*, 8:145. doi:10.3389/fonc.2018.00145.

Glebov, O. (2006). Flotillin-1 defines a clathrin-independent endocytic pathway in mammalian cells. *Nat Cell Biol.*, 46–54. doi:10.1038/ncb1342

Gleyzer, N. (2005). Control of mitochondrial transcription specificity factors (TFB1M and TFB2M) by nuclear respiratory factors (NRF-1 and NRF-2) and PGC-1 family coactivators. *Mol Cell Biol*, 25(4):1354-66. doi:10.1128/MCB.25.4.1354-1366.2005

Gnopo, Y. (2017). Designer outer membrane vesicles as immunomodulatory systems - Reprogramming bacteria for vaccine delivery. *Adv Drug Deliv Rev.*, 114:132-142. doi:10.1016/j.addr.2017.05.003.

Goettsch, C. (2016). Sortilin mediates vascular calcification via its recruitment into extracellular vesicles. *J Clin Invest.*, 126(4):1323-36. doi:10.1172/JCI80851

Gomari, H. (2018). Targeted cancer therapy using engineered exosome as a natural drug delivery vehicle. *Onco Targets Ther*, 5753–5762. doi:10.2147/ott.s173110

Göran Ronquist, K. (2019). Extracellular vesicles and energy metabolism. *Clin Chim Acta.*, 488:116-121. doi:10.1016/j.cca.2018.10.044.

Gould, D. (2013). Cancer cachexia prevention via physical exercise: molecular mechanisms. *J Cachexia Sarcopenia Muscle*, 111–124. doi:10.1007/s13539-012-0096-0

Groot Kormelink, T. (2018). The role of extracellular vesicles when innate meets adaptive. *Semin Immunopathol.*, 40(5):439-452. doi:10.1007/s00281-018-0681-1.

Guescini, M. (2017). Extracellular Vesicles Released by Oxidatively Injured or Intact C2C12 Myotubes Promote Distinct Responses Converging toward Myogenesis. *Int J Mol Sci*, E2488. doi:10.3390/ijms18112488

Guix, F. (2018). Detection of Aggregation-Competent Tau in Neuron-Derived Extracellular Vesicles. *Int J Mol Sci*, E663. doi:10.3390/ijms19030663

Gupta, A. (2004). Detection of fetal DNA and RNA in placenta-derived syncytiotrophoblast microparticles generated in vitro. *Clin Chem.*, 50(11):2187-90. doi:10.1373/clinchem.2004.040196.

Gupta, S. (2018). An improvised one-step sucrose cushion ultracentrifugation method for exosome isolation from culture supernatants of mesenchymal stem cells. *Stem Cell Res Ther*, 9(1):180. doi:10.1186/s13287-018-0923-0

Gutierrez-Vazquez, C. (2013). Transfer of extracellular vesicles during immune cell-cell interactions. *Immunol. Rev.*, 125–142. doi:10.1111/imr.12013

Ha, D. (2016). Exosomes as therapeutic drug carriers and delivery vehicles across biological membranes: current perspectives and future challenges. *Acta Pharm. Sin.* , 287–296. doi:10.1016/j.apsb.2016.02.001

Haga, H. (2015). Tumour cell-derived extracellular vesicles interact with mesenchymal stem cells to modulate the microenvironment and enhance cholangiocarcinoma growth. *J. Extracell. Vesicles*, 4:24900. doi:10.3402/jev.v4.24900

Hahn, G. (1991). Mammalian stress proteins HSP70 and HSP28 coinduced by nicotine and either ethanol or heat. *Mol Cell Biol*, 6034–6040. doi:10.1128/mcb.11.12.6034

Haldar, S. (2015). Chaperonin-Assisted Protein Folding: Relative Population of Asymmetric and Symmetric GroEL:GroES Complexes. *J Mol Biol*, 2244-55. doi:10.1016/j.jmb.2015.04.009

Han, C. (2019). Syncytiotrophoblast-Derived Extracellular Vesicles in Pathophysiology of Preeclampsia. *Front Physiol.*, 10:1236. doi:10.3389/fphys.2019.01236.

Han, J. (2018). Interleukin-6 induces fat loss in cancer cachexia by promoting white adipose tissue lipolysis and browning. *Lipids Health Dis*, 17: 14. doi:10.1186/s12944-018-0657-0

Handschin, C. (2008). The role of exercise and PGC1α in inflammation and chronic disease. *Nature*, 463-9. doi:10.1038/nature07206

Haney, M. (2015). Exosomes as drug delivery vehicles for Parkinson's disease therapy. *J. Control. Release*, 18–30. doi:10.1016/j.jconrel.2015.03.033

Hanson, P. (2012). Multivesicular body morphogenesis. *Annu Rev Cell Dev Biol*, 337-62. doi:10.1146/annurev-cellbio-092910-154152

Haraszti, R. (2016). High-resolution proteomic and lipidomic analysis of exosomes and microvesicles from different cell sources. *J Extracell Vesicles*, 5:32570. doi:10.3402/jev.v5.32570

Haraszti, R. (2018). Exosomes Produced from 3D Cultures of MSCs by Tangential Flow Filtration Show Higher Yield and Improved Activity. *Mol Ther*, 2838-2847. doi:10.1016/j.ymthe.2018.09.015

Hartl, F. (1992). Protein folding in the cell: the role of molecular chaperones Hsp70 and Hsp60. *Annu Rev Biophys Biomol Struct*, 293-322. doi:10.1146/annurev.bb.21.060192.001453

Hasegawa, J. (2017). PI5P and PI(3,5)P2: Minor, but Essential Phosphoinositides. *Cell Struct Funct.*, 42(1): 49–60. doi:10.1247/csf.17003

Hessvik, N. (2018). Current knowledge on exosome biogenesis and release. *Cell. Mol. Life Sci*, 193–208. doi:10.1007/s00018-017-2595-9

Heydenreich, A. (2003). Preparation and purification of cationic solid lipid nanospheres—effects on particle size, physical stability and cell toxicity. *International Journal of Pharmaceutics*, 83-7. doi:10.1016/S0378-5173(02)00688-9

Higa-Nakamine, S. (2015). Involvement of Protein Kinase D1 in Signal Transduction from the Protein Kinase C Pathway to the Tyrosine Kinase Pathway in Response to Gonadotropin-releasing Hormone. *J Biol Chem*, 25974-85. doi:10.1074/jbc.M115.681700

Hirata, E. (2017). Tumor Microenvironment and Differential Responses to Therapy. *Cold Spring Harb Perspect Med.*, 7(7): a026781. doi:10.1101/cshperspect.a026781

Hisada, Y. (2019). Cancer cell-derived tissue factor-positive extracellular vesicles. *Current Opinion in Hematology*, 349-356. doi:10.1097/MOH.0000000000000521

Hope, M. (1986). Generation of multilamellar and unilamellar phospholipid vesicles. *Chemistry and Physics of Lipids*. doi:10.1016/0009-3084(86)90065-4

Horváth, I. (2008). Membrane-associated stress proteins: More than simply chaperones. *Biochim Biophys Acta*, 1653-64. doi:10.1016/j.bbamem.2008.02.012

Huang, J. (1998). Role of calpain in skeletal-muscle protein degradation. *Proc. Natl. Acad. Sci. USA*, 12100–12105. doi:10.1073/pnas.95.21.12100

Huber, V. (2018). Tumor-derived microRNAs induce myeloid suppressor cells and predict immunotherapy resistance in melanoma. *The Journal of Clinical Investigation*, 128(12):5505-5516. doi:10.1172/JCI98060

Huotari, J. (2011). Endosome maturation. *EMBO J.*, 30(17): 3481–3500. doi:10.1038/emboj.2011.286

Hurwitz, S. (2016). Proteomic profiling of NCI-60 extracellular vesicles uncovers common protein cargo and cancer type-specific biomarkers. *Oncotarget.*, 7(52): 86999–87015. doi:10.18632/oncotarget.13569

Hutcheson, J. (2018). Extracellular vesicles in cardiovascular homeostasis and disease. *Curr Opin Cardiol*, 290-297. doi:10.1097/HCO.0000000000000510

Hyunseok, J. (2016). Size dependent classification of heat shock proteins: a mini-review. *J Exerc Rehabil*, 255–259. doi:10.12965/jer.1632642.321

Iraci, N. (2017). Extracellular vesicles are independent metabolic units with asparaginase activity. *Nat Chem Biol.*, 13(9):951-955. doi:10.1038/nchembio.2422.

Iritani, E. (1995). Upward Dead-End Ultrafiltration of Binary Protein Mixtures. *Separation science and technology*. doi:10.1080/01496399508013877

Irrcher, I. (2008). AMP-Activated Protein Kinase-Regulated Activation of the PGC-1α Promoter in Skeletal Muscle Cells. *PLoS One*, 3(10): e3614. doi:10.1371/journal.pone.0003614

Ishida, R. (2018). Physicochemical Properties of the Mammalian Molecular Chaperone HSP60. *International Journal of Molecular Sciences.* doi:10.3390/ijms19020489

Iwai, K. (2016). Isolation of human salivary extracellular vesicles by iodixanol density gradient ultracentrifugation and their characterizations. *J Extracell Vesicles*, 5:30829. doi:10.3402/jev.v5.30829

IZON. (2014). *qNano training modules.*

Jang, S. (2013). Bioinspired exosome-mimetic nanovesicles for targeted delivery of chemotherapeutics to malignant tumors. *ACS Nano*, 7698-710. doi:10.1021/nn402232g

Ji, Q. (2020). Primary tumors release ITGBL1-rich extracellular vesicles to promote distal metastatic tumor growth through fibroblast-niche formation. *Nat Commun*, 1211. doi:10.1038/s41467-020-14869-x

Jia, Y. (2016). miRNAs in Urine Extracellular Vesicles as Predictors of Early-Stage Diabetic Nephropathy. *J Diabetes Res.*, 2016:7932765. doi:10.1155/2016/7932765

Joffe, L. (2016). Potential Roles of Fungal Extracellular Vesicles during Infection. *mSphere*, e00099-16. doi:10.1128/mSphere.00099-16

Joseph, A. (2006). Control of gene expression and mitochondrial biogenesis in the muscular adaptation to endurance exercise. *Essays in Biochemistry*, 13–29. doi: 10.1042/bse0420013

Jovic, M. (2010). The early endosome: a busy sorting station for proteins at the crossroads. *Histol Histopathol.*, 25(1): 99–112. doi:10.14670/hh-25.99

Jun, S. (2013). Acinetobacter baumannii outer membrane vesicles elicit a potent innate immune response via membrane proteins. *PLoS One.*, 8(8):e71751. doi:10.1371/journal.pone.0071751.

Kalra, H. (2016). Focus on Extracellular Vesicles: Introducing the Next Small Big Thing. *Int J Mol Sci.*, 17(2):170. doi:10.3390/ijms17020170

Kang, C. (2013). Extracellular Vesicles Derived from Gut Microbiota, Especially Akkermansia muciniphila, Protect the Progression of Dextran Sulfate Sodium-Induced Colitis. *PLoS One.*, 8(10): e76520. doi:10.1371/journal.pone.0076520

Karlin, S. (2000). Heat shock protein 60 sequence comparisons: duplications, lateral transfer, and mitocondrial ecolution. *Proc Natl Acad Sci USA*, 11348-53. doi:10.1073/pnas.97.21.11348

Karnati, H. (2019). Neuronal Enriched Extracellular Vesicle Proteins as Biomarkers for Traumatic Brain Injury. *J Neurotrauma*, 975-987. doi:10.1089/neu.2018.5898

Kauppi, M. (2002). The small GTPase Rab22 interacts with EEA1 and controls endosomal membrane trafficking. *J Cell Sci.*, 115(Pt 5):899-911.

Kayacan, O. (2006). Impact of TNF-alpha and IL-6 levels on development of cachexia in newly diagnosed NSCLC patients. *Am J Clin Oncol*, 29(4):328-35. doi:10.1097/01.coc.0000221300.72657.e0

Kaye, S. (1988). The multidrug resistance phenotype. *Br J Cancer.*, 58(6): 691–694. doi:10.1038/bjc.1988.291.

Keklikoglou, I. (2019). Chemotherapy elicits pro-metastatic extracellular vesicles in breast cancer models. *Nat. Cell Biol*, 190–202. doi:10.1038/s41556-018-0256-3

Kerr, J. (1972). Apoptosis: A Basic Biological Phenomenon with Wide-ranging Implications in Tissue Kinetics. *Br J Cancer*, 239–257. doi:10.1038/bjc.1972.33

Kesimer, M. (2009). Characterization of exosome-like vesicles released from human tracheobronchial ciliated epithelium: a possible role in innate defense. *FASEB J*, 1858-68. doi:10.1096/fj.08-119131

Kesimer, M. (2015). Physical characterization and profiling of airway epithelial derived exosomes using light scattering. *Methods*, 87:59-63. doi:10.1016/j.ymeth.2015.03.013

Khal, J. (2005). Expression of the ubiquitin-proteasome pathway and muscle loss in experimental cancer cachexia. *Br J Cancer*, 93(7): 774–780. doi:10.1038/sj.bjc.6602780

Khatua, A. (2009). Exosomes packaging APOBEC3G confer human immunodeficiency virus resistance to recipient cells. *J. Virol*, 512–521. doi:10.1128/jvi.01658-08

Kim, D. (2018). Mastocytosis-derived extracellular vesicles exhibit a mast cell signature, transfer KIT to stellate cells, and promote their activation. *Proc Natl Acad Sci U S A.*, 115(45):E10692-E10701. doi: 10.1073/pnas.1809938115

Kim, M. (2016). Development of exosome-encapsulated paclitaxel to overcome MDR in cancer cells. *Nanomedicine.*, 12(3):655-664. doi:10.1016/j.nano.2015.10.012.

Kim, M. (2019). Delivery of High Mobility Group Box-1 siRNA Using Brain-Targeting Exosomes for Ischemic Stroke Therapy. *J Biomed Nanotechnol*, 2401-2412. doi:10.1166/jbn.2019.2866

Kim, O. (2015). Bacterial protoplast-derived nanovesicles as vaccine delivery system against bacterial infection. *Nano Lett.*, 15(1):266-74. doi:10.1021/nl503508h

Kim, O. (2017). Bacterial protoplast-derived nanovesicles for tumor targeted delivery of chemotherapeutics. *Biomaterials*, 68-79. doi:10.1016/j.biomaterials.2016.10.037

Kim, S. (1983). Preparation of multivesicular liposomes. . *Biochim Biophys Acta*, 339-48. doi:10.1016/0005-2736(83)90504-7

Kisho, O. (2018). HSP-enriched properties of extracellular vesicles involve survival of metastatic oral cancer cells. *Journal of Cellular Biochemistry*, 7350-7362. doi:10.1002/jcb.27039

Kleijmeer, M. (2001). Antigen loading of MHC class I molecules in the endocytic tract. *Traffic.*, 2(2):124-37. doi:10.1034/j.1600-0854.2001.020207.x

Klumperman, J. (2014). The complex ultrastructure of the endolysosomal system. *Cold Spring Harb Perspect Biol.*, 6(10):a016857. doi:10.1101/cshperspect.a016857

Knijff-Dutmer, E. (2002). Elevated levels of platelet microparticles are associated with disease activity in rheumatoid arthritis. *Arthritis Rheum.*, 46(6):1498-503. doi:10.1002/art.10312

Ko, S. (2019). Cancer-derived small extracellular vesicles promote angiogenesis by heparin-bound, bevacizumab-insensitive VEGF, independent of vesicle uptake. *Commun Biol.*, 2:386. doi:10.1038/s42003-019-0609-x.

Kobayashi, Y. (2018). Circulating extracellular vesicles are associated with lipid and insulin metabolism. *Am J Physiol Endocrinol Metab.*, 315(4):E574-E582. doi:10.1152/ajpendo.00160.2018.

Koistinen, H. (2002). Regulation of glucose transport in human skeletal muscle. *Ann Med*, 410-418. doi:10.1080/078538902321012351

Kojima, K. (2014). ESCRT-0 Protein Hepatocyte Growth Factor-regulated Tyrosine Kinase Substrate (Hrs) Is Targeted to Endosomes Independently of Signal-transducing Adaptor Molecule (STAM) and the Complex Formation with STAM Promotes Its Endosomal Dissociation. *J Biol Chem*, 33296–33310. doi:10.1074/jbc.M114.578245

Koliha, N. (2016). A novel multiplex bead-based platform highlights the diversity of extracellular vesicles. *J Extracell Vesicles*, 5:29975. doi:10.3402/jev.v5.29975

Konoshenko, M. (2018). Isolation of Extracellular Vesicles: General Methodologies and Latest Trends. *Biomed Res Int*, 8545347. doi:10.1155/2018/8545347

Kosanovic, D. (2019). Enhanced circulating levels of CD3 cells-derived extracellular vesicles in different forms of pulmonary hypertension. *Pulm Circ.*, 9(3): 2045894019864357. doi:10.1177/2045894019864357

Koukourakis, M. (2006). Oxygen and glucose consumption in gastrointestinal adenocarcinomas: correlation with markers of hypoxia, acidity and anaerobic glycolysis. *Cancer Sci.*, 97(10):1056-60. doi:10.1111/j.1349-7006.2006.00298.x

Kouwaki, T. (2017). Extracellular Vesicles Deliver Host and Virus RNA and Regulate Innate Immune Response. *Int. J. Mol. Sci*, 666. doi:10.3390/ijms18030666

Kowal, J. (2016). Proteomic comparison defines novel markers to characterize heterogeneous populations of extracellular vesicle subtypes. *Proc. Natl. Acad. Sci. U.S. A*, E968–E977. doi:10.1073/pnas.1521230113

Kraft, J. (2014). Emerging research and clinical development trends of liposome and lipid nanoparticle drug delivery systems. *J Pharm Sci*, 29-52. doi:10.1002/jps.23773

Kulp, A. (2010). Biological functions and biogenesis of secreted bacterial outer membrane vesicles. *Annu Rev Microbiol.*, 64:163-84. doi:10.1146/annurev.micro.091208.073413

Kurten, R. (2001). Self-assembly and binding of a sorting nexin to sorting endosomes. *J Cell Sci.*, 114(Pt 9):1743-56.

Kyrana, E. (2012). Molecular mechanisms of cachexia in chronic disease. *Expert Rev Endocrinol Metab*, 7(1):73-90. doi:10.1586/eem.11.87

Lakhter, A. (2015). Minireview: Emerging Roles for Extracellular Vesicles in Diabetes and Related Metabolic Disorders. *Mol Endocrinol.*, 29(11):1535-48. doi: 10.1210/me.2015-1206.

Larsson, N. (1998). Mitochondrial transcription factor A is necessary for mtDNA maintenance and embryogenesis in mice. *Nat Genet*, 18(3):231-6. doi:10.1038/ng0398-231

Lässer, C. (2018). Subpopulations of extracellular vesicles and their therapeutic potential. *Mol Aspects Med*, 1-14. doi:10.1016/j.mam.2018.02.002

Laulagnier, K. (2004). PLD2 is enriched on exosomes and its activity is correlated to the release of exosomes. *FEBS Lett*, 11-4. doi:10.1016/j.febslet.2004.06.082

Laulagnier, K. (2018). Amyloid precursor protein products concentrate in a subset of exosomes specifically endocytosed by neurons. *Cell. Mol. Life Sci*, 757–773. doi:10.1007/s00018-017-2664-0

Lawson, J. (2017). Selective secretion of microRNAs from lung cancer cells via extracellular vesicles promotes CAMK1D-mediated tube formation in endothelial cells. *Oncotarget.*, 8(48): 83913–83924. doi:10.18632/oncotarget.19996

Lee, C. (2018). Discovery of a diagnostic biomarker for colon cancer through proteomic profiling of small extracellular vesicles. *BMC Cancer.*, 18(1):1058. doi:10.1186/s12885-018-4952-y.

Lee, E. (2009). Gram-positive bacteria produce membrane vesicles: proteomics-based characterization of Staphylococcus aureus-derived membrane vesicles. *Proteomics.*, 9(24):5425-36. doi:10.1002/pmic.200900338.

Lee, J. (2013). Staphylococcus aureus Extracellular Vesicles Carry Biologically Active β-Lactamase. *Antimicrob Agents Chemother.*, 57(6): 2589–2595. doi:10.1128/AAC.00522-12

Lemaire, Q. (2019). Isolation of microglia-derived extracellular vesicles: towards miRNA signatures and neuroprotection. *J Nanobiotechnology*, 17: 119. doi:10.1186/s12951-019-0551-6

Lentz, B. (2003). Exposure of platelet membrane phosphatidylserine regulates blood coagulation. *Prog Lipid Res.*, 42(5):423-38. doi:10.1016/s0163-7827(03)00025-0

Li, M. (2017). Lactobacillus-derived extracellular vesicles enhance host immune responses against vancomycin-resistant enterococci. *BMC Microbiol*, 66. doi:10.1186/s12866-017-0977-7

Li, W. (2014). Rab27A regulates exosome secretion from lung adenocarcinoma cells A549: involvement of EPI64. *APMIS*, 122(11):1080-7. doi:10.1111/apm.12261.

Li, Y. (2003). Hydrogen peroxide stimulates ubiquitin-conjugating activity and expression of genes for specific E2 and E3 proteins in skeletal muscle myotubes. *Am J Physiol Cell Physiol.*, C806-12. doi:10.1152/ajpcell.00129.2003

Li, Z. (2002). Roles of heat-shock proteins in antigen presentation and cross-presentation. *Curr Opin Immunol*, 45-51. doi:10.1016/s0952-7915(01)00297-7

Liang, G. (2018). Engineered exosome-mediated delivery of functionally active miR-26a and its enhanced suppression effect in HepG2 cells. *Int. J. Nanomed*, 585–599. doi:10.2147/ijn.s15445

Lichtenberg, D. (1984). Structural Characteristics of Phospholipid Multilamellar Liposomes . *Journal of pharmaceutical sciences*. doi:10.1002/jps.2600730134

Lin, J. (2002). Peroxisome Proliferator-activated Receptor γ Coactivator 1β (PGC-1β), A Novel PGC-1-related Transcription Coactivator Associated with Host Cell Factor. *Journal of Biological Chemistry*, 1645-1648. doi:10.1074/jbc.C100631200

Lin, J. (2005). Metabolic control through the PGC-1 family of transcription coactivators. *Cell Metab*, 1(6):361-70. doi:10.1016/j.cmet.2005.05.004

Lin, Y. (2018). Exosome-liposome hybrid nanoparticles deliver CRISPR/Cas9 system in MSCs. . *Adv. Sci.* , 5:1700611. doi:10.1002/advs.201700611

Lira, F. (2014). Exercise training as treatment in cancer cachexia. *Appl Physiol Nutr Metab*, 679-86. doi:10.1139/apnm-2013-0554

Liu, P. (2007). Rab-Regulated Interaction of Early Endosomes with Lipid Droplets. *Biochim Biophys Acta.*, 1773(6): 784–793. doi:10.1016/j.bbamcr.2007.02.004

Liu, W. (2019). A novel pan-cancer biomarker plasma heat shock protein 90alpha and its diagnosis determinants in clinic. *Cancer Sci.*, 110(9): 2941–2959. doi:10.1111/cas.14143

Liu, Y. (2015). Targeted exosome-mediated delivery of opioid receptor Mu siRNA for the treatment of morphine relapse. *Sci. Rep*, 5:17543. doi:10.1038/srep17543

Logozzi, M. (2009). High levels of exosomes expressing CD63 and caveolin-1 in plasma of melanoma patients. *PLoS One*, 4(4):e5219. doi:10.1371/journal.pone.0005219

Lopes-Rodrigues, V. (2017). Identification of the metabolic alterations associated with the multidrug resistant phenotype in cancer and their intercellular transfer mediated by extracellular vesicles. *Sci Rep.*, 44541. doi:10.1038/srep44541.

Lopez-Verrilli, M. (2013). Schwann cell-derived exosomes enhance axonal regeneration in the peripheral nervous system. *Glia.*, 61(11):1795-806. doi:10.1002/glia.22558

Lotvall, J. (2014). Minimal experimental requirements for definition of extracellular vesicles and their functions: a position statement from the international society for extracellular vesicles. *J. Extracell. Vesicles.*, 3:26913. doi:10.3402/jev.v3.26913

Lou, G. (2015). Exosomes derived from miR-122-modified adipose tissue-derived MSCs increase chemosensitivity of hepatocellular carcinoma. *J Hematol Oncol*, 122. doi:10.1186/s13045-015-0220-7

Luan, X. (2017). Engineering exosomes as refined biological nanoplatforms for drug delivery. *Acta Pharmacol Sin*, 754–763. doi:10.1038/aps.2017.12

Lunavat, T. (2015). Small RNA deep sequencing discriminates subsets of extracellular vesicles released by melanoma cells--Evidence of unique microRNA cargos. *RNA Biol.*, 12(8):810-23. doi:10.1080/15476286.2015.1056975.

Lund, P. (2003). The chaperonins: perspectives from the Archaea. *Biochem Soc Trans*, 681-5. doi:10.1042/bst0310681

Lv, C. (2018). A PEG-based method for the isolation of urinary exosomes and its application in renal fibrosis diagnostics using cargo miR-29c and miR-21 analysis. *Int Urol Nephrol*, 973-982. doi:10.1007/s11255-017-1779-4

Lydic, T. (2015). Rapid and comprehensive 'shotgun' lipidome profiling of colorectal cancer cell derived exosomes. *Methods*, 83-95. doi:10.1016/j.ymeth.2015.04.014

Maacha, S. (2019). Extracellular vesicles-mediated intercellular communication: roles in the tumor microenvironment and anti-cancer drug resistance. *Mol Cancer.*, 18: 55. doi:10.1186/s12943-019-0965-7

Maas, S. (2014). Quantification and size-profiling of extracellular vesicles using tunable resistive pulse sensing. *J Vis Exp*, e51623. doi:10.3791/51623

Macario, A. (2005). Sick chaperones cellular stress and disease. *N Engl J Med*, 1489-501. doi:10.1056/NEJMra050111

MacDonald, P. (2005). Calcium increases endocytotic vesicle size and accelerates membrane fission in insulin-secreting INS-1 cells. *J Cell Sci.*, 118(Pt 24):5911-20. doi:10.1242/jcs.02685

Machtinger, R. (2016). Extracellular vesicles: roles in gamete maturation, fertilization and embryo implantation. *Hum Reprod Update.*, 22(2):182-93. doi:10.1093/humupd/dmv055.

Madeddu, C. (2009). Medroxyprogesterone acetate in the management of cancer cachexia. *Expert Opin Pharmacother*, 10(8):1359-66. doi:10.1517/14656560902960162

Maëva, D. (2017). Characterisation of adipocyte-derived extracellular vesicle subtypes identifies distinct protein and lipid signatures for large and small extracellular vesicles. *J Extracell Vesicles.*, 6(1): 1305677. doi:10.1080/20013078.2017.1305677.

Malik, M. (2012). Microemulsion method: A novel route to synthesize organic and inorganic nanomaterials: 1st Nano Update. *Arabian Journal of Chemistry*, 397-417. doi:10.1016/j.arabjc.2010.09.027

Malvern. (2009). *user manual.* England.

Marcilla, A. (2014). Extracellular vesicles in parasitic diseases. *J Extracell Vesicles.*, 3:25040. doi:10.3402/jev.v3.25040.

Markov, O. (2019). Immunotherapy Based on Dendritic Cell-Targeted/-Derived Extracellular Vesicles-A Novel Strategy for Enhancement of the Anti-tumor Immune Response. *Front Pharmacol.*, 10:1152. doi:10.3389/fphar.2019.01152.

Martínez-Redondo, V. (2015). The hitchhiker's guide to PGC-1α isoform structure and biological functions. *Diabetologia*, 58(9):1969-77. doi:10.1007/s00125-015-3671-z

Martínez-Redondo, V. (2016). Peroxisome Proliferator-activated Receptor γ Coactivator-1 α Isoforms Selectively Regulate Multiple Splicing Events on Target Genes. *J Biol Chem*, 291(29): 15169–15184. doi:10.1074/jbc.M115.705822

Mashburn-Warren, L. (2008). Interaction of quorum signals with outer membrane lipids: insights into prokaryotic membrane vesicle formation. *Mol Microbiol.*, 69(2):491-502. doi:10.1111/j.1365-2958.2008.06302.x

Masiero, E. (2009). Autophagy is required to maintain muscle mass. *Cell Metabolism*, 507-15. doi:10.1016/j.cmet.2009.10.008.

Matsuzaki, K. (2017). MiR-21-5p in urinary extracellular vesicles is a novel biomarker of urothelial carcinoma. *Oncotarget.*, 8(15): 24668–24678. doi:10.18632/oncotarget.14969

Mc Clements, D. (2012). Nanoemulsions versus microemulsions: terminology, differences, and similarities. *Soft Matter*. doi:10.1039/C2SM06903B

Mellisho, E. (2017). Identification and characteristics of extracellular vesicles from bovine blastocysts produced in vitro. *PLoS One.*, 12(5):e0178306. doi:10.1371/journal.pone.0178306.

Menay, F. (2017). Exosomes Isolated from Ascites of T-Cell Lymphoma-Bearing Mice Expressing Surface CD24 and HSP-90 Induce a Tumor-Specific Immune Response. *Front Immunol.*, 8:286. doi:10.3389/fimmu.2017.00286.

Mendt, M. (2019). Mesenchymal stem cell-derived exosomes for clinical use. *Bone Marrow Transplant*, 789-792. doi:10.1038/s41409-019-0616-z

Merendino, A. (2010). Hsp60 Is Actively Secreted by Human Tumor Cells. *PLoS ONE*. doi:10.1371/journal.pone.0009247

Migliano, S. (2018). ESCRT and Membrane Protein Ubiquitination. *Prog Mol Subcell Biol*, 107-135. doi:10.1007/978-3-319-96704-2_4

Mills, J. (1998). Apoptotic membrane blebbing is regulated by myosin light chain phosphorylation. *J Cell Biol.*, 140(3):627-36. doi:10.1083/jcb.140.3.627

Mimms, L. (1981). Phospholipid vesicle formation and transmembrane protein incorporation using octyl glucoside. *Biochemistry*. doi:10.1021/bi00507a028

Mincheva-Nilsson, L. (2014). Placenta-derived exosomes and syncytiotrophoblast microparticles and their role in human reproduction: immune modulation for pregnancy success. *Am J Reprod Immunol.*, 72(5):440-57. doi:10.1111/aji.12311.

Minciacchi, V. (2015). Extracellular vesicles in cancer: exosomes, microvesicles and the emerging role of large oncosomes. *Semin Cell Dev Biol.*, 40:41-51. doi:10.1016/j.semcdb.2015.02.010.

Mitsuhashi, S. (2016). Luminal Extracellular Vesicles (EVs) in Inflammatory Bowel Disease (IBD) Exhibit Proinflammatory Effects on Epithelial Cells and Macrophages. *Inflamm Bowel Dis.*, 22(7):1587-95. doi:10.1097/MIB.0000000000000840.

Miura, S. (2008). Isoform-specific increases in murine skeletal muscle peroxisome proliferator-activated receptor-gamma coactivator-1alpha (PGC-1alpha) mRNA in response to beta2-adrenergic receptor activation and exercise. *Endocrinology*, 149(9):4527-33. doi:10.1210/en.2008-0466

Mol, E. (2017). Higher functionality of extracellular vesicles isolated using size-exclusion chromatography compared to ultracentrifugation. *Nanomedicine*, 2061-2065. doi:10.1016/j.nano.2017.03.011

Momen-Heravi, F. (2012). Alternative methods for characterization of extracellular vesicles. *Front Physiol.*, 3:354. doi: 10.3389/fphys.2012.00354

Moon, P. (2016). Identification of Developmental Endothelial Locus-1 on Circulating Extracellular Vesicles as a Novel Biomarker for Early Breast Cancer Detection. *clinical cancer research*, 22(7):1757-66. doi:10.1158/1078-0432.CCR-15-0654

Morio, H. (2018). Cancer-Type OATP1B3 mRNA in Extracellular Vesicles as a Promising Candidate for a Serum-Based Colorectal Cancer Biomarker. *Biol Pharm Bull.*, 41(3):445-449. doi:10.1248/bpb.b17-00743.

Mulcahy, L. (2014). Routes and mechanisms of extracellular vesicle uptake. *J Extracell Vesicles.* doi:10.3402/jev.v3.24641.

Müller, I. (2003). Intravascular tissue factor initiates coagulation via circulating microvesicles and platelets. *FASEB J.*, 17(3):476-8. doi:10.1096/fj.02-0574fje

Munoz, J. (2013). Delivery of Functional Anti-miR-9 by Mesenchymal Stem Cell-derived Exosomes to Glioblastoma Multiforme Cells Conferred Chemosensitivity. *Mol Ther Nucleic Acids*, e126. doi:10.1038/mtna.2013.60

Nagano, M. (2019). Rab5-mediated endosome formation is regulated at the trans-Golgi network. *Commun Biol.*, 419. doi:10.1038/s42003-019-0670-5

Narkar, V. A. (2017). PGC1α Promoter Methylation and Nucleosome Repositioning: Insights Into Exercise and Metabolic Regulation in Skeletal Muscle. *Endocrinology*, 158(7): 2084–2085. doi:10.1210/en.2017-00439

Naseri, Z. (2018). Exosome-mediated delivery of functionally active miRNA-142-3p inhibitor reduces tumorigenicity of breast cancer in vitro and in vivo. *Int. J. Nanomed*, 7727–7747. doi:10.2147/ijn.s18238

Nawaz, M. (2018). Extracellular Vesicles and Matrix Remodeling Enzymes: The Emerging Roles in Extracellular Matrix Remodeling, Progression of Diseases and Tissue Repair. *Cells.*, E167. doi:10.3390/cells7100167.

Nguyen, D. (2016). Characterization of Microvesicles Released from Human Red Blood Cells. *Cell Physiol Biochem.*, 38(3):1085-99. doi:10.1159/000443059

Nielsen, E. (1999). Rab5 regulates motility of early endosomes on microtubules. *Nat Cell Biol.*, 1(6):376-82. doi:10.1038/14075

Nielsen, K. (1999). A Single-Ring Mitochondrial Chaperonin (Hsp60-Hsp10) Can Substitute for GroEL-GroES In Vivo. *J Bacteriol*, 5871-5. doi:10.1128/JB.181.18.5871-5875.1999

Nielsen, M. (2015). Elevated atherosclerosis-related gene expression, monocyte activation and microparticle-release are related to increased lipoprotein-associated oxidative stress in familial hypercholesterolemia. *PLoS One.*, 10(4):e0121516. doi:10.1371/journal.pone.0121516

Nik, A. (2017). Extracellular Vesicles As Mediators of Cardiovascular Calcification. *Front Cardiovasc Med.*, 4: 78. doi:10.3389/fcvm.2017.00078

Nishida, N. (2006). Angiogenesis in Cancer. *Vasc Health Risk Manag.*, 2(3): 213–219. doi:10.2147/vhrm.2006.2.3.213

Nixon, B. (2019). Proteomic Profiling of Mouse Epididymosomes Reveals their Contributions to Post-testicular Sperm Maturation. *Mol Cell Proteomics.*, 18(Suppl 1):S91-S108. doi:10.1074/mcp.RA118.000946.

Nomura, S. (2017). Extracellular vesicles and blood diseases. *Int J Hematol*, 392-405. doi: 10.1007/s12185-017-2180-x

Nordin, J. (2015). Ultrafiltration with size-exclusion liquid chromatography for high yield isolation of extracellular vesicles preserving intact biophysical and functional properties. *Nanomedicine*, 879-83. doi: 10.1016/j.nano.2015.01.003

Nowak, T. J. (1990). 70-kDa heat shock protein and c-fos gene expression after transient ischemia. *Stroke*, 107-11.

Oda, H. (1995). Interaction of the microtubule cytoskeleton with endocytic vesicles and cytoplasmic dynein in cultured rat hepatocytes. *J Biol Chem.*, 270(25):15242-9. doi:10.1074/jbc.270.25.15242

Ofir-Birin, Y. (2017). Pathogen-derived extracellular vesicles coordinate social behaviour and host manipulation. *Semin Cell Dev Biol*, 83-90. doi:10.1016/j.semcdb.2017.03.004

Ohtani, N. (2013). Roles and mechanisms of cellular senescence in regulation of tissue homeostasis. *Cancer Sci.*, 104(5):525-30. doi:10.1111/cas.12118.

O'Loughlin, A. (2012). Exosomes and the emerging field of exosome-based gene therapy. *Curr Gene Ther*, 262-74. doi:10.2174/156652312802083594

O'Neill, C. (2019). Role of Extracellular Vesicles (EVs) in Cell Stress Response and Resistance to Cancer Therapy. *Cancers (Basel).*, E136. doi:10.3390/cancers11020136.

O'Neill, H. (2008). Exosomes secreted by bacterially infected macrophages are proinflammatory. *Sci Signal.*, 1(6):pe8. doi:10.1126/stke.16pe8

Osteikoetxea, X. (2015). Differential detergent sensitivity of extracellular vesicle subpopulations. *Org Biomol Chem*, 9775-82. doi:10.1039/c5ob01451d

Ostrowski, K. (1999). Pro- and anti-inflammatory cytokine balance in strenuous exercise in humans. *J Physiol*, 287–291. doi:10.1111/j.1469-7793.1999.287ad.x

P. Y. Che, S. (2017). Tissue Factor-Expressing Tumor-Derived Extracellular Vesicles Activate Quiescent Endothelial Cells via Protease-Activated Receptor-1. *Front. Oncol.* doi:10.3389/fonc.2017.00261

Padrão, A. (2017). Long-term exercise training prevents mammary tumorigenesis-induced muscle wasting in rats through the regulation of TWEAK signalling. *Acta Physiol (Oxf)*, 803-813. doi:10.1111/apha.12721

Pagano, A. (2004). In Vitro Formation of Recycling Vesicles from Endosomes Requires Adaptor Protein-1/Clathrin and Is Regulated by Rab4 and the Connector Rabaptin-5. *Molecular Biology of the Cell.*, 4990–5000. doi:10.1091/mbc.e04-04-0355.

Palikaras, K. (2014). Mitochondrial homeostasis: the interplay between mitophagy and mitochondrial biogenesis. *Exp Gerontol.*, 56:182-8. doi:10.1016/j.exger.2014.01.021

Pang, B. (2020). Extracellular vesicles: the next generation of biomarkers for liquid biopsy-based prostate cancer diagnosis. *Theranostics.*, 2309–2326. doi:10.7150/thno.39486

Pascua-Maestro, R. (2018). Extracellular Vesicles Secreted by Astroglial Cells Transport Apolipoprotein D to Neurons and Mediate Neuronal Survival Upon Oxidative Stress. *Front Cell Neurosci*, 12: 526. doi:10.3389/fncel.2018.00526

Patel, G. (2019). Comparative analysis of exosome isolation methods using culture supernatant for optimum yield, purity and downstream applications. *Sci Rep*, 5335. doi:10.1038/s41598-019-41800-2

Patel, H. (2017). TNF-α and cancer cachexia: Molecular insights and clinical implications. *Life Sci.*, 170:56-63. doi:10.1016/j.lfs.2016.11.033

Patton, M. (2020). Hypoxia alters the release and size distribution of extracellular vesicles in pancreatic cancer cells to support their adaptive survival. *J Cell Biochem.*, 121(1):828-839. doi:10.1002/jcb.29328.

Paul, P. (2010). Targeted ablation of TRAF6 inhibits skeletal muscle wasting in mice. *J Cell Biol*, 191(7):1395-411. doi:10.1083/jcb.201006098

Pedersen, K. (2017). Specific and Generic Isolation of Extracellular Vesicles with Magnetic Beads. *Methods Mol Biol.*, 1660:65-87. doi:10.1007/978-1-4939-7253-1_7

Pegtel, D. (2014). Extracellular vesicles as modulators of cell-to-cell communication in the healthy and diseased brain. *Philos Trans R Soc Lond B Biol Sci*, 369(1652): 20130516. doi:10.1098/rstb.2013.0516

Penna, F. (2013). Autophagic Degradation Contributes to Muscle Wasting in. *Am J Pathol*, 182(4):1367-78. doi:10.1016/j.ajpath.2012.12.023

Penna, F. (2019). The Skeletal Muscle as an Active Player Against Cancer Cachexia. *Front. Physiol*, 10: 41. doi:10.3389/fphys.2019.00041

Perut, F. (2019). Extracellular Nanovesicles Secreted by Human Osteosarcoma Cells Promote Angiogenesis. *Cancers (Basel).*, 11(6). doi:10.3390/cancers11060779.

Pfrieger, F. (2018). Cholesterol and the journey of extracellular vesicles. *J. Lipid Res.*, 2255–2261. doi:10.1194/jlr.r084210

Pierre-Yves, M. (2014). The role of extracellular vesicles in Plasmodium and other protozoan parasites. *Cell Microbiol*, 344–354. doi:10.1111/cmi.12259

Pilegaard, H. (2003). Exercise induces transient transcriptional activation of the PGC-1alpha gene in human skeletal muscle. *J Physiol*, 546(Pt 3):851-8. doi:10.1113/jphysiol.2002.034850

Pin, F. (2015). Combination of exercise training and erythropoietin prevents cancer-induced muscle alterations. *Oncotarget*, 43202–43215. doi:10.18632/oncotarget.6439

Pirkkala, L. (2001). Roles of the heat shock transcription factors in regulation of the heat shock response and beyond. *FASEB J*, 1118-31. doi:10.1096/fj00-0294rev

Podinovskaia, M. (2018). The Endosomal Network: Mediators and Regulators of Endosome Maturation. *Progress in Molecular and Subcellular Biology.*, 1-38. doi:10.1007/978-3-319-96704-2_1.

Poliakov, A. (2009). Structural heterogeneity and protein composition of exosome-like vesicles (prostasomes) in human semen. *Prostate*, 159-67. doi:10.1002/pros.20860

Pollet, H. (2018). Plasma Membrane Lipid Domains as Platforms for Vesicle Biogenesis and Shedding? *Biomolecules*, 8(3): 94. doi:10.3390/biom8030094

Pospichalova, V. (2015). Simplified protocol for flow cytometry analysis of fluorescently labeled exosomes and microvesicles using dedicated flow cytometer. *J Extracell Vesicles*, 4:25530. doi:10.3402/jev.v4.25530

Pugholm, L. (2016). Phenotyping of Leukocytes and Leukocyte-Derived Extracellular Vesicles. *J Immunol Res.*, 2016:6391264. doi: 10.1155/2016/6391264

Puhka, M. (2017). Metabolomic Profiling of Extracellular Vesicles and Alternative Normalization Methods Reveal Enriched Metabolites and Strategies to Study Prostate Cancer-Related Changes. *Theranostics.*, 7(16): 3824–3841. doi: 10.7150/thno.19890

Puigserver, P. (1999). Activation of PPARgamma coactivator-1 through transcription factor docking. *Science*, 286(5443):1368-71. doi:10.1126/science.286.5443.1368

Puppa, M. (2014). Skeletal muscle glycoprotein 130's role in Lewis lung carcinoma-induced cachexia. *FASEBJ*, 998-1009. doi:28:998-1009

Qingfu, Z. (2018). Microfluidic Engineering of Exosomes: Editing Cellular Messages for Precision Therapeutics. *Lab Chip*, 1690–1703. doi:10.1039/c8lc00246k

Raimondo, S. (2015). Chronic myeloid leukemia-derived exosomes promote tumor growth through an autocrine mechanism. *Cell Commun Signal*, 8. doi:10.1186/s12964-015-0086-x.

Ranjbar, K. (2019). Combined Exercise Training Positively Affects Muscle Wasting in Tumor-Bearing Mice. *Med Sci Sports Exerc*, 1387-1395. doi:10.1249/MSS.0000000000001916

Reggiori, F. (2001). Sorting of proteins into multivesicular bodies: ubiquitin-dependent and -independent targeting. *EMBO J*, 5176-86. doi:10.1093/emboj/20.18.5176

Rejman, J. (2005). Role of clathrin- and caveolae-mediated endocytosis in gene transfer mediated by lipo- and polyplexes. *Mol Ther.*, 12(3):468-74. doi:10.1016/j.ymthe.2005.03.038

Ribeiro-Rodrigues, T. (2017). Exosomes secreted by cardiomyocytes subjected to ischaemia promote cardiac angiogenesis. *Cardiovasc Res.*, 113(11):1338-1350. doi:10.1093/cvr/cvx118

Richard, J. (2005). Cellular Uptake of Unconjugated TAT Peptide Involves Clathrindependent Endocytosis and Heparan Sulfate Receptors. *J Biol Chem.*, 280(15):15300-6. doi:10.1074/jbc.M401604200

Ricklefs, F. (2018). Immune evasion mediated by PD-L1 on glioblastoma-derived extracellular vesicles. *Science Advances*, eaar2766. doi:10.1126/sciadv.aar2766

Rink, J. (2005). Rab conversion as a mechanism of progression from early to late endosomes. *Cell.*, 122(5):735-49. doi:10.1016/j.cell.2005.06.043

Ritossa, F. (1962). A new puffing pattern induced by temperature shock and DNP in drosophila. *Experientia*, 571–573. doi:10.1007/BF02172188

Robert, J. (2003). Evolution of heat shock protein and immunity. *Dev Comp Immunol.*, 449-64. doi:10.1016/s0145-305x(02)00160-x

Robinson, M. (1996). Membrane dynamics in endocytosis. *Cell.*, 84(1):13-21. doi:10.1016/s0092-8674(00)80988-5

Rock, G. (1997). New concepts in coagulation. *Crit Rev Clin Lab Sci.*, 34(5):475-501. doi:10.3109/10408369709006423.

Rodrigues, M. (2013). Vesicular mechanisms of traffic of fungal molecules to the extracellular space. *Curr Opin Microbiol*, 414-20. doi:10.1016/j.mib.2013.04.002

Rodrigues, M. (2018). Role of Extracellular Vesicles in Viral and Bacterial Infections: Pathogenesis, Diagnostics, and Therapeutics. *Theranostics*, 2709–2721. doi:10.7150/thno.20576

Romancino, D. (2013). Identification and characterization of the nano-sized vesicles released by muscle cells. *FEBS Lett*, 1379-84. doi:10.1016/j.febslet.2013.03.012

Rosenberger, L. (2019). Stem cell exosomes inhibit angiogenesis and tumor growth of oral squamous cell carcinoma. *Sci. Rep*, 9:663. doi:10.1038/s41598-018-36855-6

Roucourt, B. (2015). Heparanase activates the syndecan-syntenin-ALIX exosome pathway. *Cell Res*, 412–428. doi:10.1038/cr.2015.29

Royo, F. (2017). Hepatocyte-secreted extracellular vesicles modify blood metabolome and endothelial function by an arginase-dependent mechanism. *Sci Rep.*, 7:42798. doi:10.1038/srep42798.

Russell, A. (2003). Endurance training in humans leads to fiber type-specific increases in levels of peroxisome proliferator-activated receptor-gamma coactivator-1 and peroxisome proliferator-activated receptor-alpha in skeletal muscle. *Diabetes*, 52(12):2874-81. doi:10.2337/diabetes.52.12.2874

Russell, M. (2006). Molecular mechanisms of late endosome morphology, identity and sorting. *Curr Opin Cell Biol.*, 18(4):422-8. doi:10.1016/j.ceb.2006.06.002

Saletti, R. (2017). High resolution mass spectrometry characterization of the oxidation pattern of methionine and cysteine residues in rat liver mitochondria voltage-dependent anion selective channel 3 (VDAC3). *Biochim Biophys Acta Biomembr*, 301-311. doi:10.1016/j.bbamem.2016.12.003

Saletti, R. (2018). Post-translational modifications of VDAC1 and VDAC2 cysteines from rat liver mitochondria. *Biochim Biophys Acta Bioenerg*, 806-816. doi:10.1016/j.bbabio.2018.06.007

Salomon, C. (2014). A gestational profile of placental exosomes in maternal plasma and their effects on endothelial cell migration. *PLoS One.*, 9(6):e98667. doi:10.1371/journal.pone.0098667.

Sampaio, N. (2018). Extracellular vesicles from early stage Plasmodium falciparum-infected red blood cells contain PfEMP1 and induce transcriptional changes in human monocytes. *Cell Microbiol*, e12822. doi:10.1111/cmi.12822

Sanders, P. (2005). Angiotensin II directly induces muscle protein catabolism through the ubiquitin–proteasome proteolytic pathway and may play a role in cancer cachexia. *Br J Cancer*, 425–434. doi:10.1038/sj.bjc.6602725

Sandqvist, A. (2009). Heterotrimerization of heat-shock factors 1 and 2 provides a transcriptional switch in response to distinct stimuli. *Mol Biol Cell*, 1340-7. doi:10.1091/mbc.E08-08-0864

Sansone, P. (2017). Packaging and transfer of mitochondrial DNA via exosomes regulate escape from dormancy in hormonal therapy-resistant breast cancer. *Proc Natl Acad Sci U S A.*, 114(43):E9066-E9075. doi:10.1073/pnas.1704862114.

Santamaria-Martos, F. (2019). Comparative and functional analysis of plasma membrane-derived extracellular vesicles from obese vs. nonobese women. *Clin Nutr.*, S0261-5614(19)30163-3. doi:10.1016/j.clnu.2019.04.008.

Sato, Y. (2016). Engineering hybrid exosomes by membrane fusion with liposomes. *Sci. Rep*, 6:21933. doi:10.1038/srep21933

Scarpulla, R. (2002). Nuclear activators and coactivators in mammalian mitochondrial biogenesis. *Biochim Biophys Acta*, 1576(1-2):1-14. doi:10.1016/s0167-4781(02)00343-3

Schaeffer, P. (2004). Calcineurin and calcium/calmodulin-dependent protein kinase activate distinct metabolic gene regulatory programs in cardiac muscle. *J Biol Chem.*, 279(38):39593-603. doi:10.1074/jbc.M403649200

Schey, K. (2015). Proteomics characterization of exosome cargo. *Methods*, 75-82. doi:10.1016/j.ymeth.2015.03.018

Schiro, A. (2015). Elevated levels of endothelial-derived microparticles and serum CXCL9 and SCGF-β are associated with unstable asymptomatic carotid plaques. *Sci Rep*, 16658. doi:10.1038/srep16658

Schneider, D. (2017). Mechanisms and modulation of microvesicle uptake in a model of alveolar cell communication. *J Biol Chem*, 20897-20910. doi:10.1074/jbc.M117.792416

Schuh, A. (2014). The ESCRT machinery: From the plasma membrane to endosomes and back again. *Crit Rev Biochem Mol Biol.*, 49(3): 242–261. doi:10.3109/10409238.2014.881777

Scott, C. (2011). Ion flux and the function of endosomes and lysosomes: pH is just the start. *BioEssays.*, 33(2):103-10. doi:10.1002/bies.201000108.

Senthilkumar, K. (2018). A New Approach for Loading Anticancer Drugs Into Mesenchymal Stem Cell-Derived Exosome Mimetics for Cancer Therapy. *Front Pharmacol*, 1116. doi:10.3389/fphar.2018.01116

Serban, K. (2016). Structural and functional characterization of endothelial microparticles released by cigarette smoke. *Sci Rep.*, 6: 31596. doi:10.1038/srep31596

Silva, K. (2015). Inhibition of Stat3 Activation Suppresses Caspase-3 and the Ubiquitin-Proteasome System, Leading to Preservation of Muscle Mass in Cancer Cachexia. *J Biol Chem*, 290(17): 11177–11187. doi:10.1074/jbc.M115.641514

Silverman, J. (2016). Disease Mechanisms in ALS: Misfolded SOD1 Transferred Through Exosome-Dependent and Exosome-Independent Pathways. *Cell Mol Neurobiol*, 377–381. doi:10.1007/s10571-015-0294-3

Sitar, S. (2015). Size characterization and quantification of exosomes by asymmetrical-flow field-flow fractionation. *Anal Chem*, 87(18):9225-33. doi:10.1021/acs.analchem.5b01636

Sivamohan, R. (1999). Liquid chromatography used to size-separate the amphiphilic-molecules stabilized nano-particles of cds in the 1–10nm range. *Nanostructured Materials*, 89-94. doi:10.1016/S0965-9773(99)00072-0

Skotland, T. (2017). Lipids in exosomes: Current knowledge and the way forward. *Prog Lipid Res*, 30-41. doi:10.1016/j.plipres.2017.03.001

Skotland, T. (2019). Exosomal lipid composition and the role of ether lipids and phosphoinositides in exosome biology. *J Lipid Res*, 9-18. doi:10.1194/jlr.R084343

Skottvoll, F. (2019). Ultracentrifugation versus kit exosome isolation: nanoLC-MS and other tools reveal similar performance biomarkers, but also contaminations. *Future Sci*, OA 5:FSO359. doi:10.4155/fsoa-2018-0088

Soekmadji, C. (2019). *Extracellular Vesicles in Health and Disease*. Tratto da Coursera.

Sokolova, V. (2011). Characterisation of exosomes derived from human cells by nanoparticle tracking analysis and scanning electron microscopy. *Colloids Surf B Biointerfaces*, 146-50. doi:10.1016/j.colsurfb.2011.05.013

Solans, C. (1997). Surfactants for microemulsions. *Current opinion in colloid & interface science*, 464-471. doi:10.1016/S1359-0294(97)80093-3

Soler, N. (2008). Virus-like vesicles and extracellular DNA produced by hyperthermophilic archaea of the order Thermococcales. *Res Microbiol.*, 159(5):390-9. doi:10.1016/j.resmic.2008.04.015.

Somji, S. (1999). Expression of the constitutive and inducible forms of heat shock protein 70 in human proximal tubule cells exposed to heat, sodium arsenite, and CdCl(2). *Environ Health Perspect*, 887–893. doi:10.1289/ehp.99107887

Sousa, D. (2015). Intercellular Transfer of Cancer Drug Resistance Traits by Extracellular Vesicles. *Trends Mol Med.*, 21(10):595-608. doi:10.1016/j.molmed.2015.08.002

Spinazzola, A. (2009). Mitochondrial diseases: a cross-talk between mitochondrial and nuclear genomes. *Adv Exp Med Biol*, 652:69-84. doi:10.1007/978-90-481-2813-6_6

Sproviero, D. (2018). Pathological Proteins Are Transported by Extracellular Vesicles of Sporadic Amyotrophic Lateral Sclerosis Patients. *Front Neurosci.*, 12:487. doi:10.3389/fnins.2018.00487

Stenmark, H. (2009). Rab GTPases as coordinators of vesicle traffic. *Nat Rev Mol Cell Biol.*, 10(8):513-25. doi:10.1038/nrm2728

Stevenson, T. (2018). Immunization with outer membrane vesicles displaying conserved surface polysaccharide antigen elicits broadly antimicrobial antibodies. *Proc Natl Acad Sci U S A*, 115(14):E3106-E3115. doi:10.1073/pnas.1718341115.

Suades, R. (2012). Circulating and platelet-derived microparticles in human blood enhance thrombosis on atherosclerotic plaques. *Thromb Haemost.*, 108(6):1208-19. doi:10.1160/TH12-07-0486

Suades, R. (2015). High levels of TSP1+/CD142+ platelet-derived microparticles characterise young patients with high cardiovascular risk and subclinical atherosclerosis. *Thromb Haemost.*, 114(6):1310-21. doi:10.1160/TH15-04-0325

Sullivan, R. (2016). Epididymosomes: Role of extracellular microvesicles in sperm maturation. *Front Biosci (Schol Ed).*, 8:106-14. doi:10.2741/s450.

Sun, D. (2010). A novel nanoparticle drug delivery system: the anti-inflammatory activity of curcumin is enhanced when encapsulated in exosomes. *Mol Ther*, 1606-14. doi: 10.1038/mt.2010.105

Sun, S. (2006). Mechanics of Enveloped Virus Entry into Host Cells. *Biophys J*, L10–L12. doi:10.1529/biophysj.105.074203

Surman, M. (2017). Deciphering the role of ectosomes in cancer development and progression: focus on the proteome. *Clin. Exp. Metastasis*, 34 273–289. doi:10.1007/s10585-017-9844-z

Szatanek, R. (2015). Isolation of extracellular vesicles: determining the correct approach. *Int. J. Mol. Med.*, 11–17. doi:10.3892/ijmm.2015.2194

Taha, E. (2019). Roles of Extracellular HSPs as Biomarkers in Immune Surveillance and Immune Evasion. *Int. J. Mol. Sci.*, E4588. doi:10.3390/ijms20184588

Taldone, T. (2014). Protein chaperones: a composition of matter. *Expert Opin Ther Pat*, 501-18. doi:10.1517/13543776.2014.887681

Tardif, N. (2013). Autophagic-lysosomal pathway is the main proteolytic system modified in the skeletal muscle of esophageal cancer patients. *The American Journal of Clinical Nutrition*, 1485–1492. doi:10.3945/ajcn.113.063859

Taylor, D. (2015). Methods of isolating extracellular vesicles impact down-stream analyses of their cargoes. *Methods.*, 87:3-10. doi:10.1016/j.ymeth.2015.02.019

Tazi, E. (2010). Treatment of Cachexia in Oncology. *Indian J Palliat Care*, 16(3): 129–137. doi:10.4103/0973-1075.73644

Théry, C. (2006). Isolation and characterization of exosomes from cell culture supernatants and biological fluids. *Curr Protoc Cell Biol*, Unit 3.22. doi:10.1002/0471143030.cb0322s30

Théry, C. (2018). Minimal information for studies of extracellular vesicles 2018 (MISEV2018): a position statement of the International Society for Extracellular Vesicles and update of the MISEV2014 guidelines. *J Extracell Vesicles*, 1535750. doi: 10.1080/20013078.2018.1535750

Thomas, G. (2009). Cancer cell-derived microparticles bearing P-selectin glycoprotein ligand 1 accelerate thrombus formation in vivo. *J Exp Med.*, 206(9):1913-27. doi:10.1084/jem.20082297.

Thompson, A. (2016). Extracellular vesicles in neurodegenerative disease — pathogenesis to biomarkers. *Nat Rev Neurol*, 346–357. doi:10.1038/nrneurol.2016.68

Thompson, M. (1998). Signalling pathways regulating protein turnover in skeletal muscle. *Cell Sign*, 1-11. doi:10.1016/s0898-6568(97)00076-4

Tian, T. (2018). Surface functionalized exosomes as targeted drug delivery vehicles for cerebral ischemia therapy. *Biomaterials*, 137-149. doi:10.1016/j.biomaterials.2017.10.012

Tian, Y. (2014). A doxorubicin delivery platform using engineered natural membrane vesicle exosomes for targeted tumor therapy. *Biomaterials*, 2383-90. doi:10.1016/j.biomaterials.2013.11.083

Tijerina, A. (2004). The biochemical basis of metabolism in cancer cachexia. *Dimens Crit Care Nurs*, 23(6):237-43. doi:10.1097/00003465-200411000-00001

Timár, C. (2013). Antibacterial effect of microvesicles released from human neutrophilic granulocytes. *Blood.*, 121(3):510-8. doi:10.1182/blood-2012-05-431114.

Tissot, J. (2013). Blood microvesicles: From proteomics to physiology. *ScienceDirect*, 38-52. doi:10.1016/j.trprot.2013.04.004

Tixeira, R. (2017). Defining the morphologic features and products of cell disassembly during apoptosis. *Apoptosis*, 475–477. doi:10.1007/s10495-017-1345-7

Tominaga, N. (2015). Brain metastatic cancer cells release microRNA-181c-containing extracellular vesicles capable of destructing blood-brain barrier. *Nat Commun.*, 6:6716. doi:10.1038/ncomms7716.

Tracey, K. (1986). Shock and tissue injury induced by recombinant human cachectin. *Science*, 234(4775):470-4. doi:10.1126/science.3764421

Tracey, K. (1988). Cachectin/tumor necrosis factor induces cachexia, anemia, and inflammation. *J Exp Med*, 167(3): 1211–1227. doi:10.1084/jem.167.3.1211

Tramontano, A. (2010). Circulating Endothelial Microparticles in Diabetes Mellitus. *Mediators of Inflammation.*, 1-8. doi:10.1155/2010/250476

Tricarico, C. (2017). Biology and biogenesis of shed microvesicles. *Small GTPases*, 220-232. doi:10.1080/21541248.2016.1215283

Tripisciano, C. (2017). Different Potential of Extracellular Vesicles to Support Thrombin Generation: Contributions of Phosphatidylserine, Tissue Factor, and Cellular Origin. *Sci Rep.*, 7(1):6522. doi:10.1038/s41598-017-03262-2.

Trotta, M. (1996). Phase behaviour of microemulsion systems containing lecithin and lysolecithin as surfactants. *International journal of Pharmaceutics*. doi:10.1016/S0378-5173(96)04688-1

Tseng, Y. (2015). Preclinical Investigation of the Novel Histone Deacetylase Inhibitor AR-42 in the Treatment of Cancer-Induced Cachexia. *J Natl Cancer Inst*, djv274. doi:10.1093/jnci/djv274

Tuena de Gómez-Puyou, M. (1983). Regulation of the synthesis and hydrolysis of ATP by mitochondrial ATPase. Role of the natural ATPase inhibitor protein. *J Biol Chem*, 258(22):13680-4.

Tunici, P. (1999). In vivo modulation of 73 kDa heat shock cognate and 78 kDa glucose-regulating protein gene expression in rat liver and brain by ethanol. *Alcohol Clin Exp Res*, 1861-7.

Turturici, G. (2014). Extracellular membrane vesicles as a mechanism of cell-to-cell communication: advantages and disadvantages. *Am. J. Physiol. Cell Physiol.*, 306 C621–C633. doi:10.1152/ajpcell.00228.2013.

Vagner, T. (2018). Large extracellular vesicles carry most of the tumour DNA circulating in prostate cancer patient plasma. *J Extracell Vesicles.*, 7(1): 1505403. doi:10.1080/20013078.2018.1505403

Valencia, K. (2014). miRNA cargo within exosome-like vesicle transfer influences metastatic bone colonization. *The Journal of Neuroscience*, 39(47), 9269–9273. doi:10.1523/jneurosci.0147-18.2019

Vallin, J. (2019). The role of the molecular chaperone CCT in protein folding and mediation of cytoskeleton-associated processes: implications for cancer cell biology. *Cell Stress and Chaperones*, 17–27. doi:10.1007/s12192-018-0949-3

van der Pol, L. (2015). Outer membrane vesicles as platform vaccine technology. *Biotechnol J*, 1689–1706. doi:10.1002/biot.201400395

van der Vos, K. (2016). Directly visualized glioblastoma-derived extracellular vesicles transfer RNA to microglia/macrophages in the brain. *Neuro Oncol.*, 18(1):58-69. doi:10.1093/neuonc/nov244.

Van Deun, J. (2014). The impact of disparate isolation methods for extracellular vesicles on downstream RNA profiling. *J. Extracell. Vesicles*, 18:3. doi:10.3402/jev.v3.24858

Vargas-Roig, L. (1997). Heat shock proteins and cell proliferation in human breast cancer biopsy samples. *Cancer Detect Prev*, 441-51.

Vazirabadi, G. (2003). Epstein-Barr virus latent membrane protein-1 (LMP-1) and lytic LMP-1 localization in plasma membrane-derived extracellular vesicles and intracellular virions. *J Gen Virol*, 1997-2008. doi:10.1099/vir.0.19156-0

Veerman, R. (2019). Immune Cell-Derived Extracellular Vesicles - Functions and Therapeutic Applications. *Trends Mol Med.*, 25(5):382-394. doi:10.1016/j.molmed.2019.02.003

Ventura-Clapier, R. (2008). Transcriptional control of mitochondrial biogenesis: the central role of PGC-1alpha. *Cardiovascular Research*, 208-17. doi:10.1093/cvr/cvn098

Vilasi, S. (2014). Human Hsp60 with Its Mitochondrial Import Signal Occurs in Solution as Heptamers and Tetradecamers Remarkably Stable over a Wide Range of Concentrations. *PLoS One*, 9(5): e97657. doi:10.1371/journal.pone.0097657

Von Haehling, S. (2014). Treatment of Cachexia: An Overview of Recent Developments. *J Am Med Dir Assoc*, 866-72. doi:10.1016/j.jamda.2014.09.007

Vorkapic, D. (2016). Multifaceted roles of extracellular DNA in bacterial physiology. *Curr Genet*, 71–79. doi:10.1007/s00294-015-0514-x

Vu, L. (2019). Tumor-secreted extracellular vesicles promote the activation of cancer-associated fibroblasts via the transfer of microRNA-125b. *J Extracell Vesicles.*, 8(1): 1599680. doi:10.1080/20013078.2019.1599680

Wagner, M. (1999). Induction of stress proteins in human endothelial cells by heavy metal ions and heat shock. *Am J Physiol*, 1026-33. doi:10.1152/ajplung.1999.277.5.L1026

Wahlund, C. (2017). Exosomes from antigen-pulsed dendritic cells induce stronger antigen-specific immune responses than microvesicles in vivo. *Scientific Reports*, 17095. doi:10.1038/s41598-017-16609-6

Wallberg, A. (2003). Coordination of p300-mediated chromatin remodeling and TRAP/mediator function through coactivator PGC-1alpha. *Mol Cell*, 12(5):1137-49. doi:10.1016/s1097-2765(03)00391-5

Wandinger-Ness, A. (2014). Rab Proteins and the Compartmentalization of the Endosomal System. *Cold Spring Harb Perspect Biol.*, 6(11): a022616. doi:10.1101/cshperspect.a022616

Wang, S. (2018). Mesenchymal Stem Cell-Derived Extracellular Vesicles Suppresses iNOS Expression and Ameliorates Neural Impairment in Alzheimer's Disease Mice. *J Alzheimers Dis*, 1005-1013. doi:10.3233/JAD-170848

Wang, X. (2010). Caspase-3 cleaves specific 19 S proteasome subunits in skeletal muscle stimulating proteasome activity. *J Biol Chem.*, 285(28):21249-57. doi:10.1074/jbc.M109.041707

Wang, Y. (2017). Global scientific trends on exosome research during 2007-2016: a bibliometric analysis. *Oncotarget*, 48460-48470. doi:10.18632/oncotarget.17223

Wang, Y. (2019). Extracellular Vesicles (EVs) from Lung Adenocarcinoma Cells Promote Human Umbilical Vein Endothelial Cell (HUVEC) Angiogenesis through Yes Kinase-associated Protein (YAP) Transport. *Int J Biol Sci.*, 15(10):2110-2118. doi:10.7150/ijbs.31605

Wegele, H. (2004). Hsp70 and Hsp90—a relay team for protein folding. *Reviews of Physiology, Biochemistry and Pharmacology*. doi:10.1007/s10254-003-0021-1

Weiss, R. (2018). Differential Interaction of Platelet-Derived Extracellular Vesicles with Leukocyte Subsets in Human Whole Blood. *Sci Rep.*, 8(1):6598. doi:10.1038/s41598-018-25047-x

Wenz, T. (2009). PGC-1alpha activation as a therapeutic approach in mitochondrial disease. *IUBMB Life*, 1051-62. doi:10.1002/iub.261

Wenzel, E. (2018). Concerted ESCRT and clathrin recruitment waves define the timing and morphology of intraluminal vesicle formation. *Nat Commun.*, 2932. doi:10.1038/s41467-018-05345-8

Westerblad, H. (2010). Skeletal muscle: Energy metabolism, fiber types, fatigue and adaptability. *Experimental Cell Research*, 3093-3099. doi:10.1016/j.yexcr.2010.05.019

Whitley, D. (1999). Heat shock proteins: A review of the molecular chaperones. *Journal of Vascular Surgery*, 748-51. doi:10.1016/s0741-5214(99)70329-0

Wilcke, M. (2000). Rab11 Regulates the Compartmentalization of Early Endosomes Required for Efficient Transport from Early Endosomes to the Trans-Golgi Network. *J Cell Biol.*, 151(6): 1207–1220. doi:10.1083/jcb.151.6.1207

Williams, A. (2019). Mesenchymal Stem Cell-Derived Exosomes Provide Neuroprotection and Improve Long-Term Neurologic Outcomes in a Swine Model of Traumatic Brain Injury and Hemorrhagic Shock. *J Neurotrauma*, 54-60. doi:10.1089/neu.2018.5711

Willms, E. (2018). Extracellular vesicle heterogeneity: subpopulations, isolation techniques, and diverse functions in cancer progression. *Front. Immunol.*, 9:738. doi:10.3389/fimmu.2018.00738

Wolf, P. (1967). The nature and significance of platelet products in human plasma. *Br J Haematol.*, 269-88. doi:10.1111/j.1365-2141.1967.tb08741.x

Wu, C. (2019). Extracellular vesicles derived from natural killer cells use multiple cytotoxic proteins and killing mechanisms to target cancer cells. *J Extracell Vesicles.*, 8(1):1588538. doi:10.1080/20013078.2019.1588538.

Wu, G. (2015). Altered microRNA Expression Profiles of Extracellular Vesicles in Nasal Mucus From Patients With Allergic Rhinitis. *Allergy Asthma Immunol Res.*, 7(5):449-57. doi:10.4168/aair.2015.7.5.449

Wu, H. (2007). Calpain-calcineurin signaling in the pathogenesis of calcium-dependent disorder. *Acta Med Okayama*, 61(3):123-37. doi:10.18926/AMO/32905

Wu, J. (2018). Exosome-Mimetic Nanovesicles from Hepatocytes promote hepatocyte proliferation in vitro and liver regeneration in vivo. *Sci Rep*, 2471. doi:10.1038/s41598-018-20505-y

Xu, D. (2013). The role of exosomes and microRNAs in senescence and aging. *Adv Drug Deliv Rev.*, 65(3):368-75. doi:10.1016/j.addr.2012.07.010.

Yang, C. (2019). Effects of extracellular vesicles on placentation and pregnancy disorders. *Reproduction.*, 158(5):R189-R196. doi:10.1530/REP-19-0147.

Yang, J. (2017). Exosome Mediated Delivery of miR-124 Promotes Neurogenesis after Ischemia. *Mol Ther Nucleic Acids*, 278-287. doi:10.1016/j.omtn.2017.04.010

Yang, L. (2019). Long non-coding RNA HOTAIR promotes exosome secretion by regulating RAB35 and SNAP23 in hepatocellular carcinoma. *Mol Cancer.*, 18(1):78. doi:10.1186/s12943-019-0990-6.

Yang, Y. (2018). Inflammation leads to distinct populations of extracellular vesicles from microglia. *J Neuroinflammation*, 168. doi:10.1186/s12974-018-1204-7

Yarana, C. (2018). Extracellular Vesicles Released by Cardiomyocytes in a Doxorubicin-Induced Cardiac Injury Mouse Model Contain Protein Biomarkers of Early Cardiac Injury. *Clin Cancer Res.*, 24(7):1644-1653. doi:10.1158/1078-0432.CCR-17-2046

Yoshida, T. (2015). Mechanisms of Cachexia in Chronic Disease States. *Am J Med Sci*, 350(4): 250–256. doi:10.1097/MAJ.0000000000000511

Yuana, Y. (2013). Extracellular vesicles in physiological and pathological conditions. *Blood Rev.*, 27(1):31-9. doi:10.1016/j.blre.2012.12.002.

Yuana, Y. (2014). Co-isolation of extracellular vesicles and high-density lipoproteins using density gradient ultracentrifugation. *J Extracell Vesicles*, 3: 10. doi:10.3402/jev.v3.23262

Yujun, H. (2007). Proteomics-based identification of HSP60 as a tumor-associated antigen in colorectal cancer. *Proteomic Clinical Applications*, 336-42. doi:10.1002/prca.200600718

Zahka, J. (1985). Practical Aspects of Tangential Flow Filtration in Cell Separations. doi:10.1021/bk-1985-0271.ch003

Zeng, F. (2018). Extracellular vesicle-mediated MHC cross-dressing in immune homeostasis, transplantation, infectious diseases, and cancer. *Semin Immunopathol.*, 40(5):477-490. doi:10.1007/s00281-018-0679-8.

Zhang, B. (2014). Immunotherapeutic Potential of Extracellular Vesicles. *Front Immunol.*, 5: 518. doi:10.3389/fimmu.2014.00518

Zhang, L. (2017). Skeletal Muscle-Specific Overexpression of PGC-1α Induces Fiber-Type Conversion through Enhanced Mitochondrial Respiration and Fatty Acid Oxidation in Mice and Pigs. *Int J Biol Sci*, 13(9): 1152–1162. doi:10.7150/ijbs.20132

Zhang, Z. (2014). Comparison of ultracentrifugation and density gradient separation methods for isolating Tca8113 human tongue cancer cell line-derived exosomes. *Oncol. Lett.*, 1701–1706. doi:10.3892/ol.2014.2373

Zhao, L. (2016). Phosphatidylserine exposing-platelets and microparticles promote procoagulant activity in colon cancer patients. *J Exp Clin Cancer Res*, 35: 54. doi:10.1186/s13046-016-0328-9

Zhou, T. (2018). Development and validation of a clinically applicable score to classify cachexia stages in advanced cancer patients. *J Cachexia Sarcopenia Muscle*, 9(2): 306–314. doi:10.1002/jcsm.12275

Zwicker, J. (2008). Tissue factor-bearing microparticles and cancer. *Semin Thromb Hemost.*, 34(2):195-8. doi:10.1055/s-2008-1079260.